CD20+ T cells: Phenotype, origin and presence in the tumour microenvironment

By

Muath Mohammed Suliman

Supervisors: Prof John Curnow

Prof Ben Willcox

A thesis submitted to The University of Birmingham for the Degree of DOCTOR OF PHILOSOPHY

Institute of Immunology and Immunotherapy

College of Medical and Dental Science

University of Birmingham

July 2021

Abstract

CD20 is well-known as a lineage marker for B cells in human, although the presence of CD20+ T cells has been reported previously (Schuh et al., 2016). In my experiments we sorted memory CD8+CD20+ and CD20- T cells and subsequently analysed TCRβ CDR3 sequences to determine clonal overlap between populations. I was able to demonstrate TCRβ CDR3 amino acid sequences within the CD20+ T cells that were not found in the CD20- T cells population, suggesting the presence of unique T cell clones. This data suggests possible thymic origin of at least some CD20+ T cells, or an early expression of CD20+ following activation of naïve T cells. This does not however refute the trogocytosis theory where some T cells acquire CD20 from B cell. I analysed a number of published mass cytometry datasets and determined that memory CD20+ T cells express higher levels of CD127, CD27, CD28, PD-1 and CD57 especially by the effector memory (Tem) and effector memory CD45RA revertant (Temra) subsets, suggesting a possible late differentiation state of the CD20+ T cells. Further phenotyping revealed a novel population of CD20+Vα7.2+CD161+ cells in the peripheral blood of healthy donors, which are potentially CD20+ mucosal-invariant T (MAIT) cells. In colon cancer, CD20+ T cells were found within tumour tissue, adjacent normal tissue and showed fewer CD20+ T cells expressing the marker CD39. This may indicate lower numbers of CD20+ T cells within tumour-reactive T cell pool and requires further investigation. Using mass cytometry datasets from colorectal cancer patients, and melanoma patients receiving anti- programmed cells death (PD-1) or anti-cytotoxic T lymphocyte-associated protein-4 (CTLA-4), CD20+ T cells showed similar phenotypes to those found in healthy peripheral blood. Importantly, they produced higher levels of cytokines compared to the CD20- T cells including; TNF-α, IFN-γ, IL-2, IL-17, and MIP-1β. My data, including both primary data and analysis of published datasets, indicates that CD20+ T cells can originate as a separate lineage, in addition to acquiring CD20 by

trogocytosis. CD20+ T cells were found to be more highly differentiated, with increased cytokine production and contained a high frequency of CD20+ Vα7.2+CD161+ cells. Although there was no detectable difference in cancer, future work will be required to determine if they play any role within the tumour microenvironment or other pathological scenarios.

ACKNOWLEDGEMENTS

Personal acknowledgements

I would like to thank Prof. John Curnow for supervising me after being through difficult times during my PhD journey. No words can express my gratitude for him being so patients and supportive and being there for me whenever I needed his support. He believed on me when other seeded doubt inside my head that I would not be able to do it.

During my journey, I had to go through difficult exams, however, with the support of my family I could go through what I thought to be impossible for me to go through. My mother, my father and my brothers, I will be in your debt to the end of this world. You have been always there when I needed you. You took care of my sons during my divorce and you never put me under any kind of stress. You have believed in me and supported me in all the possible ways and thank you would never express what I feel about you.

Thank you so much Dr Graham Wallace for supporting me during my transfer from my previous supervisor and thank you for your justice with the decision you made for me. Thank you to my friends in Birmingham and in Saudi Arabia for their continuous support and advice. For those who made it so difficult for me during my PhD, thank you; because what does not kill you will make you stronger.

Scientific acknowledgements

My thanks to all of the technical facility staff who supported me during this journey; especially the flow and mass cytometry facility staff: Dr Shahram Golbabapour and Dr Adriana Flores-Langarica. Also, thanks to the EBV group in Cancer Sciences for their hospitality and support during moving the lab and to all other members who supported me during my project. Finally, I would like to thank King Khalid University for funding me and providing me with the scholarship to pursue my PhD.

Impact of COVID-19

Due to the COVID-19 pandemic, and the national and international lockdown, I was not able to use the lab facilities during the whole of this period of time. The original plan was to develop a mass cytometry panel that would allow us to phenotype the CD20+ T cells within healthy individuals, cancer tissue and normal adjacent tissue. We managed to get the necessary ethical approval to supply the required tissues. We developed and ordered the panel and performed the necessary optimisation. However, the lockdown came and we could not perform the experiments. I tried to assess CD20+ T cells tissue images using the Vectra machine, but, due to technical issues, we could not detect the cells and decided to use confocal microscopy just before the lockdown. I established a collaboration with Prof Graham Anderson to do experiments on thymic tissue, but because of COVID-19, all the scheduled operations were cancelled and no new tissue was available. We wanted to do single cell RNA-sequencing as well, however, that could not be done while the lab facilities were closed. Saudi Arabia gave the evacuation of the Saudi citizens in UK the priority and time line and when I came back to Saudi Arabia, my UK VISA expired and could not be renewed after that, because of COVID-19 pandemic and the national lockdown in Saudi Arabia, We therefore decided to use the available online tools, such as using mass cytometry datasets from FlowRepository to answer some of our questions about CD20+ T cells.

Table of Contents

Table of figures

List of tables

Abbreviations

APC	**Antigen-presenting cells**
B cells	B lymphocytes
BSA	Bovine serum albumin
Ca2+	Calcium ion
CAR	Chimeric antigen receptor
CCR6	C-C chemokine receptor-6
CCR7	C-C chemokine receptor-7
CCR9	C-C chemokine receptor-9
CD1d	major histocompatibility complex (MHC) class I-like glycoprotein
CD3	Cluster of differentiation-3
CD62L	L-selectin
CNS	Central nervus system
COVID-19	Coronavirus disease
CRC	Colorectal caner
CSF	Cerebrospinal fluid
CTLA-4	Cytotoxic T lymphocyte-associated protein-4
CXCL-13	C-X-C chemokine ligand-13
CXCR4	C-X-C chemokine receptor 4
CyTOF	Cytometry by time of flight
DAMP	Damage-associated molecular patterns
DC	Dendritic cell
DN	Double negative
DP	Double positive
EBV	Epstein-Barr virus
EDTA	Ethylenediaminetetraacetic acid
ETP	Early thymic progenitors
FACS	Fluorescence activated cell sorting
FDA	Food and Drug Administration
Foxp-3	Forkhead box protein-3
GM-CSF	Granulocyte-macrophage colony stimulating factor
GraA	Granzyme A
GraB	Granzyme B
HBRC	Human Biomaterial Resource Centre
HLA-DR	Human leukocyte antigen – DR isotype
ICAM-1	Intracellular adhesion molecule-1
IFNγ	Interferon-γ
Ig	Immunoglobulin
IgA	Immunoglobulin A
IgE	Immunoglobulin E
IgG	Immunoglobulin G
IgM	Immunoglobulin M
IL-17	interleukin- 17
IL-2	Interleukin-2
IL-21	interleukin- 21
IL-22	interleukin- 22
IL-2Rβ	Interlukin-2β receptor
IL-4	Interleukin-4

IL-6	Interleukin-6
IL-7	Interleukin-7
iNKT	Invariant natural killer T cell
ITP	Idiopathic thrombocytopenic purpura
KLRG1	Killer cell lectin like receptor G1
LMCV	lymphocytic choriomeningitis virus
LTβR	lymphotoxin beta receptor
mAB	Monoclonal antibodies
MAIT cells	Mucosal associated invariant T cells
Matched blood	Blood obtained before the operation from the same patient
MHC	Major histocompatibility complex
MIP-1β	Macrophage inflammatory protein β
MOG	myelin oligodendrocyte glycoprotein
MR-1	Major histocompatibility complex class I-related gene protein
MS	Multiple sclerosis
NK cell	Natural killer cell
NKG7	Natural killer cell granule 7
NKT	Natural killer T cells
PAMP	Pathogen-associated molecular pattern
PBMCs	Peripheral blood mononuclear cells
PBS	Phosphate-buffer saline
PD-1	Programmed cell death
PRF1	Perforin 1
PSGL-1	P-selectin glycoprotein ligand-
RA	Rheumatoid arthritis
RAG-1	Recombinase activating genes 1
RAG-2	Recombinase activating genes 2
rmT cells	Tissue resident memory T cells
RTX	Rituximab
SELL	L-selectin gene
T cells	T lymphocytes
TC-1	T cell one cytokines
TCF7	Transcription factor 7
Tcm	Central memory
TCR	T-cell receptor
TCRγδ	T-cell receptor gamma-delta
Tem	Effector memory
Temra	Effector memory CD45RA revertant
Th1	T helper 1
Th17	T helper 17
Th2	T helper 2
TIM-3	T-cell immunoglobulin mucin receptor-3
TNFa	Tumour necrosis factor-α
Trm cellsTregs	Tissue resident memory T cellsRegulatory T cells
Tstm	T memory stem cell
tTSNe	t-distributed stochastic neighbour embedding
VCAM-1	Vascular adhesion molecule-1
VDJ	Variable, diversity and joining
Vα7.2	TCRAV7S2

Chapter One: Introduction

1 Introduction

1.1 Overview of the immune system

The immune system represents the main defence system of the body against foreign pathogens, by maintaining a balance between pathogen clearance and preventing excessive tissue damage and destruction. The importance of the immune system can be illustrated using dysfunctional immune system outcomes, which can range from disease manifestation and immunodeficiency disorders to an over-activated immune system, resulting in the development of autoimmunity disorders (Brodin and Davis, 2017).

The immune system consists of two main subsystems, each with a different function. However, both subsystems work together to reach optimum protection of the body against a wide variety of pathogens. One of the subsystems is the innate immune system, which functions as the first line of defence and is known by its ability to recognise threats through shared molecular recognition receptors that can detect pathogen-associated molecular patterns (PAMPs) and damage-associated molecular patterns (DAMPs). The other subsystem is the adaptive immune system, which operates alternatively through the expression of unique receptors that are far more specific than innate receptors. These receptors are developed during gene rearrangement as a stage of adaptive immune cell development.

A pathogen breaching the skin and sub-mucosal layer results in the activation of the innate immune system, which senses pathogens through their expressed receptors. This detection usually results in the activation of the innate immune cells; especially tissue resident macrophages and the initiation of an immune response and, eventually, the recruiting of other innate immune cells and the release of recruiting factors for adaptive immune cells (Turvey and Broide, 2010, Gasteiger and Rudensky, 2014).

The recruiting factors released by the activated innate immune cells affect specific types of adaptive immune cell that are developed to act against a specific pathogen. These cells undergo clonal expansion through the proliferation of activated cells to control the pathogen threat. This activation process require longer time than activating innate immune cells; however, the first encounter with that pathogen usually results in the formation of memory cells that can clear the same pathogen in a faster time upon a second exposure (Call et al., 2002, MacLeod et al., 2010).

1.1.1 Adaptive immune system

Unlike the innate immune system, the adaptive immune system acts through a wide range of receptors, each targeting a specific component of the pathogen. Adaptive immune cells can also generate long-lived memory cells that rapidly clear pathogens upon a second encounter. The adaptive immune system consists of two types of cell: B lymphocytes (B cells) and T lymphocytes (T cells). Each of those cells has different functions and mechanisms of action, as will be discussed in the next subsections (Murphy and Weaver, 2016).

1.1.1.1 B lymphocytes

The generation of B cells starts in foetal liver and then continues in bone marrow, which is responsible for the maintenance of B cell numbers throughout life (Jung and Alt, 2004). The B-cell mechanism of action relies on the expression of a specific immunoglobulin (Ig) B-cell receptor. Activated B cells also have the ability to differentiate into antibody-secreting plasma cells and the development of memory B-cell formation (Zhang et al., 2016). During the development of B cells, sequential gene rearrangement is required to generate unique Ig receptors through the expression of endonuclease recombinase activating genes 1 and 2 (RAG1 and RAG2). The rearrangement of variable, diversity and joining (VDJ) gene segments is controlled by RAG1-2, which support their recombinase activity and allow them

to generate diverse specific B-cell receptors to target different types of pathogens (Jung and Alt, 2004).

At first, and during the formation of pre-B-cell receptors, successful gene rearrangement results in the formation of a heavy chain that is bound to the cell membrane (Tonegawa, 1983, Melchers, 2005). Next, another gene rearrangement is triggered to form the light chain that binds with the heavy chain to form immunoglobulin M (IgM) B-cell receptors (Pieper et al., 2013). The gene rearrangement process can however result in the formation of B-cell receptors that are able to target self-antigens. These auto-reactive B cells undergo clonal deletion by editing the receptor to another B-cell receptor that targets non-self-antigens (Nemazee and Hogquist, 2003, Goodnow et al., 2005).

The IgM+ mature B cells migrate from the bone marrow to the secondary lymphoid organs for further maturation and to await their activation by cognate antigens. The activation of the B cells can be classified into two main categories: T-dependent activation and T-independent activation. To illustrate, T-dependent B-cell responses require a signal from the T cells to be activated, whereas T-independent responses activate B cells without a T-cell signal (Liu et al., 1991). However, the T-dependent activation of B cells results in the entrance of B cells to germinal centres for further somatic hypermutation and class switching of immunoglobulin to IgG, IgA or IgE, accordingly (Kranich and Krautler, 2016). The ultimate goal of this process is to produce class-switched high affinity memory B cells and antibody-secreting plasma cells.

1.1.1.2 T lymphocytes

T lymphocytes are part of the adaptive immune cells and, unlike innate immune cells, are known for their specificity to specific antigens and by their ability to generate an immunological memory. They originate from haematopoiesis in the bone marrow and

migrate to the thymus for further maturation and education. Within the thymus, T cells undergo different gene segment rearrangements in order to generate fully functional T-cell receptors (TCRs) that can recognise a wide range of different antigens (Shah and Zúñiga-Pflücker, 2014).

Approximately 95% of the TCRs generated are composed of α and β chains, which are able to recognise the peptide bound to the major histocompatibility complex (MHC) molecules presented by antigen-presenting cells (APC), such as dendritic cells (DC), macrophages and B cells. The MHC molecules can be classified into two different molecules: MHC class I (MHC-I) and MHC class II (MHC-II). Each can present antigens (peptides) to a specific subset of T cells and expressed in different types of cells. MHC-II usually presents peptides to CD4+ T cells and can be expressed by APCs, while MHC-1 usually presents peptides to CD8+ T cells and can be expressed by all nucleated cells, including APC (Rock et al., 2016).

The remainder of the T cells are usually composed of γ and δ chains that can recognise less conventional ligands including lipids, instead of peptide antigens. Generally, αβ TCRs associate with four invariant membrane chains (CD3) to form a fully functional receptor that is able to signal through to ultimately alter transcription and activate the cells (Zúñiga-Pflücker, 2004, Attaf et al., 2015).

Within the thymus, T cells are generally not fully mature and are known as thymocytes. During the maturation process, T cells usually pass through different checkpoints, known as negative and positive selection. As the focus of this thesis is on CD20+ T cells, the development, maturation, subsets and responses of T cells are discussed in more detail in the following sections.

1.2 Overview of T cells

1.2.1 T cell development

Early T-cell progenitors descending from haematopoietic stem cells in the bone marrow reside in the thymus for further differentiation and maturation that eventually seeds mature CD4 or CD8 single-positive naïve T cells (Benz et al., 2008). Recruitment of these progenitors is controlled by different mechanisms and molecular expression factors.

To illustrate, chemokine receptor- 7 (CCR7), chemokine receptor-9 (CCR9) and CXC chemokine receptor-4 CXCR4 are chemokine receptors that control the migration of early T-cell progenitors to the thymus; CCR9-, CCR7- and CXCR4-deficient mice have been shown to possess a lower number of early T-cell progenitors within their thymus compared with the control mice (Calderón and Boehm, 2011). Another mechanism controlling the migration of those progenitors is the interaction between P-selectin glycoprotein ligand-1 (PSGL-1) on the lymphoid progenitor and P-selectin on thymic endothelium cells (Rossi et al., 2005).

Furthermore, the expression of other markers that usually interact with thymic portal endothelial cells can affect the entry of early lymphoid progenitors to the thymus, such as lymphotoxin beta receptor (LTβR), intracellular adhesion molecule-1 (ICAM-1) and vascular adhesion molecule-1 (VCAM-1) (Lucas et al., 2016).

The commitment of early lymphoid progenitors towards a T-cell lineage seems to be controlled by the Notch1 signalling pathway, whereby mice that lack Notch1 function have shown impaired T-cell development due to the loss of thymocytes, but not other lineages (Radtke, 1999). At this stage, the early thymic progenitors (ETP) lack the expression of CD4 and CD8 and are referred to as double negative (DN). However, they express two different markers: CD44 and CD25, which can be used to classify this population into further subsets.

The expression of CD44 alongside CD117 identifies a subset that is capable of giving rise to αβT-cell progenitors (Porritt et al., 2004). After the different stages of transition, from CD44+CD25- (DN1) to CD44+CD25+ (DN2) to CD44-CD25+ (DN3), a successful TCR-β chain rearrangement occurs (Dudley et al., 1994) **(Fig 1.2.1)**.

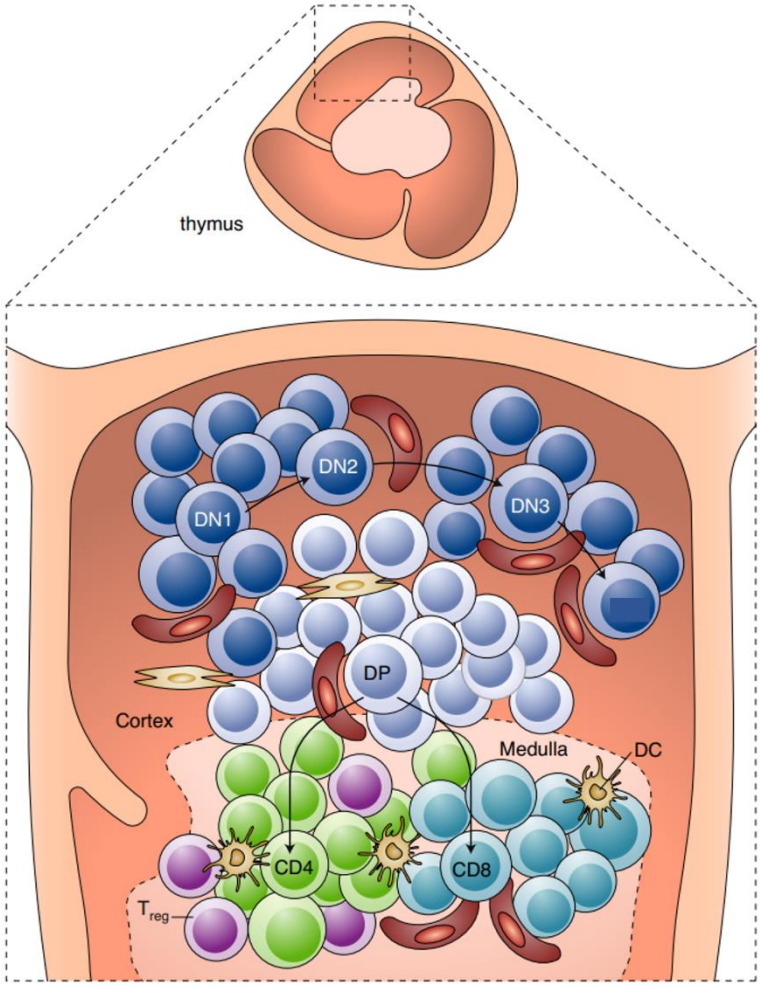

Figure.1.2.1 T cell development process in thymus.

Adapted from (Mittelbrunn and Kroemer, 2021). Diagram to show the development of T cells within the thymus. During T cells development in the thymus, migrated early lymphoid progenitors undergo through two main stages. The first to develop DN cells that will commit later to either CD4+ or CD8+ T cells. Each step performed in different part of the thymus. DN1;CD44+CD25-, DN2;CD44+CD25+, DN3;CD44-CD25+, DP; CD4+CD8+, Treg; regulatory T cells, DC; dendritic cell.

Similar to B-cell receptor rearrangement, the successful rearrangement of VDJ segments of the TCR-β receptor are controlled by RAG1-2 genes (Shinkai et al., 1992). After the generation of TCR-β receptors and CD3, a TCR-α chain starts gene rearrangement, down-regulating CD25 and expressing both CD4 and CD8. The cells at this stage are known as double positive (DP) and are prepared for positive selection (Fehling et al., 1995).

Positive selection is a process that happens within the cortical region of the thymus, by which the DP ability to interact with either MHCI or MHCII on the cortical thymic epithelial cells determines the fate of the cell and the commitment to either a CD4+ or CD8+ lineage. The cells with TCR that are unable to interact with the MHC molecule usually undergo death by neglect (Dzhagalov and Phee, 2012).

The type of MHC with which a DP thymocyte TCR interacts determines the lineage commitment. To illustrate, interaction of a TCR with MHCII develops CD4 single-positive cells, whereas interaction with MHCI will develop CD8 single-positive cells (Singer, 2002). This process ensures the development of functional T cells that are able to elicit immune responses through the appropriate MHC molecules.

Following the process outlined above, the DP thymocytes migrate through to the medulla region of the thymus by up-regulating CCR7 for another process known as negative selection. The aim of negative selection is to test the affinity of the TCR towards a self-presented antigen and self- MHC molecule on the medullary thymic epithelial cells and DCs in order to maintain immune tolerance and prevent the development of autoimmune responses (Anderson et al., 2002, Derbinski et al., 2001).

The ultimate goal of TCR rearrangement is to develop diverse TCRs that are able to target different types of pathogen; however, this process has a side effect of developing cells that can target self-antigens.

Therefore, negative selection can be a self-check process during the development of those cells, whereby cells that show activity towards self-peptide antigens are directed towards apoptosis (Bouillet et al., 2002). Passing through all the development stages within the thymus generates mature functional naïve T cells that are able to egress the thymus to the periphery and then to the lymph nodes, where they can be activated.

1.2.2 T-cell activation and differentiation

Within the lymph nodes, naïve T cells navigate through to the T-cell zone and scan through the antigens presented by the DCs using their CCR7 and L-selectin (CD62L) to enter and exit the lymph node. Until naïve T cells recognise their cognate antigens, a specialised stromal cell type, known as a T-cell zone reticular cell, which lines that zone, provides all the necessary elements for naïve T cells to search for the cognate antigen (Brinkman et al., 2013). For instance, T-cell zone reticular cells form a 3D mesh network that acts as a highway for naïve T cells to migrate and scan the antigens presented by DCs. Second, they secrete chemokine ligands CCL19 and CCl21 to guide both DCs and T cells to the T-cell zone. Third, they secrete the necessary survival factors for naïve T cells, such as interleukin-7 (IL-7), in order to increase their life span and maximise their chance of finding cognate antigens (Fletcher et al., 2015).

T cells require two types of signal to be successfully activated. First, the formation of an immunological synapse, which is a complex of TCR recognition of the peptide antigen present on the MHC molecule of the APC and transduction of the signal through CD3 subunits.

During this phase, CD4+ or CD8+, depending on the type of MHC molecule on the APC, is recruited and binds the MHC molecule to strengthen the interaction. Second, the signal is transduced through the interaction with additional molecules on the APC and T cells, known

as co-stimulatory molecules. Co-stimulation is the second signal, in addition to TCR-MHC complex signalling, to generate fully functional activated T cells. Examples are, CD80 and CD86 with the CD28 on T cells, which is considered a critical co-stimulatory signal for T cell activation. The nature of this interaction can determine the fate of the activated T cell (Smith-Garvin et al., 2009). The affinity of self-peptide engagement with MHC can determine the cell fate. To illustrate, strong affinity of the antigen in itself can determine the expansion rate of the primed CD8+ T cell, where higher affinity antigens can result in more expanded pool over the lower affinity antigens (Ozga et al., 2016). Indeed, the same finding can be noticed within CD4+ T cells (Kotov et al., 2019). In addition to promoting the expansion, the strong TCR stimulation has been shown to favour the promotion of IFN-γ producing Th1 cells over IL-4 producing Th2 cells (Bhattacharyya and Feng, 2020). On the other hand, in the periphery, a T cell receiving signal one without the co-stimulation second signal can result in cell anergy (Mueller, 2010). The co-stimulation signal can also be an inhibitory signal, rather than one of activation. Different inhibitory co-stimulation signals have been reported, the most widely known of which include programmed cell death (PD-1), T-cell immunoglobulin mucin-3 (TIM-3) and cytotoxic T lymphocyte-associated protein-4 (CTLA-4) (Fuertes Marraco et al., 2015). CTLA-4 expression can be triggered by the TCR signalling, where stronger TCR signals can induce more CTLA-4 expression (Krummel and Allison, 1996). PD-1 can be expressed during the effector phase where activated T cells that experienced more antigenic stimulation up-regulate PD-1 (Blackburn et al., 2009). Furthermore, cytokine secretion has been shown to be necessary for the expression of co-stimulatory molecules on DCs. Therefore, the activation of T cells can result in the differentiation of those cells into different effector cells, the proliferation of those cells and the production of different cytokine profiles (Smith-Garvin et al., 2009). Depending on the subset of T cells, their activation results in different types of effector cells, as discussed in the next subsection.

1.2.3 Subsets of T cells

1.2.3.1 CD4 T cells

Naïve CD4+ T cells can differentiate into several different helper effector cells, each of which shows different pro- or anti-inflammatory according to the stimuli received from the APC.

To illustrate, T helper 1 (Th1) cells are effector CD4+ T cells that are usually involved in protection against intracellular pathogens, including bacteria and viruses. Th1 cells can secrete a wide range of cytokines, such as interferon-γ (IFNγ) and interleukin-6 (IL-6), which can help to clear these pathogens. Conversely, T helper 2 (Th2) cells contribute more to immune responses against extracellular pathogens, including helminths and other parasites. They secrete different profiles of cytokines from Th1, which are known as type II immune responses, such as interleukin-4 (IL-4) (Murphy and Reiner, 2002).

The T helper 17 subset (Th17) shows a distinct cytokine profile and has been linked to different chronic inflammation and disease conditions, including multiple sclerosis (MS) and rheumatoid arthritis (RA). They are usually found within mucosal tissues and it is believed that they have a role in protecting mucosal tissue through the secretion of interleukin- 17 (IL-17), interleukin- 21 (IL-21) and interleukin- 22 (IL-22) (Crome et al., 2010). Finally, Tregs, which are different from other helper T cells in that, unlike Th1, Th2 and Th17, they have a different role, in regulating immune responses (Corthay, 2009).

1.2.3.2 CD8 T cells

Naïve CD8+ T cells can differentiate to cytotoxic CD8+ T lymphocytes that are capable of the direct killing of infected cells through their granzyme B and perforin, using a cell-to-cell contact mechanism such as Fas and Fas ligand that results in the apoptosis of the targeted cells (Andersen et al., 2006, Volpe et al., 2016). The activation of naïve CD8+ T cells results

in their proliferation and differentiation into effector cells, in order to control pathogens. After pathogen clearance, most cells die by apoptosis to contract the pool of cells except for a small proportion that develop into long-lived memory cells for future protection (Kaech et al., 2002).

Cytotoxic CD8+ T cells can also produce a high levels of pro-inflammatory cytokine, including tumour necrosis factor-α (TNFa) and interferon-γ (IFNγ), which can activate other immune cells and initiate pro-inflammatory immune responses (Falschlehner et al., 2009).

Another subset of CD8+ T cells has been shown to have a regulatory function, known as regulatory CD8 (CD8+ Treg). This subset express both forkhead box protein-3 (Foxp-3) and CD25, which are also used to characterise CD4+ Treg. CD4+ Treg have also been found within the tumour microenvironment and have suppressive capacity including within cancer patients (Chen et al., 2014).

CD8+ Treg are able to secrete suppressor cytokines, such as IL-10 and transforming growth factor β-1, and express high levels of CTLA-4 (Chen et al., 2014). Therefore, like CD4+ Tregs, CD8+ Tregs are able to provide immune tolerance and within the tumour microenvironment to supress immune responses.

1.2.3.3 Mucosal associated invariant T cells (MAIT cells).

Mucosal associated invariant T (MAIT) cells are an unconventional T cell population that are marked by their unique TCRα gene segment sequences: Vα7.2 and Jα33. Unlike conventional T cells, MAIT cells can interact with non-peptide antigens presented by the MHC-I like MR-1 molecule, especially vitamin B metabolites. They can be found in mice and humans and are enrichmed within mucosal tissues, hence their name (Godfrey et al., 2019). However, they can also be found in non-mucosal tissues where about 10% of the total

T cells within human blood can be MAIT cells and about 45% of the total liver T cells (Gherardin et al., 2018, Dusseaux et al., 2011).

MAIT cells have been shown to mature in the thymus, where DP (CD4+CD8+) cells in the thymus that interact with MR-1 expressed by other DP cells and are fated towards MAIT cells. During their development, they pass through different stages to reach fully matured MAIT cells that express CD27 and CD161 and exit to the periphery (Godfrey et al., 2019).

Based on the expression of CD4 and CD8, MAIT cells can be subdivided into further subsets: CD4-CD8-, CD4+CD8- and CD4-CD8+. CD4-CD8+ can further be divided into CD4-CD8αα+ and CD4-CD8αβ+ which constitute most of the MAIT cells within human blood (Gherardin et al., 2018). Functionally, all five subsets produce similar cytokine levels after activation, with slightly higher levels of cytokines produced by the CD8 expressing MAIT cells. However, CD4-CD8- are considered to be the most mature subset of MAIT cells (Dias et al., 2018). The ability of the cells to respond to a variety of pathogens, including bacteria, yeasts and viruses, has been shown in various studies, especially pathogens using the riboflavin-biosynthesis pathway (Godfrey et al., 2019).

1.2.3.4 Natural killer T cells (NKT cells)

Other unconventional T cells include NKT cells, which have been shown to develop in the thymus and are able to respond to lipid-based antigens. NKT cells can respond to lipids through the non-classical MHC-1 molecule (CD1d) that can be expressed on different APC, including DC, B cells, monocytes and macrophages. Two different subsets of NKT cells can be found in humans. Type I NKT cells or invariant NKT cells (iNKT), are known by their restricted TCR and the expression of Vα24. Type II NKT cells, which showed more diverse TCR and variable TCR-α chains, are more abundant in humans than iNKT (Pellicci et al., 2020). The iNKT cells showed the ability to respond to the lipid α-galactosylceramide

presented in CD1d, while type II NKT are capable of responding to different varieties of lipid antigens, but not α-galactosylceramide (Kumar and Delovitch, 2014).

In mice, iNKT show the ability to reside within different tissue and each showed the ability to regulate different immune functions, mimicking the different CD4+ T helper subsets; Th1-like iNKT, Th2-like iNKT and Th17-like iNKT (Brennan et al., 2013). The same scenario can be noticed for the type II NKT. However, two subsets can be noticed within type II NKT cells; Th1-like type II NKT and Th2-like type II NKT (Marrero et al., 2015).

Overall, NKT cells showed high similarities to natural killer cells (NK), both in morphology and phenotype (Krijgsman et al., 2018). To illustrate, iNKT cells showed the ability to express two known markers for NK cells: CD56 and CD161 (Eger et al., 2006). They show more of a memory phenotype and are able to express the co-stimulatory marker CD27 and the early activation marker CD69 (Chan et al., 2013, Kitayama et al., 2016). NKT cells represent another subset of unconventional T cells that are able to respond to lipidbased antigens and regulate the different functions of the immune system.

1.2.4 Memory T cells

One of the most important features of the adaptive immune system is the ability to generate immunological memory of an encountered antigen. This allows for the quick clearance of any re-encountered pathogens and leads to the development of vaccines through the formation of long-lived memory T (and B) cells (Jameson and Masopust, 2018).

The development of memory is believed to be another form of cell activation, whereby activated naïve T cells generate a pool of memory T cells. Attempts to define the mechanisms controlling this process can be summarised into two main categories.

First, the generation of memory T cells arises from the fact that, upon activation, naïve T cells proliferate and the two daughter cells divide into one long-lived memory T cell and one

effector T cell (Chang et al., 2014). Second, the generated memory T cells differentiate from activated T cells that have repeatedly proliferated post-activation (Jameson and Masopust, 2018). During the peak of T cell responses, two different types of cells can be distinguished based on the expression of different markers; known as terminal effector cells or short-lived effector cells and memory precursor cells. To illustrate, short-lived effector cells lack the expression the α-chain IL-7 receptor (CD127), where IL-7 is known to promote the survival of the T cells and the lack of the CD127 expression prevent the necessary survival signal by IL-7 (Joshi et al., 2007). On the other hand, CD127 expressing memory precursor cells showed the ability to persist longer than the short-lived effector cells and exhibit more memory related gene expression (Best et al., 2013).

In order to distinguish between circulating effector cells and memory cells, different markers have been investigated. Two of the CD45 isoforms, CD45RA and CD45RO, and the co-stimulatory molecule CD27 have been used to identify CD45RA-CD27+ circulating memory and CD45RA+CD27-CD62L- circulating effector cells (Hayward et al., 1989).

However, based on homing to tissues, memory T cells can be classified into three different categories; central memory (Tcm), effector memory (Tem) and effector memory CD45RA revertant (Temra) T cells. Unlike naïve T cells, memory T cells can access tissue. The various memory subsets show different trafficking and circulating routes. For example, EM T cells usually circulate between blood and tissues, while CM T cells circulate through lymphatic tissues (Jameson and Masopust, 2018). They can be distinguished through their cell surface expression of different molecules, which include CD45RA, CD45RO, CCR7 and adhesion molecule L-selectin. Naïve T cells express both CD45RA and CCR7, where CD45RA is an isoform of the cell surface tyrosine phosphatase CD45, while CCR7 is a chemokine receptor that allow T cells to home in on lymphatic organs. CM T cells express CCR7 but lack the expression of CD45RA (Earl and Baum, 2008). However, the EM expression of CCR7 is

very low as it circulates through blood routes and CCR7 influences lymphatic homing (Willinger et al., 2005, Mahnke et al., 2013). Finally, Temra are non-proliferative memory T cells, mainly within the CD8+ compartment, which are terminally differentiated and express CD45RA (Mahnke et al., 2013).

In terms of functional difference, CM T cells have been shown to have more proliferation capacity and higher interleukin-2 (IL-2) production in mouse studies. In addition, due to the localisation of CM T cells within lymph nodes, it is proposed that those cells are responsible for protecting against some chronic infections, such as that caused by the lymphocytic choriomeningitis virus (LMCV) (Wherry et al., 2003b). This was explained by their ability to proliferate and produce high level of IL-2 in response to antigenic stimulation. Equally, EM T cells can protect against other viral infections, because of their location and presence within the periphery. In fact, other studies proposed the EM to be the immediate responder cell to infection; due to their location, while CM provide sustained responses through their ability to proliferate in the secondary lymphoid organs (Hengel et al., 2003, Berenzon et al., 2003).

It has been shown that EM T cells are responsible for *Listeria monocytogenes* infection protection (Huster et al., 2006). However, new subsets of memory cells have been discovered recently, such as tissue resident memory T cells (Trm cells) and T memory stem cells (Tstm), which add further complexity to the memory phenotype **(Fig 1.2.4)**. First, Trm cells are not able to circulate and can provide tissue protection through the regulation of an inflamed tissue, the recruitment of other immune cells or the promotion of the effector functions of those cells (Danahy et al., 2017). They are defined as CXCR3+KLRG1-CCR7-CD62L-CX3CR1intermediate (Gerlach et al., 2016). They also express the tissue retention receptor CD69 and two integrins that can facilitate tissue entry; CD103 and CD49a (Mackay et al., 2013).

In comparison, Tstm cells are a population of memory cells that have been defined in mice and have a naïve-like phenotype. It was found that a proportion of cells in the CD45RA+CCR7+ compartment were expressing stem cell antigen, interlukin-2β receptor (IL-2Rβ) and CXCR3, which are known as memory markers. Researchers also showed the ability of these cells to give rise to all other memory subsets while maintaining their size within those mice (Zhang et al., 2005). In line with results from mouse studies, Tstm can be found in humans within the CD45RA+CCR7+ naïve-like phenotype; however, they are defined by the expression of CD95, CXCR3, CD58, CD11a and IL-2Rβ (Lugli et al., 2013). They can be found within circulating memory cells and in different tissues (Gattinoni et al., 2017). In humans, they showed stem cell-like properties through the ability to self-renew and differentiate to different subsets of other memory cells; including Tem and Tcm (Gattinoni et al., 2010).

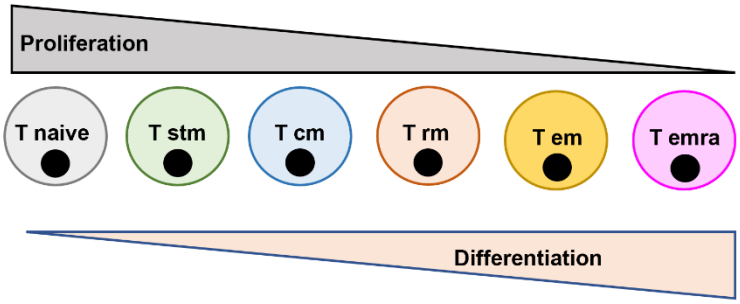

CD45RA	+	+	-	-	-	+
CD45RO	-	-	+	+	+	-
CCR7	+	+	+	-	-	-
CD27	+	+	+	+/-	+/-	-
CD95	-	+	+	+	+	+
CD69	-	-	-	+	-	-

Figure 1.2.4 T memory cells classification and phenotype**.**

Part of the activated naïve T cells develop memory T cells. According to the expression of CCR7,CD45RA, CD45RO, CD27, CD95 and CD69, resting T cells can be classified into different subsets; each with different tissue homing properties. T naive naïve T cells, Tstm; T memory stem cell, Tcm; T central memory, Trm; T resident memory, Tem; T effector memory, Ttf; T terminal effector or revertant effector memory T cells.

1.2.5 T-cell responses to cancer

Tumour-infiltrating T cells have been linked to better prognosis in different types of tumour (Fridman et al., 2012). This can be explained by the presence of tumour-specific T cells that are able to elicit direct responses to kill cancer cells, such as cytotoxic CD8+ T cells, and indirect immune responses to organise anti-tumour immune responses, such as CD4+ T cell responses.

The existence of different immunotherapies, either by the infusion of *in vitro* modified T cells, such as chimeric antigen receptor (CAR) T cells, or the use of blockade antibodies, such as checkpoint blockade therapies, can be used as evidence for the presence of tumour-specific T cells (Van der Leun et al., 2020). To illustrate, the blockade of CTLA-4 has shown promising results in different types of cancer, by preventing the inhibitory receptor effect and enhancing or inducing anti-tumour immune responses (Cha et al., 2014).

The blocking of PD-1 can enhance the responses of pre-existing tumour-specific T cells (Robert et al., 2014). Different attempts have been made to characterise and phenotype intratumoural T cells, particularly CD8+ T cells. Development in the field of single-cell analysis techniques, such as cytometry by time of flight (CyTOF) and single-cell RNA sequencing, has led to reports of being able to profile tumour-infiltrating CD8+ T cells. As a result, different heterogeneities of tumour-infiltrating CD8+ T cells have emerged within various types of tumour and between patients with the same tumour type (Van der Leun et al., 2020). To illustrate, in melanoma, three studies using independent cohorts have characterised different infiltrating subsets. The first study found naïve and cytotoxic CD8+ T cells infiltrates defined by the expression of different sets of genes including: CCR7 , transcription factor 7 (TCF7) and the L-selectin gene (SELL) for naïve cells; and perforin 1 (PRF1), granzyme A (GraA), granzyme B (GraB) and natural killer cell granule 7 (NKG7) (Tirosh et

al., 2016) for cytotoxic CD8+ T cells. The second study found a similar gene signature (Li et al., 2020a).

However, the third study found a similar signature but identified CD8+ T cells as memory-like, instead of naïve, due to the presence of different gene sets that are linked to the memory status (Sade-Feldman et al., 2019).In addition to the naïve and cytotoxic subsets that were found in the three studies, heterogeneous subsets were found in the three studies that were characterised as dysfunctional or exhausted cells due to the expression of inhibitory receptors, including PD-1, CTLA-4 and T-cell immunoglobulin mucin receptor-3 (TIM-3) (Li et al., 2020a, Sade-Feldman et al., 2019, Tirosh et al., 2016). Dysfunctional or exhausted cells have also been found in different types of cancer, such as non-small cell lung cancer and colorectal cancer (Guo et al., 2018, Zhang et al., 2018).

Regardless of nomenclature, and whether dysfunctional or exhausted, based on the level of inhibitory receptor expression, dysfunctionality can be classified into three different stages: pre-dysfunctional to early dysfunctional and then a late-dysfunctional state (Van der Leun et al., 2020). Pre-dysfunctional cells usually display low-to-intermediate inhibitory receptors in different types of cancer (Thommen et al., 2018, Fehlings et al., 2017, Chevrier et al., 2017, Wagner et al., 2019). Using two different approaches, TCR clonal sharing and an algorithm to detect transcriptional overlapping between the pre-dysfunctional and dysfunctional cells within a tumour, suggests a developmental relationship between these cells (Van der Leun et al., 2020). In non-small lung cancer, for example, the pre-dysfunctional subset displays inhibitory receptors levels that are lower than the dysfunctional subsets and using anti-PD-1 therapy restored the functions of PD-1 lower expressing CD8+ T cells (Thommen et al., 2015). Therefore, there is a possibility that the cells transit from low or intermediate inhibitory receptor expressing cells (pre-dysfunctional) to high inhibitory receptor expressing dysfunctional or exhausted cells.

Tumour-reactive cells have been found within dysfunctional CD8+ T cells (Gros et al., 2014, Inozume et al., 2010, Li et al., 2020a, Thommen et al., 2018). This can be explained by the finding that excessive antigen stimulation can drive T-cell dysfunction (Wherry et al., 2003a).

The presence of bystander T cells within the tumour microenvironment, which can be virus-specific cells, such as Epstein-Barr virus (EBV)-specific T cells, can add another challenge to detecting tumour-reactive T cells. Different candidates have been proposed as markers for tumour-specific T cells, such as CD39 and CD103 (Simoni et al., 2018b, Duhen et al., 2018). However, CD39-CD8+ T cells can also show tumour reactivity (Sade-Feldman et al., 2019). The problem of detecting tumour-specific CD8+ T cells has been reflected in chronic infections in mouse models, where excessive antigen stimulation results in the accumulation of CD8+ T cells with a dysfunctional phenotype (Wherry et al., 2003a).

It has also been shown that the infusion of tumour-specific CD8+ T cells in mouse tumour models resulted in the up-regulation of dysfunctional markers, such as PD-1, Lag-3 and CTLA-4 (Schietinger et al., 2016). Furthermore, in a human study of a melanoma cohort, a dysfunctional phenotype correlated with tumour-reactive T cells, but not a cytotoxic phenotype (Li et al., 2020a). Therefore, there is strong accumulating evidence that tumour-reactive T cells are enriched with dysfunctional (pre-dysfunctional, early and late-dysfunctional) CD8+ T cells within the tumour microenvironment. In terms of their functionality, the level of inhibitory receptors expressed by the tumour infiltrating CD8+ T cells correlates with their normal functions, where higher expression of the inhibitory receptors indicate impaired proliferation, insufficient cytokine secretion and eventually dysfunctional T cells

Although late-dysfunctional T cells lose the functions of classical cytotoxic CD8+ T cells, it has been found that late-dysfunctional CD8+ T cells are able to produce C-X-C chemokine ligand-13 (CXCL-13), which is a B-cell attractant chemokine (Li et al., 2020a, Thommen et al., 2018). This evidence was used to hypothesise the possible role of late-dysfunctional cells in organising the formation of tertiary lymphoid structures within the tumour microenvironment (Van der Leun et al., 2020). To summarise, tumour environment CD8+ T cells show a mixture of cells with naïve-like, cytotoxic and dysfunctional characteristics. This mixture contains bystander and tumour-reactive T cells, and greater numbers of dysfunctional T cells that are developed by extensive antigenic stimulation.

1.2.6 Checkpoint blockade immunotherapy

Co-inhibitory signals are used to control activated T cells and prevent unnecessary damage. Two important molecules have been investigated and used for approved immunotherapeutic blockade antibodies; CTLA-4 and PD-1 (Buchbinder and Desai, 2016). For CTLA-4, the main mechanism of action is during the activation phase of T cells. As discussed above, T cell activation require a co-stimulation signal to be fully functionally activated and to prevent entering an anergic state. One of these co-stimulation signals is the engagement of CD28 from the T cells with CD80 or CD86 on the APC that results in T cell proliferation, differentiation and the release of IL-2 (Chambers et al., 2001). During the resting state, CTLA-4 is stored intracellularly and the activation of the T cells results in the exocytosis of the CTLA-4 and the upregulation of cell surface CTLA-4 (Linsley et al., 1996). CTLA-4 has higher affinity toward CD80 and CD86 than CD28 and thus competes with CD28 for CD80 or CD86 binding and prevent the co-stimulatory signal (Chambers et al., 2001).

The binding of CTLA-4 with CD80 or CD86 on the APC results in a non-functional anergic T cell via inhibition of the CD28 signal, increasing mobility of the T cell and prevention of proper TCR-MHC presentation or direct inhibition of the TCR immune synapse (Schneider et

al., 2006, Masteller et al., 2000). On the other hand, PD-1 acts in the effector phase of the T cell activation where the ligation of PD-1 on activated T cells with PD-L1 or PD-L2 on the antigen presenting cell decreases T cell survival, reducing IFN-γ, TNF-α and IL-2 production and inhibiting cell proliferation (Keir et al., 2008).

Unlike CTLA-4, where CD80 and CD86 are expressed by experienced APC that can be found within lymph nodes, PDL-1 and PDL-2 can be expressed on a variety of cells including leukocytes, non-hematopoietic cells and cancer cells and thus PD-1 co-inhibitory signals can be induced in different types of peripheral tissues (Fife and Bluestone, 2008, Parry et al., 2005, Chen et al., 2012, Latchman et al., 2004).

The ligation of PD-1 with either PDL-1 or PDL-2 can prevent the TCR signalling through the inhibition of the phosphorylation of TCR signalling intermediates and eventually prevent T cell activation (Parry et al., 2005, Bennett et al., 2003). In fact, PD-1 can be expressed by the activated T cells to serve as a control checkpoint to prevent un-necessary prolonged activation and prevent tissue destruction (Murphy and Weaver, 2016).

However, the high PD-1 expression can result from over stimulation in situations such as chronic infections and cancer to form exhausted dysfunctional T cells that are unable to control pathogens, and where repeated activation of the T cell can result in the expression of more PD-1 by those cells (Wherry, 2011). However, the presence of such molecules led to the development of blocking antibodies to boost activation and recover the exhausted T cells that can be specific for cancer cells, where tumour-specific T cells have been shown to be more within the exhausted T cells population (Gros et al., 2014). A number of different blocking antibodies have been approved for melanoma, lung cancer, breast cancer, gastric cancer and other cancers.

Blocking antibodies can be used as monotherapy to block either CTLA-4 using ipilimumab or PD-1 using nivolumab, pembrolizumab or cemiplimab, which binds with the cell surface receptor CTLA-4 or PD-1 accordingly and prevents their interaction with the counterpart natural ligand on the other cell **(Fig 1.2.6)** (Rotte, 2019). Monotherapy blocking antibodies showed promising results through the increase of survival rates in responding patients (Rotte et al., 2018). However, combined therapy using two antibodies to block CTLA-4 and PD-1 showed better results, especially, with the response rate and disease progression (Khair et al., 2019).

Monoclonal antibodies (mAB) to block either PD-1 or CTLA-4 or both might increase the possibility of developing autoimmune disease. In normal physiological reactions, PD-1 and CTLA-4 are co-inhibitory molecules that maintain tolerance and prevent the development of autoimmunity. Autoimmunity develops from the break of the tolerance mechanisms that can result in the activation and infiltration of different self-antigen reactive T cells to the targeted tissues. Anti-PD-1 and/or anti-CTLA-4 can result in adverse effects; known as immune-related adverse effects (Elia et al., 2020). Several experiments indicate the essential roles of CTLA-4 and PD-1 in preventing autoimmunity, where the deletion of PD-1 and CTLA-4 can results in several autoimmune diseases (Klocke et al., 2016, Tivol et al., 1995). The same can be noticed in some of the patients receiving the immune checkpoint blockade therapies. Whether anti-PD-1 can induce more of these effects than anti-CTLA-4 or the other way around is not fully understood yet (Elia et al., 2020). However, the immune-relate adverse effects can range from diarrhoea, skin reactions, purities and thyroid disorders (Boutros et al., 2016). Therefore, although promising results can be found in patients receiving the therapy, some immune-related adverse effects have been found as well.

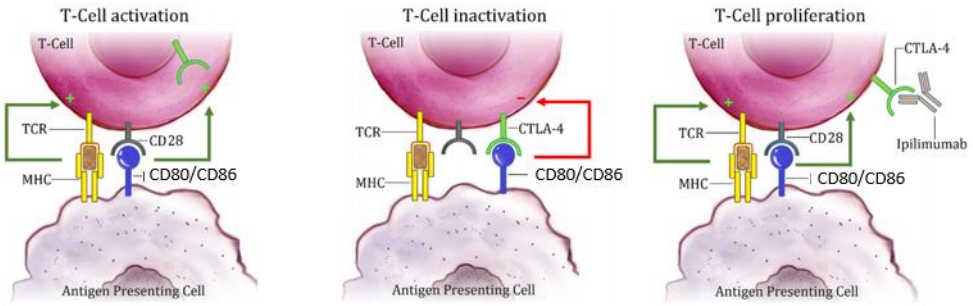

Fig. 1. Ipilimumab mechanism of action showing interaction with CTLA-4 receptor.

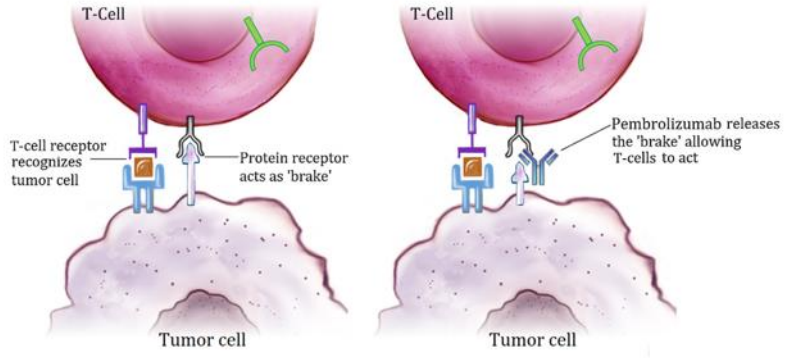

Fig. 2. Pembrolizumab interaction with PD-1 allowing T-cell to function by releasing a brake on the immune system.

Figure 0.2.6 Ipilimumab and pembrolizumab mechanism of action.

Adapted from (Wahid et al., 2017). Upon T cell activation, CTLA-4 can relocalize and transfer to the cell surface to compete with CD28 on binding to CD80 or CD86 and induce inhibitory signal. Ipilimumab binds with CTLA-4 and prevent CTLA-4 ligation with CD80/CD86 on the APC **(Fig1)**. While, Pembrolizumab binds with PD-1 on the activated T cells to prevent their interaction with PDL-1 or PDL-2 and eventually prevent the co-inhibitory signal induced by PD-1 and PDL-1 or PDL-2 ligation **(Fig2)**.TCR; T cell receptor.

1.3 CD3+ CD20+ T cells

1.3.1 Introduction to CD20

CD20 is one of the four cell receptors belonging to the membrane-spanning 4-domains subfamily A (MS4A) (Liang et al., 2001, Tedder and Engel, 1994). CD20 has been used for decades as an exclusive marker for B cells, and 95% of B cells express CD20 (Klein et al., 2013). CD20 can be expressed from the pre-B cell stage and loses expression towards the plasmablast stage; however, memory B cells still express CD20 (Schuh et al., 2016, Yokose et al., 2001).

The MS4A gene family includes up to 18 different proteins including MS4A1 encoding CD20. Due to their close chromosomal location (11q12 in human), they showed similar structures and polypeptide sequence (Eon Kuek et al., 2016). The structure of CD20 consists of three parts: cytoplasmic carboxyl-1 and amino-termini ends with an approximately 44 amino acid extracellular loop that span the membrane four times (small and large loops) to form a tetraspanin protein (Polyak et al., 1998) **(Fig. 1.3.1)**. During the activation of a human B cell line, CD20 has been shown to co-localise with CD40, MHCII and B cell receptors and play a vital role in B cell development (Petrie and Deans, 2002, Léveillé et al., 1999).

Different results have been shown regarding the targeting of CD20 using therapeutic mABs. However, no solid conclusion about the function of CD20 can be determined and this is possibly because of the different clones of mABs against CD20 that were developed. To illustrate, two different mABs can result in different effects. For example, rituximab (RTX) and LT20 are two type I mABs against CD20 but, unlike LT20, RTX can enhance adhesion of B cells. Besides, B1 and IF5 have the same isotype, but they have different antibody types and unlike IF5, B1 can induce apoptosis(Cragg et al., 2005).

The 16 anti-CD20 mABs have been classified into two subgroups based on two different schemes. In one study they were subgrouped into four different groups based on their ability to bind the extracellular loop of CD20 on two residues: alanine at position 170 and proline at position 172 (Polyak and Deans, 2002). Another attempt classified mABs into two groups based on their functional effect, whereby type I can translocate CD20 and result in antibody-dependent cellular cytotoxicity, and type II can result in homotypic aggregation and apoptosis (Cragg, 2002, Cragg et al., 2003, Cragg and Glennie, 2004). Therefore, various effects can be obtained using different mABs against CD20 and the true function of CD20 is still a matter of controversy.

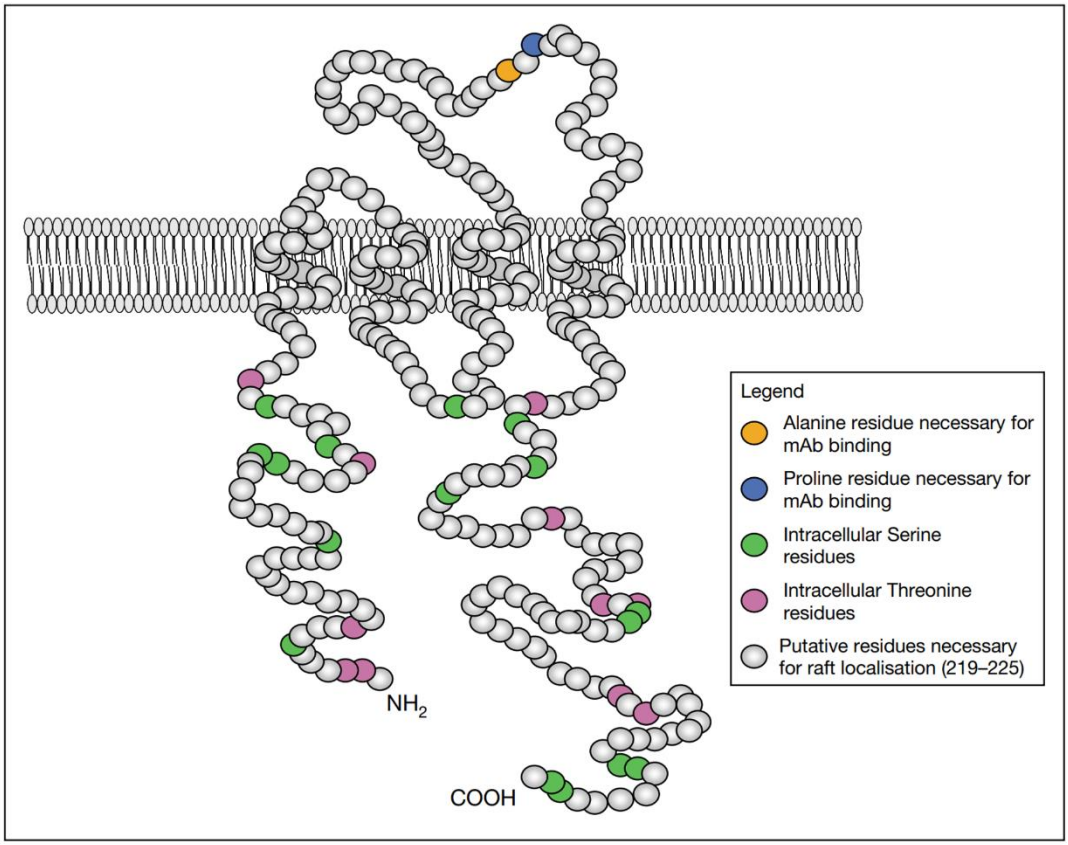

Figure 1.3.1 Structure of cell surface CD20.

Adapted from (Cragg et al., 2005). Intracellularly, one large loop ends with a C-terminus and a small loop ends with the N-terminus that contains serine and threonine which form the potential phosphorylation sites. The two loops extend and span the membrane 4 times to form one extracellular large loop that contains alanine and proline motifs that are necessary for anti-CD20 antibodies to bind, and a smaller extracellular loop.

1.3.2 Functions of CD20

To date, the natural ligand for CD20, if any, and the functions of CD20 are still controversial. Although CD20 knockout mice have been developed by homozygous mutation in the *MS4A1* gene, the mice showed normal features and functions of B cells; B cell development, maturation, differentiation, tissue homing and isotype switching (Uchida et al., 2004). However, immunizing CD20 knock out mice with T-dependent antigens resulted in reduced number of germinal centre B cells (Morsy et al., 2013). In humans, a study involving a juvenile patient with an extremely rare homozygous mutation in the CD20 gene resulting in the complete deletion of CD20 from B cells, found a normal B-cell count with a reduction in memory B cells, and normal B-cell responses to vaccination, except for T-independent antigen B-cell responses (Kuijpers et al., 2010). Therefore, mild effects can be noticed as a result of CD20 loss in both humans and mice.

In humans, different attempts to explore the function of CD20 rely on the mAB against CD20 in human B cells and B-cell lines. The targeting of CD20 by mAB, using human B cells and B cell line, can result in different scenarios for the targeted cells; for example, this can cause death in some depletion experiments or enhance survival, activation, proliferation and adhesion (Holder et al., 1995, Smeland et al., 1987, Clark and Shu, 1987, Kansas and Tedder, 1991, Tedder et al., 1986). It has been shown that targeting CD20 can, in some cases, result in the up-regulation of CD18, CD95, MHCII and CD58 (Clark and Shu, 1987, Holder et al., 1995, Kansas and Tedder, 1991, Smeland et al., 1987). It has been reported from *in vitro* studies that CD20 may have a role in B-cell activation, differentiation and proliferation (Tedder et al., 1985, Kuijpers et al., 2010). A recent study using Ramos B cell lines and human B cells, showed that CD20 maintains the B cell resting state. The deletion of CD20 from those cells resulted in transient activation of B cells (Kläsener et al., 2021).

CD20 has been reported as a calcium ion (Ca2+) channel that regulates the transport of calcium across a membrane (Kuijpers et al., 2010). This was supported by experiments where the transfection of CD20 in CD20- negative cells and 3T3 fibroblast cells resulted in an increase of cytosolic Ca2+ concentration (Kanzaki et al., 1995). Furthermore, stimulating B cells from CD20 knockout mice resulted in reduced Ca2+ flux (Uchida et al., 2004). Therefore, there is strong evidence supporting the possible role of CD20 in regulating calcium flux.

Patients undergoing treatment with anti-CD20 therapies have shown impairment of calcium intake and results demonstrate an effect on the normal functionality of B-cell receptors (Bubien et al., 1993, Kanzaki et al., 1997). *In vitro* studies from CD20 knockout mice showed normal development and activation of B cells, except for B-cell receptor function and calcium responses in the spleen (Uchida et al., 2004).

However, due to a lack of knowledge of the CD20 natural ligand and the reliance on mAB to study CD20 function, whereby each can induce different effects, the definite biological function of CD20 is still controversial. Most studies have reported a possible role of CD20 in regulating calcium flux, either as a calcium ion channel or within different cascades of actions.

1.3.3 Anti-CD20 therapies

Anti-CD20 depletion therapy has shown promising results and has been used against various diseases, such as multiple sclerosis (MS), rheumatoid arthritis (RA), lymphoma and idiopathic thrombocytopenic purpura (ITP), and as effective immunosuppressive therapy for renal transplantation patients (Hainsworth et al., 2000, Arnold et al., 2007, Edwards et al., 2004, Vo et al., 2008). Three different antibodies have been used as anti-CD20 antibodies: RTX, ocrelizumab and ofatumumab (Wilk et al., 2009).

The goal of this type of therapy is to deplete B cells and attenuate pathogenic antibody production through; antibody-dependent cellular cytotoxicity, complement-dependent cytotoxicity, antibody-dependent cellular phagocytosis and induction of apoptosis (Margoni et al., 2021).

Interestingly, in one MS study, RTX resulted in approximately 90% depletion of B cells from the cerebrospinal fluid (CSF) of those patients, in addition to an approximately 55% reduction in CSF T cells (Cross et al., 2006). The same results can be seen in patients with RA, where the detectable CD3+ CD20+ T cells were completely depleted after the administration of RTX (Wilk et al., 2009). This can indicate the possible existence of CD20+ T cells, which is discussed in more detail in the next section.

1.3.4 Origin of CD3+CD20+ T cells

The presence of CD20+ T cells was first reported in 1990 in the blood of a small patient group with HIV, and proposed as an artefact of flow cytometry (Landay et al., 1990). Later, another study showed the presence of CD20+ T cells within peripheral blood mononuclear cells (PBMCs) isolated from healthy donors. The researchers used three different clones (Leu16, B1 and IF5) to show that the binding of CD20 to a small population of CD3+ T cells was specific and not non-specific binding of the Fc receptor. Further to these studies, CD20+ T cells have been found within human thymus, bone marrow, lymph node, CSF, brain and liver tissue (Schuh et al., 2016, Wilk et al., 2009, Holley et al., 2014). Although mouse studies have not found CD20+ T cells, they have shown the presence of MS5aB1+ T cells, which has been proposed as a CD20 homology molecule (Xu et al., 2006, Yan et al., 2013). Different reports conflict with regard to the origin and development of these cells, whereby cord blood of newborn children has been scanned for the presence of CD20+ CD3+ T cells and researchers could not detect them.

Co-culturing PBMCs or purified T cells with a B cell line or primary HLA-mismatched B cells resulted in an increase in the number of CD3+ CD20+ T cells (de Bruyn et al., 2015). This was explained by a process called trogocytosis, in which a marker from one cell can be transferred to another cell as an intact protein of a protein complex, as HLA-DR transference during antigen presentation (Storie et al., 1995).

However, another paper investigated the features of CD3+ CD20+ T cells in MS and found that sorted CD3+ CD20+ T cells from healthy blood volunteers could transcribe CD20 and CD3 but not CD19 (Schuh et al., 2016). The sorted cells did not express Human leukocyte antigen – DR isotype (HLA-DR), which had been used by de Bruyn et al. (2015) to confirm that CD20 had been acquired by CD3+ CD20+ T cells via trogocytosis. Besides, previous work by our lab showed that the CD20 mRNA expression was detected in the CD3+CD20+ T cells and CD19+ B cells, but not in the CD3+CD20- T cells. While CD3 mRNA expression can be detected in both CD20+/CD20- T cells, but not CD19+ B cells (Rathbone, 2018). Furthermore, activating purified CD3+CD20+ T cells *in vitro* using mitogen and IL-2 resulted in the clonal expansion of CD3+ CD20+ T cells and did not require trogocytosis for the daughter cells to divide (Murayama et al., 1996). In addition, leukaemic CD20+ T cells have been found to proliferate clonally and were located in the spleen of a 65-year-old patient with T-cell chronic lymphocytic leukaemia (Takami et al., 1998). Collectively, the origin of CD3+ CD20+ T cells is still a matter of debate, but two explanations have been proposed: first, CD20 is transferred or trogocytosed from B cells during their interaction with T cells; and second, the existence of CD3+ CD20+ T cells in a lineage that has inherited the expression of CD20 **(Fig. 1.3.3)**. Therefore, one aim of this PhD is to investigate the possible origin of the CD20+ T cells.

1.3.5 Features and phenotype of CD3+ CD20+ T cells

CD3+CD20+ T cells show higher expression of CD8+ (about 57%) and CD45RO (about 82%) and γδ TCRs (about 14%), with of CD4+ (about 35%) and CD38+ (about 5%) (Hultin et al., 1993). Furthermore, another report showed, by comparing CD3+CD20- T cells to the CD3+CD20+ T cells, significantly higher expression of CD8 and CD45RO and significantly lower expression of CCR7, CD4 and CD38. They also showed greater expression of memory features compared with the naïve population through their higher expression of CD45RO and lower expression of CCR7. Upon activation, they were able to produce more IFN-γ, TNF-α and IL-17 than CD3+ CD20- T cells (Schuh et al., 2016). A recently published thesis by a previous colleague in our laboratory showed that CD3+CD20+ T cells from healthy volunteered blood had more CD8+ than CD4+ with predominantly memory T cells, based on the expression of CCR7 and CD45RA.

The ability of CD3+CD20+ T cells to have potent pro-inflammatory immune responses was noticed by comparing IFN-γ production. By comparing the production of IFN-γ following stimulation with PMA and ionomycin, the CD20+ subpopulation of T cells produced higher IFN-γ than the CD20-, in both the blood and CSF of MS patients. Furthermore, the potential cytotoxic effect of CD3+CD8+CD20+ T cells was noticed via their expression of perforin and granzyme and their enhanced degranulation following stimulation compared with CD3+CD8+CD20- T cells (Rathbone, 2018). No conclusive marker was found for the CD20+ T cells, just the differences in the memory/naïve and CD8/CD4 ratios compared to the CD20- T cells. Therefore, another aim of this thesis is to investigate the possible presence of other T cells subsets and unique markers to the CD20+ T cells.

1.3.6 CD3+CD20+ T cells in autoimmune diseases

CD3+CD20+ T cells can be found within RA and MS patients. CD3+CD20+ T cells have been found in the PBMCs and CSF of MS patients (Yan et al., 2013). RTX has been used to treat those patients due to the role of B cells within the central nervous system in the pathogenesis of the disease. A significant reduction in the total number of CSF T cells has been noticed within patients receiving RTX (Cross et al., 2006). This observation was used to speculate the presence of CD3+CD20+ T cells in the CSF of those patients and led to the finding of CD3+CD20+ T cells in the CSF of MS patients (Yan et al., 2013).

CD3+CD20+ T cells in MS patients produce IFN-γ and IL-17, which are known modulators that contribute to the pathogenesis of MS. Therefore, CD3+CD20+ T cells are considered to be pathogenic cells in MS patients and one of the effective results of RTX can be driven by the depletion of CD3+ CD20+ T cells (Holley et al., 2014, Schuh et al., 2016). CD3+CD20+ T cells have been found within the peripheral blood of RA patients. Those cells were found in a high activation state, in which they were able to produce IL-1β and TNF-α. They also showed lower proliferative capacity with a greater tendency towards apoptosis. Interestingly, the usage of RTX therapy for those patients resulted in the depletion of both B cells and CD3+ CD20+ T cells.

The ability of CD3+CD20+ T cells to produce IL-17, which was present in higher levels in RA patients' blood than in healthy controls, categorised CD20+ T cells as being among the pathogenic cells for RA (Wilk et al., 2009). Overall, CD3+CD20+ T cells have been linked to the pathogenesis of both RA and MS through their ability to produce IL-7 and pro-inflammatory cytokines, such as IFN- γ and TNF-α.

1.3.7 CD3+ CD20+ T cells and cancer

In contrast with autoimmune diseases for which CD3+CD20+ T cells are considered as a pathogenic subset, their ability to induce potent pro-inflammatory immune responses may be of benefit in the context of cancer, despite their presence in lymphomas and leukaemia and the variable outcomes from using RTX for those patients. A single report in the literature has tried to address the role of CD3+CD20+ T cells within ovarian cancer patients.

The report showed higher percentages of CD3+CD20+ T cells in ascitic fluid when comparing ascitic fluid from healthy donors and ovarian cancer patients. The CD20+ T cells biased toward Th1 immune responses through their ability to secrete more T cell one cytokines (TC-1) (De Bruyn et al., 2015).

However, the ability of these cells to elicit an anti-tumour immune response through the production of cytotoxic granules or their relation to the disease stage or prognosis was not addressed in the report. The ability of the CD20+ T cells to elicit a cytotoxic immune response has been reported, as discussed in the previous section. In addition, the ability of these cells to constitute a higher percentage of specific responded subsets to two EBV tetramers of the lytic cycle could indicate the importance of investigating these cells in the cancer environment (Rathbone, 2018).

As has been documented in the literature, viral infections have been proposed as the real cause of 10-15% of cancers. EBV is one of the oncogenic viruses and the infection can be asymptomatic in 90% of the 14% of the healthy population that has EBV viremia (Song et al., 2019). It has been shown to infect more than 90% of all humans and is associated with epithelial, lymphocyte and smooth muscle derived tumours (Shannon-Lowe and Rickinson, 2019, Vickers, 2017). The EBV infection can occur in children and adults and usually transmit through saliva to reach eventually lymph nodes and infect B cells (Ravi et al., 2000,

Tugizov et al., 2013). The EBV life cycle involves the expression of six nuclear antigens and two membrane proteins; known as lytic antigens. As previously shown, CD20+ T cells showed higher response to two of the EBV lytic antigens (Rathbone, 2018).

To summarise, CD3+CD20+ T cells are a subset of T cells with more CD8+ memory phenotype. They can exist in different sites of the body and have been reported as potent active pathogenic cells in autoimmunity diseases and higher IFN-γ producers in ovarian cancer. The real function of CD20 has not yet been identified, although some reports have suggested that the receptor' controls calcium trafficking through the cell membrane. The role of these cells within cancer patients has not been explored in different types of cancer **(Fig 1.3.7)**.

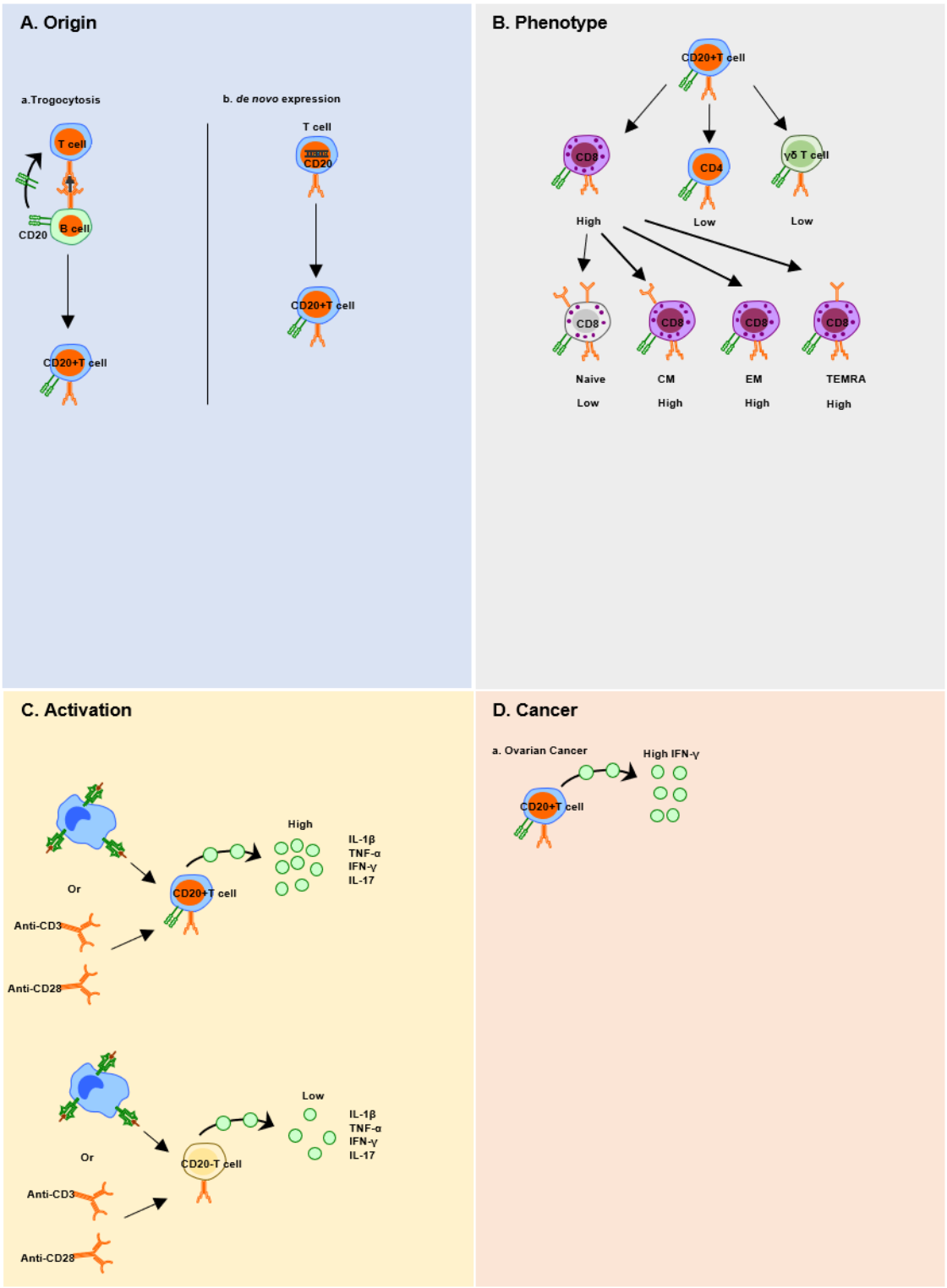

Figure 1.3.7 Summary of the previous findings about CD20+ T cells.

The possible explanations of the presence of CD20+ T cells **(A).** Reported findings about CD20+ T cells phenotype **(B)**. Cytokines produced upon activation (**C).** The reported functions of CD20+ T cells in cancer **(D).**

1.4 Aims

We hypothesise that CD3+CD20+ T cells can be found within the tumour microenvironment, healthy individuals and different tissues of the body. These cells show a cytotoxic ability and specificity to mount anti-tumour immune responses and express several inhibitory receptors, which may affect their ability to maintain an effective anti-tumour immune response. The aims of the research are as follows:

1- To investigate the frequency and the presence of CD3+CD20+ T cells within healthy individuals.

2- To determine the clonal relationship between CD3+CD20+ and CD3+CD20- T cells.

3- To investigate the antigen specificity of CD3+CD20+ T cells towards oncogenic viruses.

4- To investigate the phenotype of CD20+ T cells within healthy individuals.

5- To investigate the phenotype of CD20+ T cells within cancer patients.

6- To determine the possible relation of the CD3+CD20+ T cells to the response to checkpoint blockade therapy.

Chapter Two: Methods

2. Methods

2.1. Digestion of tumour tissues

All tumour tissues were obtained from the Human Biomaterial Resource Centre (HBRCs) under the application number 18-321 (colon cancer n= 3 and breast cancer n=1). Upon arrival of the tissue, the tissues were transferred to a Petri dish adding 1ml of phosphate-buffer saline (PBS). The tissues were minced into small pieces, about $1cm^3$, and transferred using a pasteur pipette into 15 ml conical tubes. Then, 60 µl of Liberase DL (13U/ml) and Liberase TL (13U/ml) from ROCHE and 6µl of DNASE I (100mg/ml) were added to the same tube. The tube was incubated in the auto-shaker for 45 minutes at 37℃. After 45 minutes, the tube was vortexed for 15 seconds and cells were filtered using a 70µM cell strainer. The digested cells were used for further analysis.

2.2. Isolation of PBMCs from healthy blood and matched blood

Human blood from healthy volunteers and matched blood from cancer patients were collected from healthy donors in anti-coagulated Ethylenediaminetetraacetic acid (EDTA) plastic tubes under the ethics number ERN_18-0746 and under HBRCs application number 18-321. The Ficoll-Paque density gradient method was used to obtain separate layers of plasma, PBMCs and red blood cells with granulocytes, as per the manufacturer's instructions (GE Healthcare). Briefly, the blood was collected and diluted 1:1 with PBS. Then, 25ml of the diluted blood was transferred into another 50ml tube containing 15ml of Ficoll-Paque solution (GE Healthcare), where the blood was gently layered on the Ficoll-Paque solution, avoiding any mixing. The tubes were then centrifuged for 45 minutes with no brake at 400g and at normal lab temperature. After the centrifugation, the PBMCs were aspirated into another 50ml Falcon tube and diluted 1:2 using PBS, to dilute any of the Ficoll-Paque solution that aspirated with the PBMCs. The tubes were then centrifuged for 20 minutes at 300g and 4ºC. PBMCs were kept on ice until analysis.

2.3 Flow cytometry

All cells to be analysed by flow cytometry were stained in 96 well plates, incubating them with the following antibodies for 30 minutes **(Table 2.3.1)**, diluted at a pre-determined titration in fluorescence-activated cell sorting (FACS) buffer (PBS with 2% (v/v) FBS, 0.02% (w/v) sodium azide and 2 mM EDTA).

The stained cells for flow cytometry analysis were centrifuged at 300*g* for 4 minutes, supernatant was removed and the cell pellet resuspended in 100µl of FACS buffer. The cells were filtered through a 100µm nylon mesh and transferred to FACS tubes with 300µl of FACS buffer. Stained cells were used for either analysis using BD LSRFortessa X-20 flow cytometer or sorting using BD FACSAria fusion, and the results were analysed using FlowJo software v10.5.

Table 2.3 Flow cytometer antibodies used.

Specificity	Flourochrome	Company	Cat. No	Clone	Dilution
CD3	BV510	BioLegend	314526	OKT3	1/100
CD8a	APC	eBioscience	17-0087	SK1	1/1000
CD20	PE	Biolegend	302306	2H7	1/20
CD19	Bv605	BioLegend	302244	HIB19	1/320
CD45RA	PE-Texas Red	BD Biosciences	562298	HI100	1/800
CCR7	Alexa Fluor 488	BioLegend	353206	G043H7	1/20
CD39	PE/Cy7	BioLegend	328212	A1	1/100
Mouse IgG2bκ	PE	BioLegend	400314	MPC-11	1/20

2.4 CD8+ enrichment

Using isolated PBMCs, CD8+ T cells were isolated by negative isolation using MACS column technology (CD8+ T cell isolation kit;130-096-495). Isolated PBMCs were centrifuged at 400*g* for 5 minutes and re-suspended in 40µl MACS buffer (PBS, 0.5% w/v bovine serum albumin (BSA), 2 mM EDTA and pH 7.2) per 10^7 total cells at 2-8°C. Next, 10µl of biotin-antibody cocktail was added per 10^7 total cells and incubated for 5 minutes at 2-8°C, then, 30µl of MACS buffer per 10^7 cells wasadded.

20µl of a CD8+ T cell microbeads cocktail per 10^7 cells was added and cells were incubated for 10 minutes at 2-8°C. Next, unlabelled CD8+ T cells were collected by transferring the stained PBMCs suspension to the column washed through by adding 3X 3ml of MACS buffer.

2.5 TCRβ sequencing

After many attempts to sort adequate numbers of CD20+ T cells, 10000 or more cells were sorted from three different donors in addition to CD20- T cells. Due to the lower percent of CD20+ T cells within the blood of healthy donors, 12 different attempts were required to generate enough cells from three different donors. Cells were sorted in 300µl of RNAprotect cell reagent (Qiagen, cat No; 76526) and frozen at -20°C. Frozen vials were sent to I-repertoire for RNA extraction and CDR3β TCR sequencing using Illumina MiSeq technology and v2 500-cycle kit **(Fig 2.5.1)**. The data obtained from the company were row data, including shared and un-shared amino acid sequences and their frequency from each cell subset within each donor. I-repertoire provided an analysis portal tool that provide different analysis tools, including V-gene usage heatmap and tree map from the amino acid sequence frequencies **(Fig 2.5.2)**.

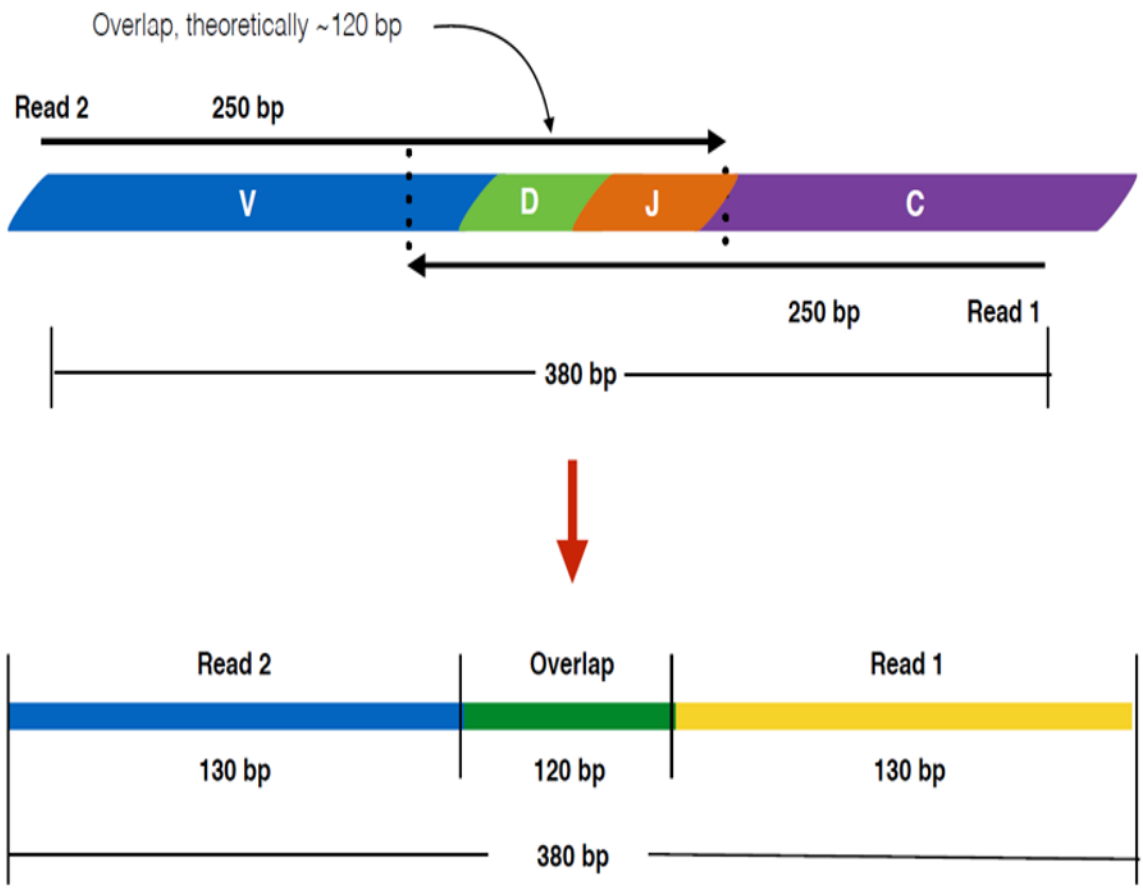

Figure 2.5.1 Read stitching and CDR3β sequences identification.

Using paired-end read and V-C primers, read one starts from the C gene segment and moves towards the V-gene segment; whereases, read two starts from the V gene segment and moves towards the C gene segment. The software demultiplex the data based on the molecular barcode used, read one and read two stitches and the read stitching breakdown for the human long-read primers.

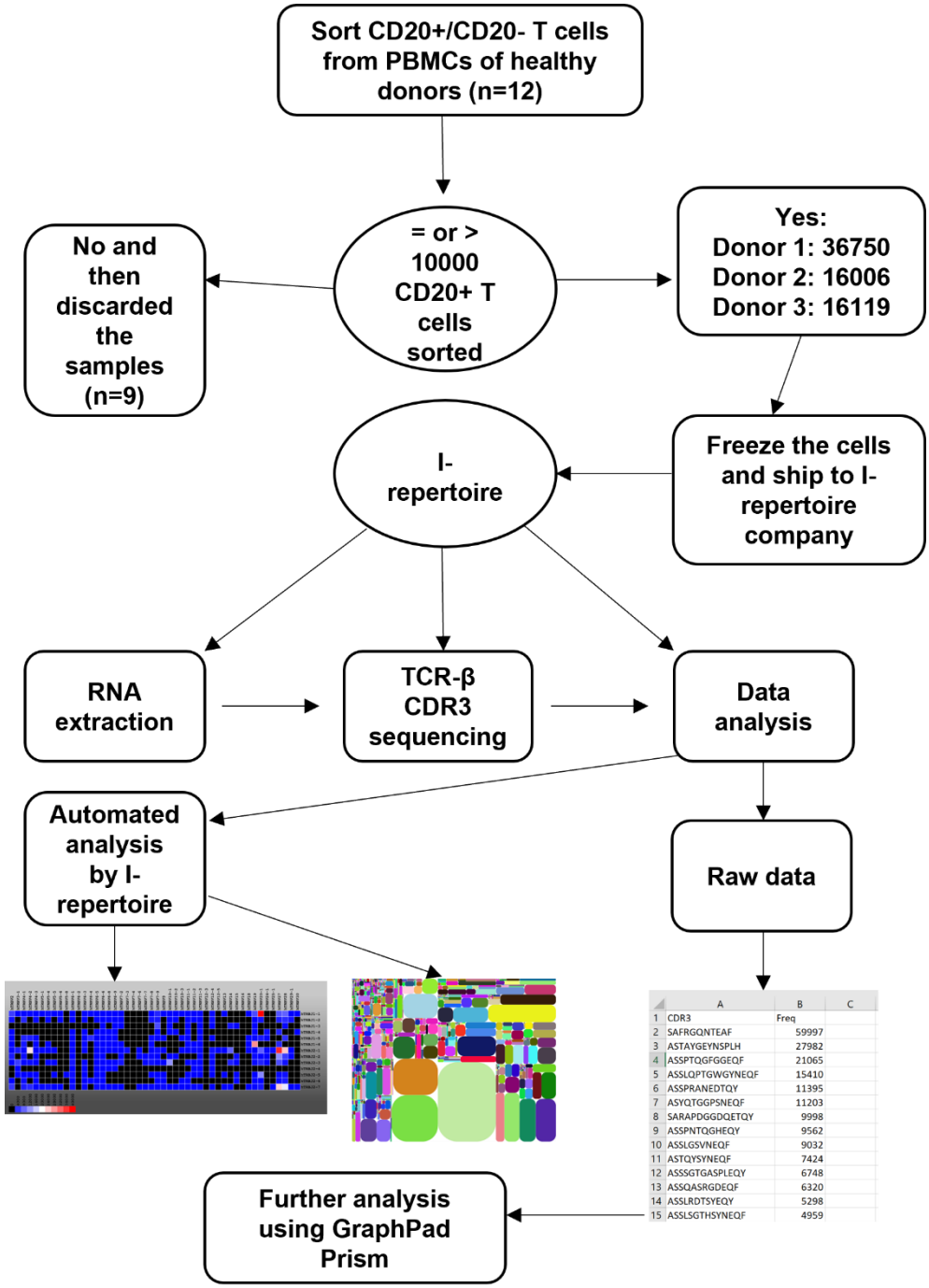

Figure 2.5.2 The T cell receptor sequencing analysis flow chart.

A flow chart to show the pre-process of the generated TCR-sequencing data, starting by the criteria of sorting CD20+ T cells. The successful sorted cells were sent to I-repertoire for TCR-β CDR3 sequencing. The sequence data were provided as row data and automated analysis by I-repertoire.

2.6 Tetramer staining

Using APC-labelled tetramers towards two EBV lytic cycle peptides; YVL (Amino acid sequence: YVLDHLIVV) and GLC (Amino acid sequence: GLCTLVAML), PBMC isolated from HLA-A*02-positive healthy donors were used for the staining (Moosmann et al., 2010). Isolated PBMCs were counted and $1-2\times10^{6}$ cells were re-suspended in 50µl FACS buffer and 1µl from each tetramer were used. Cells were incubated for 30 minutes at 37°C. Next, 100µl of FACS buffer was added and cells centrifuged at 400*g* for 5 minutes prior to flow cytometry staining as described before **(section 2.3)**.

2.7 Datasets

Due to COVID-19 pandemic and locked accesses to the laboratories, we used different online datasets from previously published papers and uploaded experiments. All the studies were selected according to the presence of an anti-CD20 antibody within the panel, the presence of mass cytometry data and the relevance of the experiment to cancer. Three different studies were uploaded from a FlowRepository website (https://flowrepository.org) out of four total selected experiments, where one was excluded due to the quality of the staining **(Fig 2.7.1)**. The first data were PBMCs isolated from 10 healthy donors (Toghi Eshghi et al., 2019). The second were from colorectal cancer (CRC) patients; which includes samples from tumour tissue, normal adjacent tissue, lymph nodes and matched blood from the same patient (de Vries et al., 2020) Finally, the third dataset was PBMCs isolated from melanoma patients received anti-PD-1 or CTLA-4 inhibitor therapies that were *in-vitro* stimulated using anti-CD3 and anti-CD28 and compared to un-stimulated cells (Spidlen et al., 2012) **(Table 2.7.1)**.

2.7.1 Mass cytometry dataset from healthy donors

Previously published datasets used PBMCs isolated from 10 healthy donors and stained with mass-conjugated monoclonal antibodies, both commercially available conjugated antibodies,

and in-house conjugated antibodies using Multi-Metal Maxpar Kits **(Table 2.7.1.1)** (Toghi Eshghi et al., 2019). The data were provided as live-single-CD45+ cells.

2.7.2 Mass cytometry data from colorectal cancer patients (CRC)

Datasets from CRC patients included; tumour tissue (n=35), matched tumour-associated lymph nodes (n=26), healthy mucosal tissue (n=17) and matched blood obtained before surgery (n=19) that was obtained from 31 patients in total, where five samples were obtained from the same patient. The mass cytometry staining method and tissue processing were described in the published study (de Vries et al., 2020). The patients used in this study had not received any previous therapies before the study, except five patients who received either chemotherapy, radiation therapy and/ or hormone therapy **(Table 2.7.2.1)**. The antibody panel used for the mass cytometry staining is shown in **Table 2.7.2.2**. The data were provided as live-single CD45+ cells.

2.7.3 Mass cytometry dataset from melanoma patients receiving anti-PD-1 or anti-CTLA-4.

Dataset from 64 melanoma patients receiving anti-PD-1 or anti-CTLA-4 were also re-analysed. The samples were blood samples obtained from patients before the treatment administration. The patients received anti-PD-1 or anti-CTLA-4 after blood drawing according to the FDA approved dosage schedule **(Table 2.7.3.1)**. The treatment response rate was determined based on Response Evaluation Criteria In Solid Tumors 1.1 and maintaining progression-free survival for at least 180 days. Further information can be found in the published paper (Subrahmanyam et al., 2018). Briefly, 96-well-U-bottom plates were used for the staining of the samples, where each sample was split into two different wells. One of the wells was unstimulated PBMCs and the other well was stimulated with PMA and ionomycin prior to the staining; each well contained 2×10^6 cells. The list of the antibodies

used and all methods of staining can be found in the published paper (Subrahmanyam et al., 2018) with antibodies listed in **Table 2.7.3.2**.

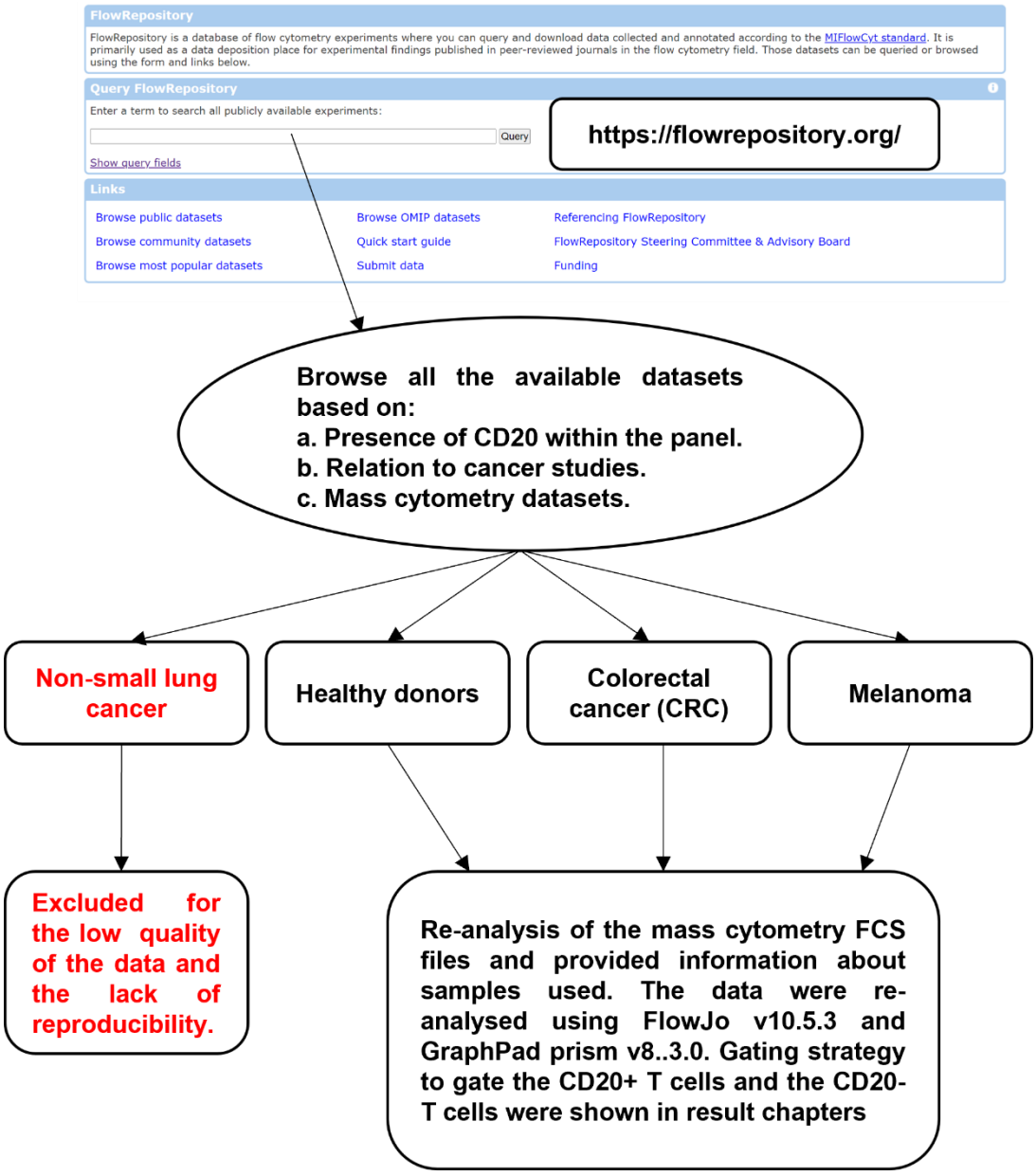

Figure 2.7.1 The dataset selection criteria flow chart.

All the datasets search were performed on FlowRepository websites. The search were based on specific criteria and 4 different datasets were downloaded. One of the datasets from non-small lung cancer were excluded due to lower quality of the data and the lack of reproducibility; CD20+ T cells memory phenotype were low. The exclusion criteria included detecting more doublets, insufficient information provided about the experiment and lack of reproducibility (e.g. higher presence of CD20+ T cells among the naïve population).. The other three datasets were downloaded as FCS files and re-analysed using FlowJo v10.5.3. The other information provided, including demographic, sex, type and number of samples and type of treatment were used in addition to the percentages and cell counts from FlowJo and analysed using GraphPad Prism.

Table 2.7.1 Datasets used in the thesis.

Dataset	**Figures**	**FlowRepository Code**	**Reference**
Healthy donors	(4.2.1), (4.2.2), (4.2.3), (4.2.4), (4.2.5), (4.2.6), (4.2.7), (4.2.8) and (4.2.9)	FR-FCM-Z24F	(Toghi Eshghi et al., 2019)
Colorectal cancer	(5.2.4), (5.2.5), (5.2.6), (5.2.7), (5.2.8), (5.2.9), (5.2.10), (5.2.11), (5.2.12), (5.2.14)	FR-FCM-Z24H	(de Vries et al., 2020)
Melanoma	(6.2.1), (6.2.2), (6.2.3), (6.2.4), (6.2.5), (6.2.6), (6.2.7), (6.2.8), (6.2.9), (6.2.10)	FR-FCM-ZYKP	(Subrahmanyam et al., 2018)

Table 2.7.1.1 List of antibodies used for the staining (Toghi Eshghi et al., 2019).

Mass	Metal	Target	Source	Vendor	Clone
89	Y	CD45	Fluidigm		HI30
115	In	CD57	Custom	Biolegend	HCD57
140	Ce	EQ Beads			
141	Pr	CD49d	Fluidigm		9F10
142	Nd	CCR4	Custom	R&D	205410
143	Nd	CD127	Fluidigm		A019D5
144	Nd	Granzyme B	Custom	Biolegend	GB11
145	Nd	CD4	Fluidigm		RPA-T4
146	Nd	IgD	Fluidigm		IA6-2
147	Sm	CD7	Fluidigm		CD7-6B7
148	Nd	CD16	Fluidigm		3G8
149	Sm	Granzyme A	Custom	Biolegend	CB9
150	Nd	CD103	Custom	Biolegend	Ber-ACT8
151	Eu	CD123	Fluidigm		6H6
152	Sm	TCR-γδ	Custom	Life Technologies	SA6.E9
154	Sm	CD3	Fluidigm		UCHT1
155	Gd	CD27	Fluidigm		L128
156	Gd	CXCR3	Fluidigm		G025H7
157	Gd	CD19	Custom	Biolegend	HIB19
158	Gd	Vα7.2	Custom	Biolegend	3C10
159	Tb	CD11c	Fluidigm		Bu15
160	Gd	CD56	Custom	Miltenyi	REA196
161	Dy	CD66	Custom	BD	B1.1
CD162	Dy	Foxp3	Fluidigm		PCH101

163	Dy	CD20	Custom	Biolegend	2H7
164	Du	CD161	Fluidigm		HP-3G10
165	Ho	CD45RO	Fluidigm		UCHL1
166	Er	FcεRI	Custom	Biolegend	AER-37 (CRA-1
167	Er	CCR7	Fluidigm		G043H7
168	Er	CD8	Fluidigm		SK1
169	Tm	CD25	Fluidigm		2A3
170	Er	CD45RA	Fluidigm		HI100
171	Yb	CD1c	Custom	Biolegend	L161
172	Yb	CD14	Custom	Biolegend	M5E2
173	Yb	PD-1	Custom	Biolegend	EH12.2H7
174	Yb	HLA-DR	Fluidigm		L243
175	Lu	Perforin	Fluidigm		B-D48
176	Yb	CD38	Custom	Biolegend	HIT2
191	Ir	Nucleic acid	Fluidigm		
192	Pt	Cisplatin	Fluidigm		
193	Ir	Nucleic acid			
195	Pt	Cisplatin	Fluidigm		
209	Bi	CD11b	Fluidigm		ICRF-44

Table 2.7.2.1Summary of CRC patients used in the dataset (de Vries et al., 2020).

Patient	Tumour	Normal tissue	Lymph node	PBMC	Location	Clinical stage	Therapy
S00016	√	×	×	√	Rectum	I (T2N0M0)	√
S00030	√	×	√	√	Ascendens	II (T3N0M0)	×
S00044	√	×	√	√	Sigmoid	III (T3N2M0)	×
S00045	√	×	×	√	Rectum	III (T3N1M0)	√
S00046	√	×	√	×	Ascendens	I (T2N0M0)	×
S00049	√	×	√	×	Ascendens	II (T3N0M0)	×
S00050	√	×	√	√	Sigmoid	III (T2N1M0)	×
S00052	√	×	√	×	Ascendens	III (T3N2M0)	×
S00056	√	×	√	√	Sigmoid	IV (T1N0M1)	×
S00084	√	×	√	√	Sigmoid	II (T3N0M0)	×
S00096-1	√	×	√	×	Sigmoid	I (T2N0M0)	×
S00096-2	√	×	√	×	Transversum	I (T2N0M0)	×
S00096-3	√	×	√	×	Transversum	I (T2N0M0)	×
S00096-4	√	×	√	×	Ascendens	I (T2N0M0)	×
S00096-5	√	×	√	×	Ascendens	I (T2N0M0)	×
S00102	√	×	√	√	Ascendens	III (T4N1M0)	×
S00104	√	×	√	×	Ascendens	III (T4N1M0)	×
S00105	√	×	√	×	Sigmoid	I (T2N0M0)	×
S00117	√	√	√	√	Rectum	I (T2N0M0)	×
S00120	√	√	×	√	Rectum	III (T3N1M0)	√
S00133	√	√	×	×	Sigmoid	III (T3N1M0)	×
S00138	√	√	√	√	Sigmoid	III (T1N1M0)	×
S00140	√	√	×	√	Rectum	I (T2N0M0)	√
S00141	√	√	×	×	Sigmoid	IV (T3N1M1)	×

S00143	√	√	√	×	Coecum	II (T4N0M0)	×
S00146	√	√	√	√	Rectum	I (T2N0M0)	√
S00150	√	√	√	×	Ascendens	II (T4N0M0)	×
S00151	√	√	√	√	Coecum	I (T2N0M0)	×
S00155	√	√	×	√	Rectum	I (T1N0M0)	×
S00159	√	√	√	×	Coecum	III (T3N1M0)	×
S00164	√	√	√	√	Descendens	II (T3N0M0)	×
S00167	√	√	√	×	Ascendens	I (T2N0M0)	×
S00172	√	√	×	√	Rectum	I (T2N0M0)	×
S00184	√	√	√	√	Sigmoid	III (T1N1M0)	×
S00202	√	√	×	√	Transversum	II (T3N0M0)	×

Table 2.7.2.2 List of antibodies used for staining (de Vries et al., 2020).

Antibodies	Clone	Source	Identifier
Anti-human CD45	HI30	Fluidigm	Cat# 3089003B
Anti-human CD14	Tük4	ThermoFisher Scientific	Cat# Q10064
Anti-human CD86	IT2.2	Biolegend	Cat# 305435
Anti-human CCR6	G034E3	Fluidigm	Cat# 3141003A
Anti-human CD40	5C3	Fluidigm	Cat# 3142010B
Anti-human ICOS	C398.4A	Fluidigm	Cat# 3143025B
Anti-human CD69	FN50	Fluidigm	Cat# 3144018B
Anti-human CD4	RPA-T4	Fluidigm	Cat# 3145001B
Anti-human CD8α	RPA-T8	Fluidigm	Cat# 3146001B
Anti-human CD115/CSF1R	9-4D2-1E4	Sony	Cat# 2336510
Anti-human CD16	3G8	Fluidigm	Cat# 3148004B
Anti-human CD25	2A3	Fluidigm	Cat# 3149010B
Anti-human ICAM-1	HCD54	Biolegend	Cat# 322702
Anti-human CD123/IL-3Rα	6H6	Fluidigm	Cat# 3151001B
Anti-human TCR-γδ	11F2	Fluidigm	Cat# 3152008B
Anti-human CD7	CD7-6B7	Fluidigm	Cat# 3153014B
Anti-human FAS	DX2	Biolegend	Cat# 305631
Anti-human CD103	Ber-ACT8	Sony	Cat# 2351010
Anti-human PD-L1	29E.2°3	Fluidigm	Cat# 3156026B
Anti-human CD122/IL-2Rβ	TU27	Biolegend	Cat# 339015
Anti-human CCR7	G043H7	Fluidigm	Cat# 3159003°
Anti-human CD163	GHI/61	Sony	Cat# 2268010
Anti-human KLRG1	REA261	Miltenyi Biotec	Cat# 120-014-229
Anti-human CD11c	Bu15	Fluidigm	Cat# 3162005B

Anti-human CD20	2H7	BioLegend	Cat# 302343
Anti-human CD161	HP-3G10	Fluidigm	Cat# 3164009B
Anti-human CD127/IL-7Rα	AO19D5	Fluidigm	Cat# 3165008B
Anti-human CD44	BJ18	Fluidigm	Cat# 3166001B
Anti-human CD27	O323	Fluidigm	Cat# 3167002B
Anti-human CD335/NKp46	9E2	Sony	Cat# 2259510
Anti-human CXCR3	G025H7	Biolegend	Cat# 353733
Anti-human CD3	UCHT1	Fluidigm	Cat# 3170001B
Anti-human CD28	CD28.2	Biolegend	Cat# 302937
Anti-human CD38	HIT2	Fluidigm	Cat# 3172007B
Anti-human CD45RO	UCHL1	Biolegend	Cat# 304239
Anti-human HLA-DR	L243	Fluidigm	Cat# 3174001B
Anti-human PD-1	EH12.2H7	Fluidigm	Cat# 3175008B
Anti-human CD56	NCAM16.2	Fluidigm	Cat# 3176008B
Anti-human CD11b	ICRF44	Fluidigm	Cat# 3209003B

Table 2.7.3.1 Summary of the patients used (Subrahmanyam et al., 2018).

		ANTI-CTLA-4		ANTI-PD-1	
		responders	**non-responders**	**responders**	**non-responders**
AGE	< 30	0	1	0	0
	30–39	0	1	2	0
	40–49	1	4	2	2
	50–59	3	0	6	6
	60–69	4	5	4	6
	> 70	2	3	7	5
GENDER	Female	4	4	8	7
	Male	6	10	13	12

2.7.3.2 List of antibodies used for staining (Subrahmanyam et al., 2018).

Metal label	Target	Antibody clone
115In	Dead cells	n/a
140Ce	Beads	n/a
141Pr	CD25	M-A251
142^{Nd}	CD19	HIB19
143Nd	IL-10	JES3-9D7
144Nd	IL-4	MP4-25D2
145Nd	CD4	RPA-T4
146Nd	CD8	RPA-T8
147Sm	CD20	2H7
148Nd	CD57	HCD57
149Sm	CTLA-4	14D3
150Nd	MIP-1β	D21–1351
151Eu	CD107a	H4A3
152Sm	TNFa	Mab11
153Eu	CD45RA	HI100
154Sm	CD3	UCHT1
155Gd	CD28	L293
156Gd	CD38	HB-7
157Gd	HLA-DR	G46–6
158Gd	CD33	WM53
159 Tb	GMCSF	BVD2-21C11
160Gd	CD14	M5E2
161Dy	IFNγ	4S.B3
162Dy	CD69	FN50
163Dy	TCRγδ	B1
164Dy	IL-17	N49–853
165Ho	CD127	A019D5
166Er	IL-2	MQ1-17 h12
167Er	CD27	L128
168Er	CD154 (CD40L)	24–31
169Tm	CCR7	150503
170Er	PD1	EH12.1
171Yb	Granzyme B	GB11
172Yb	PD-L2	24F.10C12
173Yb	Perforin	B-D48
174Yb	CD16	3G8
175Lu	PD-L1	29E.2A3
176Yb	CD56	NCAM16.2
191Ir	DNA1	n/a
193Ir	DNA2	n/a

2.8 Data and statistical analysis

All flow cytometry data and mass cytometry data were analysed using FlowJo v10.5.3 and statistical data generated using GraphPad Prism v8.3.0. I-repertoire data analysis pipeline and GraphPad Prism were used to analyse TCR repertoire and determine CDR3 sequences.

Chapter Three: Investigating the origin of CD20+ T cells

3.1 Introduction

The presence of CD20+ T cells was first reported in 1990 in the blood of a small patient group with HIV (Landay et al., 1990). However, reports in the literature provide conflicting data on the origin of CD20+ CD3+ T cells. Cord blood was analysed for the presence of CD20+ CD3+ T cells but they could not be detected (de Bruyn et al., 2015). Co-culturing peripheral blood mononuclear cells or purified T cells with a B cell line or primary HLA-mismatched B cells resulted in an increase in the number of CD3+ CD20+ T cells (de Bruyn et al., 2015). This was explained by a process called trogocytosis, where a marker from one cell can be transferred to another cell as intact protein or as a protein complex, similar to HLA-DR transference during antigen presentation (Storie et al., 1995). On the other hand, another paper intensively investigated the features of CD3+ CD20+ T cells in MS, and found that sorted CD3+ CD20+ T cells from healthy blood volunteers can transcribe CD20 and CD3, but not CD19 (Schuh et al., 2016).

Those sorted cells did not express HLADR which was used by de Bruyn et al., 2015 to confirm that CD20 has been acquired by CD3+ CD20+ T cells via trogocytosis. Therefore, due to the uncertainty about the origin of those cells, the aim of this chapter is to investigate the origin of the CD20+ T cells via deep analysis using TCR repertoire of the pre-sorted CD3+CD19-CD8+CD45RA- CD20+ or CD20- T cells. This would reveal the similarity between the two populations and the number of shared and unique clones from each population.

3.1.1 Hypothesis

We hypothesised that these cells can be found within normal healthy individuals, and unlike the trogoytosis hypothesis, the CD20+ T cells will show some unique clones and not found in the CD20- T cells population.

3.2 Results

3.2.1 CD20+CD19- population expressing CD3

First, a gating strategy was established to assess CD3 expression on the live single CD20+CD19- and CD20+CD19+ (B cell) positive populations. Healthy PBMC isolated from seven different donors were used to gate a population of single live cells. From the single live cells, CD20+CD19- and CD20+CD19+ populations were gated for the expression of CD3 **(Fig. 3.2.1A)**. CD20+ gates were set according to the PE-conjugated isotype control to minimise the contamination of any non-specific binding of the PE conjugated anti-CD20 antibody. The same gating strategy was used for the seven different healthy donors and CD3 expression was assessed in each population. The expression of CD3 by CD20+CD19+ cells was almost zero for all the donors. However, unlike CD20+CD19+ population, it was clear that almost all CD20+CD19- cells expressed CD3; this was observed for all seven donors **(Fig. 3.2.1B)**.

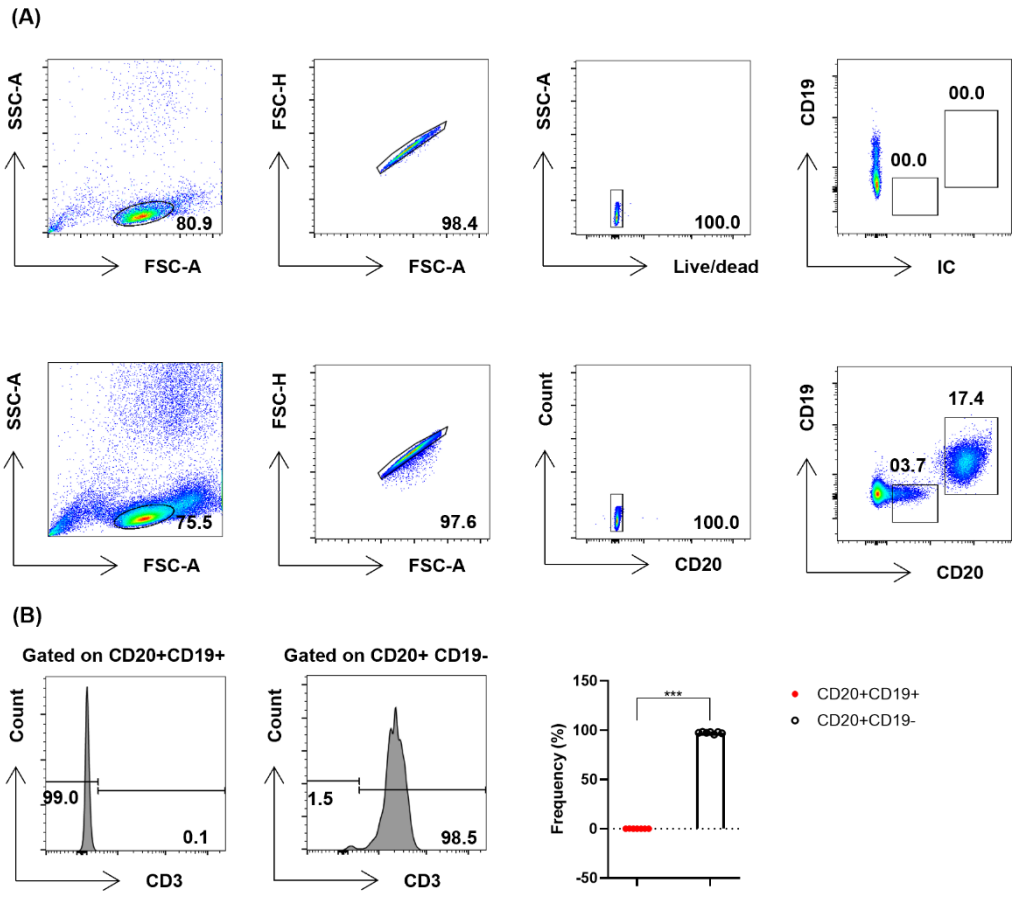

Figure 3.2.1. CD20+CD19- population expressing CD3.

Gating strategy to assess CD3 expression on CD20+CD19- and CD20+CD19+ cells using PBMC isolated from healthy donors. Representative of the CD3 expression from CD20+CD19- and CD20+CD19+ for isotype control and CD20 (same donor) (**A**) and the percent CD3+ on CD20+CD19+ and CD20+CD19- populations (n=7) **(B).** Mann-Whitney test. *** P = 0.001. FSC-A; forward light scatter area; SSC-A; side light scatter area; FSC-H; forward light scatter height. IC; isotype control.

3.2.2 CD20+CD19-CD3+ T cells usually comprise more CD8+ T cells than CD8- T cells

Following the assessment of CD3 expression on the CD20+CD19- population, isolated PBMC from seven healthy donors were used for further analysis of the CD20+CD19-CD3+ population, designed to assess the expression of CD8. CD8+ and CD8- populations were gated from the live CD3+CD19- single cells. An isotype control PE conjugated antibody was used to set the gates for the CD20+ cells **(Fig. 3.2.2A)**. In general, CD20+ T cells were detected in both the CD8+ and CD8- T cells subsets. However, CD20+ cells within the CD8+ population were significantly higher than in the CD8- population. The same result was observed across all the seven donors that were used for this analysis; CD8+ CD20+ T cells comprised a significantly higher percentage of the CD3+ T cells compared to the CD20+ CD8- T cells **(Fig. 3.2.2B)**.

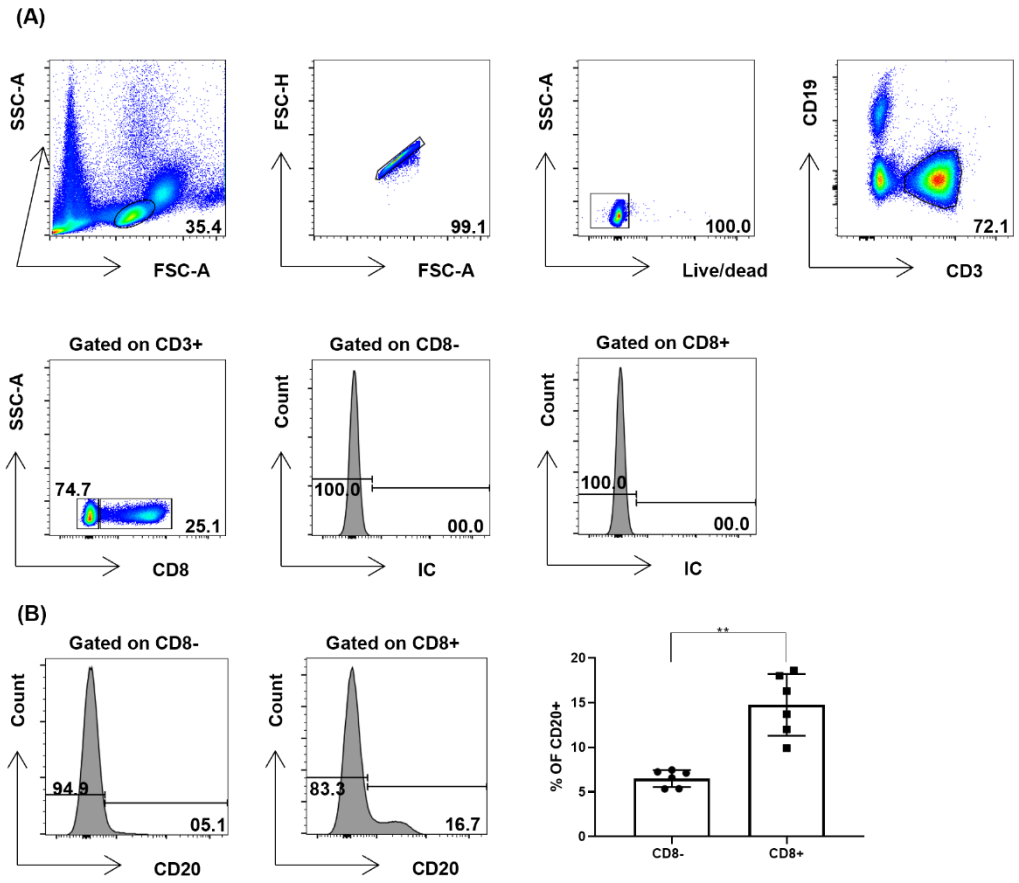

Figure 3.2.2 CD20+CD19-CD3+ T cells usually comprise more CD8+ T cells than CD8- T cells.

Gating strategy to assess CD20 expression on CD8+ or CD8- cells using PBMCs isolated from healthy donors **(A).** Representative of the CD20 expression from CD8+ and CD8- cells (same donor) and the percent CD20+ on CD8+ and CD8- populations (n=7) **(B).** Mann-Whitney test; ** P =0.0022. FSC-A; forward light scatter area; SSC-A; side light scatter area; FSC-H; forward light scatter height. IC; isotype control.

3.2.3 CD20+ T cells are enriched in the memory compartment

Further analysis of the CD20+ T cell population from three different healthy donors was used to assess the memory phenotype. Naïve, central memory (Tcm), effector memory (Tem) and revertant effector memory RA+ (Temra) populations were gated according to the expression of CD45RA and CCR7. Naïve cells were identified by their expression of CD45RA and CCR7; Tcm lack the expression of CD45RA but retain CCR7; Temra lack the expression of CCR7 but re-express CD45RA; and Tem lack the expression of both CD45RA and CCR7 **(Fig. 3.2.3A)**. Next, the expression of CD20 was assessed for each population using PBMCs isolated from normal heathy donors. CD20+ T cells were enriched within the memory compartment compared to the naïve population **(Fig. 3.2.3B)**. Indeed, the same shift towards a memory phenotype was found across three different healthy donors, where the CD20+ naïve population comprised less than 10% of the total CD8+ population. In addition, Tcm and Tem showed significantly higher percentages compared to the naïve population within the CD20+CD8+ population. On the other hand, unlike the CD20+ population, naïve cells showed the highest percentage compared to Tcm, Tem and Temra within the CD20-CD8+ population **(Fig. 3.2.3C)**.

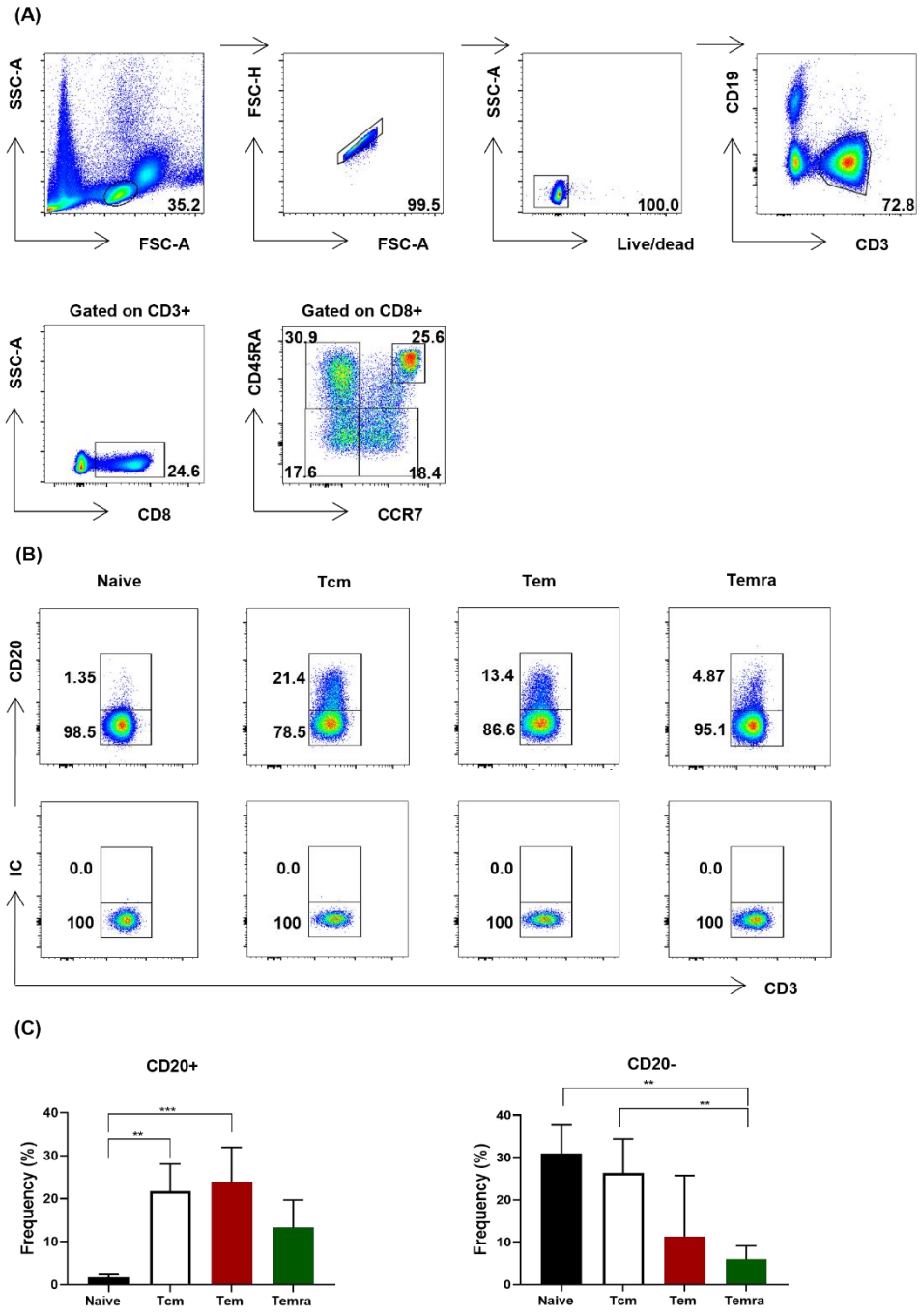

Figure 3.2.3 CD20+ T cells are enriched in the memory compartment.

Gating strategy to identify different CD8+ memory T cell subsets; including naïve (CCR7+CD45RA+), Tem (CCR7-CD45RA-), Tcm (CCR7+CD45RA-) and Temra (CCR7-CD45RA+) **(A).** Comparing CD20 expression on different CD8+ memory subsets to isotype control, the numbers represent the percentages of each subset from the same donor **(B).** The frequency of CD20+ and CD20- cells in different memory CD8+ T cell subsets (n=3) **(C)**. Mann-Whitney test. *** P = 0.0005, ** P = 0.005. FSC-A; forward light scatter area; SSC-A; side light scatter area; FSC-H; forward light scatter height, Tcm; central memory, Tem, effector memory, Temra; revertant effector memory.

3.2.4 Sorting of CD20+ and CD20- T cells.

Next, CD20+ and CD20- T cells were sorted to high purity using FACS from twelve different healthy donors and successful sorting were from three healthy donors, as described before **(Fig 2.5.2)**. CD8+ T cells were first enriched from the isolated PBMC using magnetic beads, and then used for staining and sorting. Using isotype control stained PBMC, CD20+ and CD20- T cells gates were set from the CD3+CD19-CD8+CD45RA- population and sorted into different tubes **(Fig. 3.2.4A)**. A small proportion of the sorted cells was used to assess the purity of the sorted cells from each of the three healthy donors. The sorted cells showed a 100% pure population of both the CD20+ and CD20- T cells **(Fig. 3.2.4B)**.

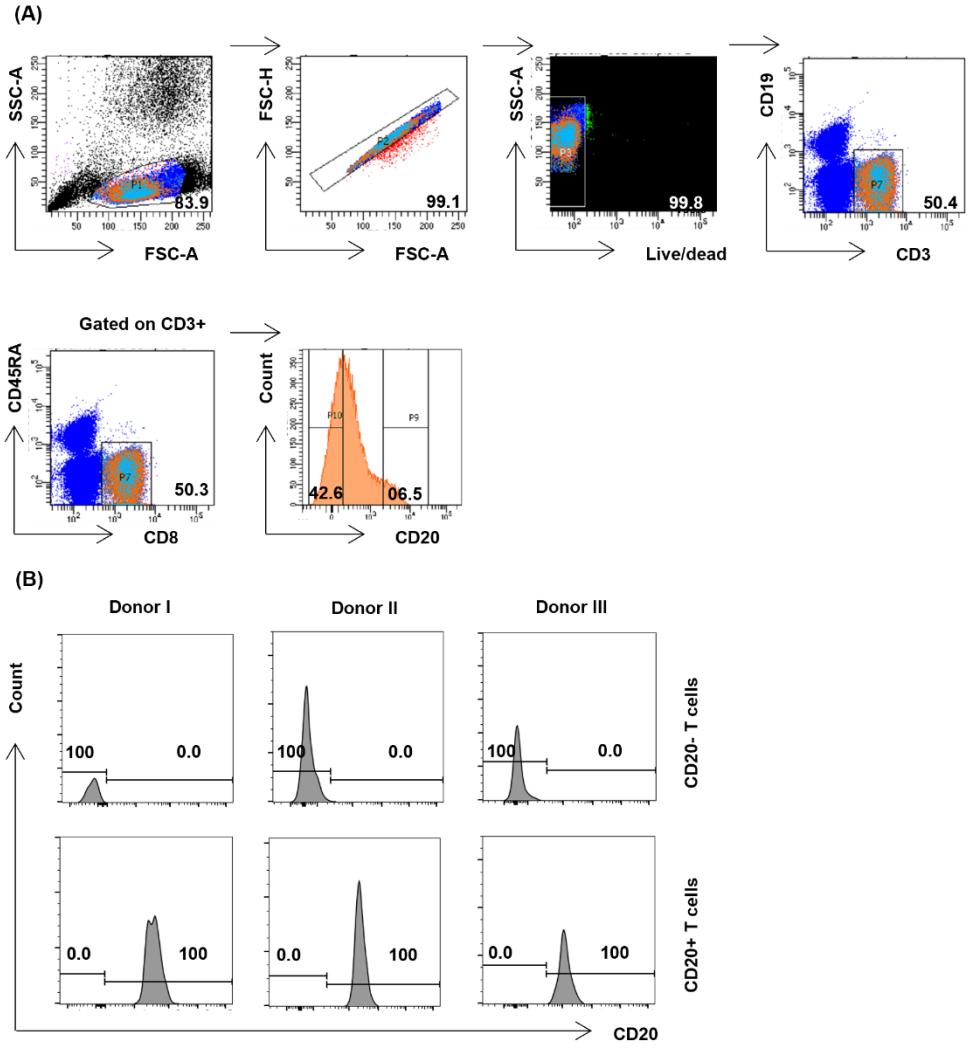

Figure 3.2.4 Sorting of CD20+ and CD20- T cells.

Gating strategy to sort live CD3+CD8+CD45RA-CD20+/- T cells from enriched CD8+ T cells from PBMCs isolated from healthy donors **(A).** Purity of the sorted cells (n=3) **(B).** FSC-A; forward light scatter area; SSC-A; side light scatter area; FSC-H; forward light scatter height.

3.2.5 TCR-β sequence repertoire shows similarity between donors

The sorted CD20+ and CD20-CD8+ T cells were used for T cell receptor sequencing, which can be used to assess the repertoire similarity between the two populations. Sorted cells from three independent donors were sent to I-repertoire company for further RNA- extraction, TCRβ CDR3-sequencing and alignment of the data. The frequency of the CDR3 reads from the aligned amino acid sequences data was plotted for CD20+ and CD20- populations from each donor, as shown in the illustrative flow chart for TCR-sequencing data processing **(Fig 2.5.2)**. Interestingly, shared sequences between the CD20+ and CD20-CD8+ T cells populations were less than 10% across all the three samples. Though, the CD20- population showed a more diverse repertoire compared to the CD20+ cells, the percent of unique sequences in the CD20- population was more than 60% in all the three donors compared to less than 30% of the sequences being unique to the CD20+CD8+ T cells **(Fig. 3.2.5A)**. Overall, the results were consistent across all the three donors and CD20+CD8+ T cells showed unique sequences that were absent from the CD20- T cell repertoire, as well as a smaller proportion that were shared between the two populations.

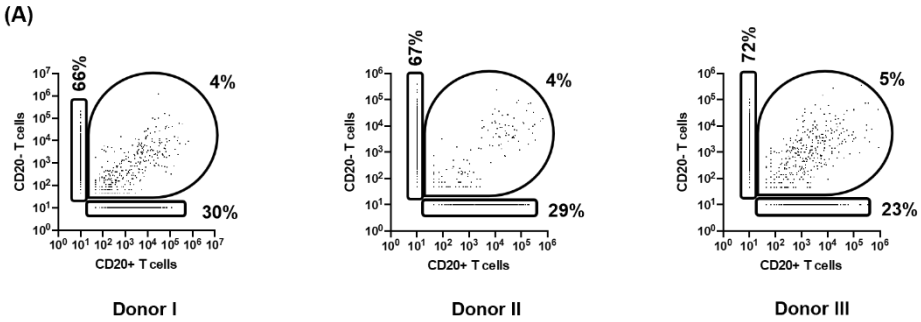

Figure 3.2.5 TCR-β sequence repertoire shows similarity between donors.

The number of reads obtained from the aligned TCRβ CDR3 amino acid sequences for CD20-CD8+ T cells (Y) and CD20+CD8+ T cells (X) were plotted to show unique and shared sequences between CD3+CD8+CD45RA-CD20+/- populations (n=3) **(A)**.

3.2.6 CD20-CD8+ T cell repertoire showed more diversity compared to CD20+CD8+ T cells.

The TCRβ CDR3 aligned amino acid sequences from each population from all the three donors were plotted to show the top 10 most expressed sequences and their percentages from the total repertoire. Every sequence unique to the CD20+ or CD20-CD8+ T cells compared to the other population from the same donor is indicated by the red colour text. Overall, the CD20-CD8+ T cell repertoire showed more diversity compared to the CD20+CD8+ T cell. In addition, the top 10 most expressed sequences within CD20- and CD20+ CD8+ T cell populations were different between the three donors **(Fig. 3.2.6)**.

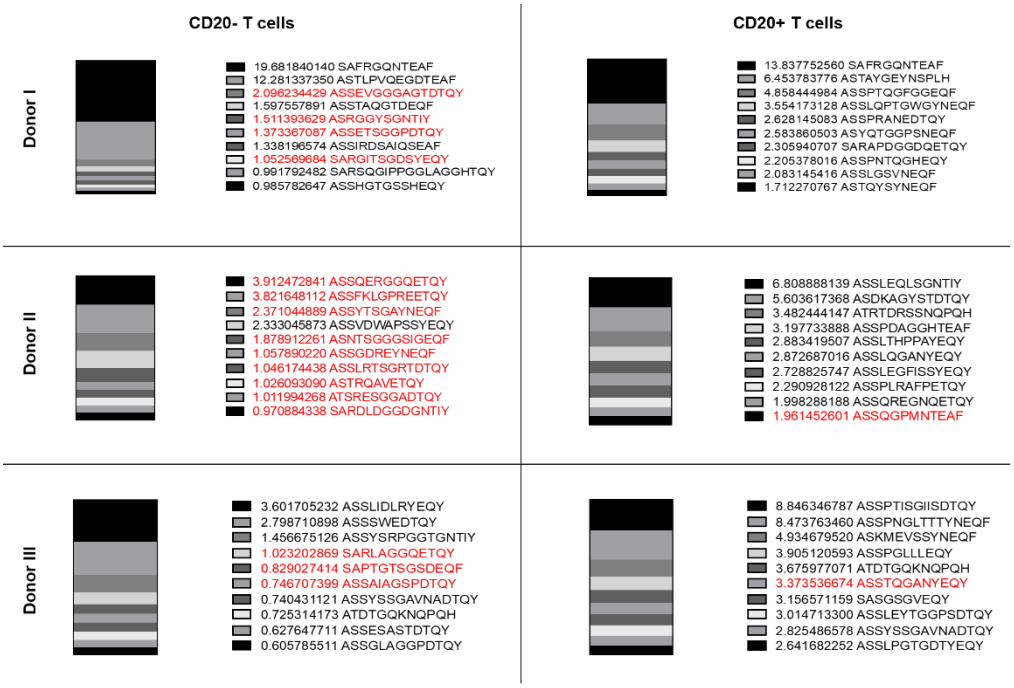

Figure 3.2.6 CD20-CD8+ T cell repertoire showed more diversity compared to CD20+CD8+ T cells.

The top 10 most expressed amino acid sequences from CD20+/CD20- T cells within each donor were plotted with their percentages from the total CDR3β amino acid sequenced repertoire. The red text indicates the sequences that are unique to this population and to this donor compared with CD20- T cells sequences from the same donor.

3.2.7 Comparison of the shared sequences between different donors

Despite the presence of unique TCRβ CDR3 amino acid sequences that can be found in either CD20+ or CD20- populations, there are also shared sequences between CD20+ and CD20- T cells. Based on the frequencies of all of the shared sequences, the frequencies for the CD20+ T cells were plotted on the X-axis, while the frequencies for the CD20- T cells were plotted on the Y-axis **(Fig. 3.2.7A)**. In all the three donors, CD20+ and CD20- shared amino acid sequences showed a correlation coefficient close to +1 Despite this degree of correlation, the level of expression of some of these shared amino acid sequences varied considerably between the two populations **(Fig. 3.2.7A)**. A tree map for each population from each donor was generated by the I-repertoire automated data analysis pipeline. The tree map generated used the V gene, J gene and the CDR3β amino acid sequence, where each (assumed) clone represents a rectangular. The size of each rectangle reflects the frequency of that clone and demonstrates the diversity between donors. However, the CD20+CD8+ T cell population showed less diversity as compared to the CD20-CD8+ T cell population with more expanded clones comparing to the CD20- population **(Fig. 3.2.7B)**.

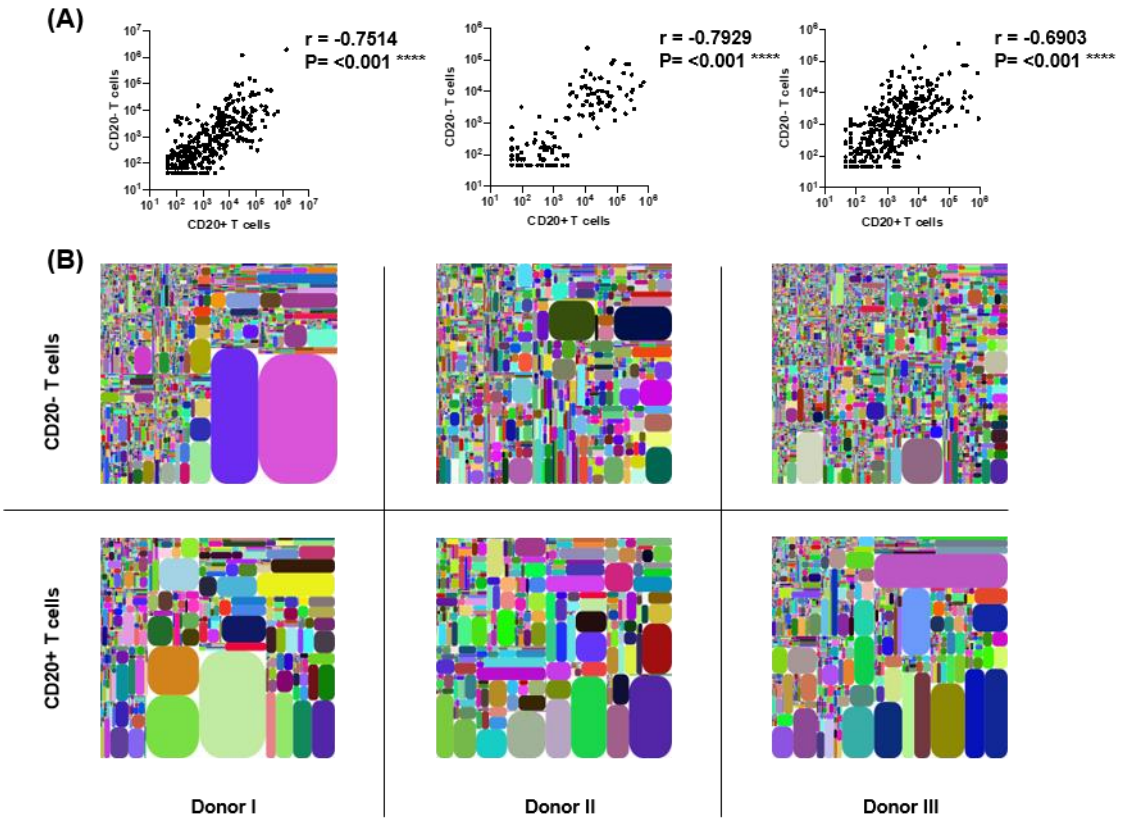

Figure 3.2.7 Comparison of the shared sequences between different donors.

Frequency of TCRβCDR3 aligned amino acid reads from CD20+ (X) and CD20- T cells (Y)from three different donors. In order to more easily visualize shared sequence amino acid reads, data is not shown where the read could not be detected in one of the populations **(A)**. Next assumed clones (using V gene, J gene and the unique CDR3 sequence) for each population were depicted in the tree map, where each rectangle reflect a shared clone that varies in size according to the frequency of that clone **(B).**

3.2.8 V-J gene segment usage comparison between CD20+ and CD20- T cells.

Next, V-J gene segment usage in the CDR3β amino acid sequences was investigated to identify the differences between CD20+ and CD20-CD8+ populations within each donor, using the automated data analysis pipeline by I-repertoire. Overall, the CD20- population showed more usage of specific V and J genes when compared to the CD20+ which were low or absent from the heatmap. However, CD20+ populations showed higher usage of other V and J genes comparing to the CD20- population across the three donors **(Fig 3.2.8A,B,C)**. To illustrate, in donor I, CD20+ T cells showed higher usage of the V gene (hTRBV4-2) and the J gene (hTRBJ2-1), while CD20- T cells from the same donor showed very low usage of those genes. CD20+ T cell usage of the V gene (hTRBV7-4) and the J gene (hTRBJ2-4) were low compared to the CD20- T cells, which suggests a more restricted profile of the CD20+ T cells compare to the diverse repertoire of the CD20- T cells.

(A)

Donor I

CD20+ T cells

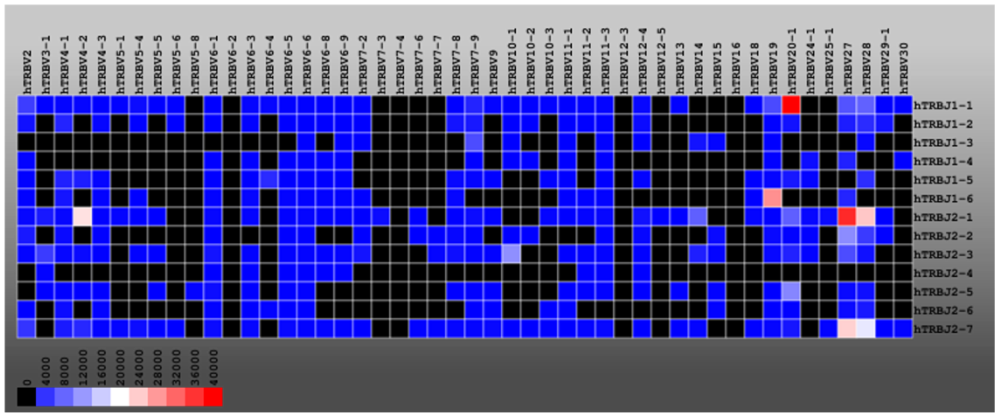

CD20- T cells

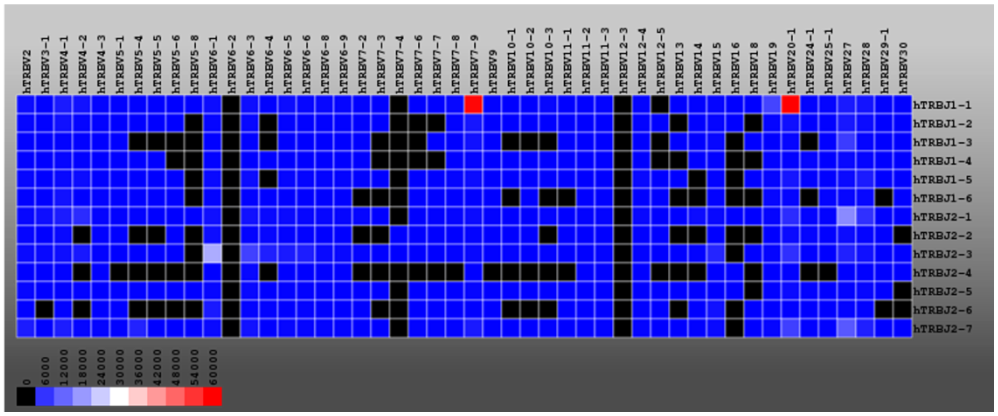

(B)

Donor II

CD20+ T cells

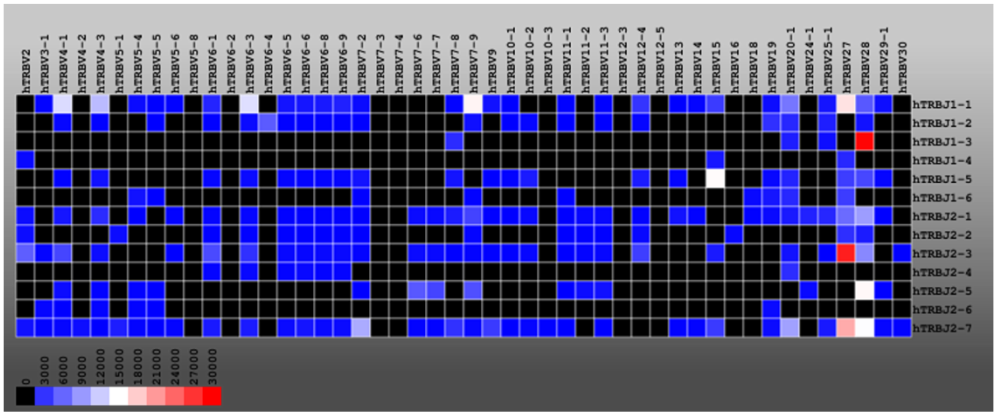

CD20- T cells

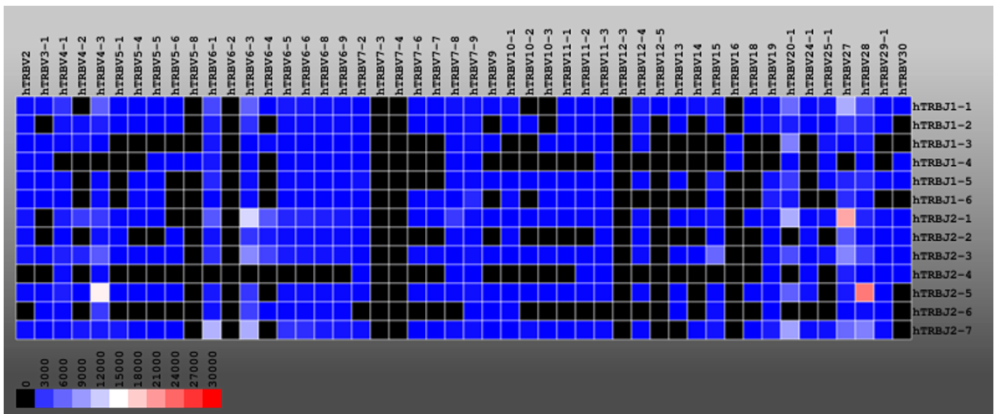

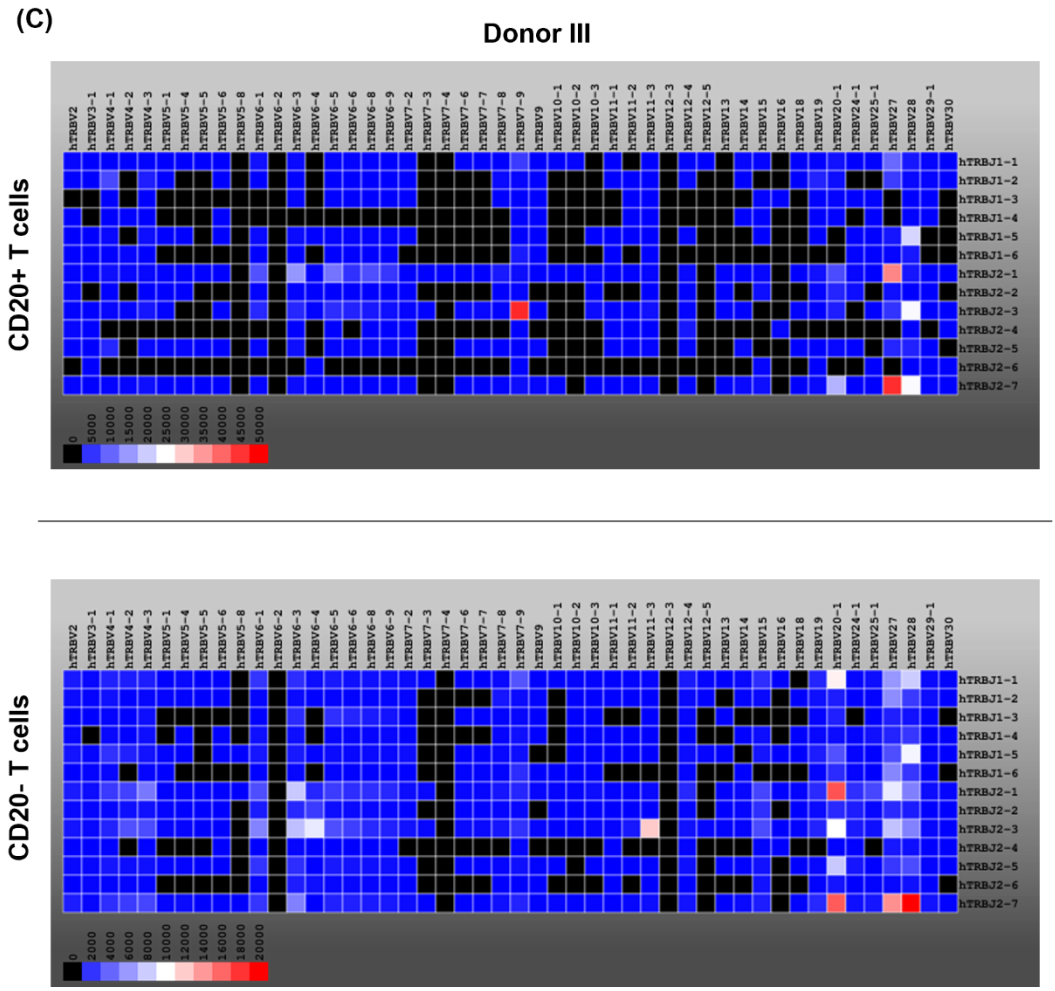

Figure 3.2.8 V-J gene segment usage comparison between CD20+ and CD20- T cells.

V-J gene segment usage in the CDR3β amino acid sequences generated by I-repertoire, in a heatmap for each population (rows) and from three different donors; donor I **(A)**, donor II **(B)**, donor III **(C)**. The frequency of the V genes (horizontal) and J genes (vertical) frequently used to build the amino acid sequences are reflected by the colour; where red means more frequent usage. The actual number relating to the colour is indicated at the bottom of each plot.

3.2.9 CD20+ T cells showed a higher response to HLA-A2.1 restricted EBV epitopes YVL and GLC compared to CD20- T cells.

Following the TCR repertoire analysis of the CD20+ and CD20- T cells, antigen specificity of those population to EBV was assessed using tetramer staining of three different donors. Isolated PBMC from three EBV+ HLA-A*02-positive donors, who were different to the donors used for the TCR-sequencing analysis, was used for the tetramer staining assessing reactivity toward two common EBV lytic cycle peptides (YVL from the latent membrane protein 2A and GLC from the immediate-early protein BRLF1). The gating for tetramer positive cells and CD20+ cells used the isotype control tetramer FMO **(Fig. 3.2.9A)**. Using the previous established gating, the percent of the tetramer positive cells from the memory CD20+ and the memory CD20-CD8+ populations was examined for three different donors. Although comparing the CD20+ T cells reactivity to YVL and GLC peptides revealed variations in their response, for both GLC and YVL, CD20+ tetramer+ T cells were higher than CD20- tetramer+ T cells across all three donors **(Fig. 3.2.9B)**.

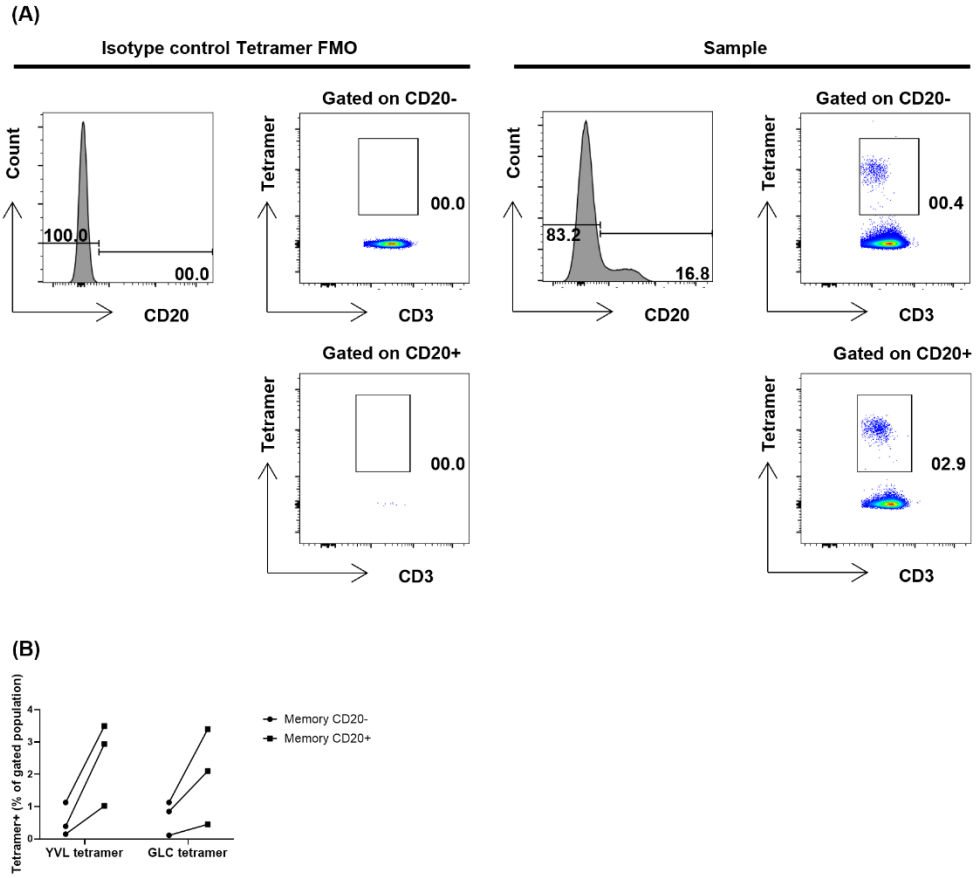

Figure 3.2.9 CD20+ T cells showed a higher response to HLA-A2.1 restricted EBV epitopes YVL and GLC compared to CD20- T cells.

Representative gating to show EBV-specific CD3+CD8+ memory T cells from PBMCs isolated from healthy donors. Comparison between isotype control FMO and CD20 EBV tetramer-stained PBMCs **(A)**. Representative plot to show the percent of CD3+CD8+ memory CD20+/CD20- T cells from HLA-A*02 positive healthy donors that have specific T cells towards two common EBV-lytic cycle peptides; YVL and GLC (n=3) **(B)**. FMO; fluorescence minus one, YVL; YVLDHLIVV, GLC; GLCTLVAML and IC; isotype control.

3.3 Discussion

First the presence of CD20+ T cells was determined through the expression of CD3 in the CD20+CD19- and not in the CD20+CD19+ population, where over 90% of the CD20+CD19- cells expressed CD3. Unlike theCD20+CD19+ population, CD3 expression on the CD20+CD19- population were almost zero **(Fig 3.2.1A,B)**. These data are consistent with previous reports demonstrating the presence of CD20+ T cells within different organs, including blood of healthy donors (Schuh et al., 2016, Wilk et al., 2009, Holley et al., 2014). Further to the data from flow cytometry, CD20+ T cells transcription of CD20, but, not CD19, has been shown previously (Schuh et al., 2016, Rathbone, 2018).

In agreement with published data, we found that CD20+ T cells were more dominant in the CD8+ memory compartment **(Fig 3.2.2A,B)**. Naïve CD20+ T cells were significantly lower than other memory compartments (Tem, Tcm and Temra), indicating that the CD20+ T cells constitute are more antigen experienced population **(Fig 3.2.3B,C)**. This in itself suggests that CD20 can be expressed on T cells after a certain trigger such as, activation in a particular microenvironment. CD20+ T cells have been shown to be more cytotoxic than CD20- T cells after *in vitro* activation, (Schuh et al., 2016). In addition, human B cell studies using monoclonal antibodies to ligate CD20 showed enhancement of survival, activation and proliferation of those cells (Clark and Shu, 1987, Holder et al., 1995, Smeland et al., 1987), indicating a role for CD20 on T cells. Hence, *in vitro* activation of CD20+ and CD20- T cells resulted in higher cytotoxicity and cytokine production by CD20+ over CD20- T cell and this would indicate the possible effects of CD20 expression on T cells activation and cytotoxicity (von Essen et al., 2019).

However, there is conflicting data on the origin of CD20+ T cells where it has been proposed to be a result of trogocytosis. We decided to assess the TCR sequences of pre-sorted CD20+ and CD20-CD8+ T cells (de Bruyn et al., 2015). The usage of TCR-sequencing would give

the chance to analyse the repertoire of each population and determine the similarities between the CD20+ and the CD20- T cell clones. To illustrate, the trogocytosis theory for the CD20+ T cells would result in high similarities between the CD20- and CD20+ repertoires. Using the same gating strategy for detection, we managed to sort CD3+CD19-CD8+CD45RA-CD20+ and CD20- T cells to high purity, where sorted cells showed up to 99% purity **(Fig 3.2.4A,B)**.

Due to technical challenges, as CD20+ T cells constitute a small percent of the total number of the T cells compared to the CD20- T cells, only three donors were used in this analysis. It is therefore possible that the results are not truly representative. CD20+ T cells showed up to 30% of unique amino acid sequences from their total repertoire that could not be detected in the CD20- T cell repertoire, and this was consistent across 3 different healthy donors **(Fig 3.2.5A,B)**. Furthermore, the CD20+ T cells unique amino acid sequences were abundant, and two of the three donors showed unique amino acid sequences among the top 10 highly expressed amino acid sequences. The presence of unique sequences in the small fraction of CD20+ T cells compared to the high percentage of CD20- T cells would make the trogocytosis theory a less likely explanation for the presence of CD20+ T cells. The presence of the unique sequences to the CD20+ T cells can support the presence of unique CD20+ T cells that had been educated in the thymus and exited to the periphery as CD20+ T cells, or who permanently switched on CD20 in the periphery following their activation. However, the existence of shared sequences between the two population suggests post-thymic induction of CD20 in some of the progeny, mirroring the story for peripheral and thymic Treg (Murphy and Weaver, 2016). Indeed, repertoire analysis of thymic derived Treg (CD4+CD25+) and peripheral induced Treg (CD4+CD25-) showed largely diverse repertoires, and though showed similar immunological functions (Lathrop et al., 2011). Therefore, the composition of unique and shared sequences of the CD20+ T cells would emphasise the presence of thymic and peripheral derived CD20+ T cells. V-J gene usage supported the sequence data

differences between CD20+ and CD20- T cells. Further to the TCR repertoire, to analyse the responses to one of the high prevalence viral infections among humans, two EBV lytic cycle peptides were used to assess CD20+ and CD20- T cells responses using tetramer technology (Moosmann et al., 2010).

The frequency of tetramer+ cells was higher in the memory CD20+ compartment for all three donors **(Fig 3.2.9B)**. This would suggest the presence of numbers of high EBV-specific CD8+ T cells within the CD20+T cells compartments. However, only three donors have been used for the experiment and only two EBV lytic peptides, so this would need further studies using bigger sample cohorts and other EBV related peptides to determine the possible role of CD20+ T cells in the EBV responses and their specificity to EBV.

The trogocytosis theory states that CD20 has been transferred to the T cells from their interaction with B cells, which means that these cells were CD20- before the interaction. The presence of high EBV-specific cells among the CD20+ T cells may indicate a possible previous interaction of those cells with B cells and would support the trogocytosis theory as CD20 is a well known lineage marker for B cells. This is because the main reservoir for the EBV can be the B cells (Delecluse et al., 2019). These data cannot refute the trogocytosis theory for the acquisition of CD20 by T cells. However, they do indicate that a more likely explanation is the presence of T cells that transcribe CD20, being both thymically derived and induced in the periphery. It is possible that multiple mechanisms are in operation that result in the presence of significant numbers of CD20+ T cells.

Chapter Four: Identifying the phenotype of CD20+ T cells in healthy individuals

4.1 Introduction

The phenotype of CD20+ T cells remain controversial, despite previous attempts to phenotype the CD20+ T cells. In most published studies, researchers used flow cytometry to assess the phenotype of the CD20+ T cells, which can add a limitation to the number of markers that can be used in each experiment. It has been shown that CD20+ T cells usually comprise more of the CD8+ subset, as compared to CD4+, with a predominantly memory phenotype (Schuh et al., 2016). It has also been proposed that the CD20+ T cells are more cytotoxic than the CD20- T cells, with higher production of pro-inflammatory cytokines upon stimulation (Schuh et al., 2016, von Essen et al., 2019). CD20+T cells from the peripheral blood of patients with MS expressed more CCR6 and were able to produce higher quantities of TNFα and IFNγ upon stimulation. In RA, higher expression of activation markers such as CD25, CD49a and CD69 and other markers such as CD161 were found within the CD20+ T cells as compared to the CD20- T cells.

There are currently no known unique markers on CD20+ T cells, or detailed information on their phenotype. The main aim of this chapter was therefore to use more complex phenotyping to examine CD20+ T cells. Due to the COVID-19 pandemic I was unable to access the lab for these experiments. Instead, I have re-analysed data from previously published datasets (Toghi Eshghi et al., 2019).

4.1.1 Aims

1- Determine phenotypic differences between CD20+ and CD20- T cells.

2- Assess the possibility of distinguishable and unique marker for CD20+ T cells.

4.2 Results

4.2.1 Mass cytometry data replicate the results from flow cytometry

In order to examine the sensitivity of mass cytometry to detect the low percentage of CD20+ T cells, previous gating strategies used for flow cytometry were applied to the mass data, in particular to assess the memory phenotype of the cells. Live single cells were used to gate CD3+CD19- TCRγδ- cells and then they were divided into CD4+ and CD8+ populations. Next, CD20 expression was assessed for the CD4+ and CD8+ populations **(Fig. 4.2.1A)**. The divided populations; CD4+ and CD8+, were subdivided into memory and naïve cells according to the expression of CCR7 and CD45RA **(Fig 4.2.1B)**. In agreement with flow cytometry data, CD20+ T cells showed a higher percentage of CD8+ than CD4+ T cells **(Fig 4.2.1C)**. In addition, there were significantly more memory than naïve cells, for both CD8+ and CD4+ populations **(Fig 4.2.1D)**. Therefore, mass cytometry data is suitable for assessing CD20+ T cell phenotype.

4.2.2 Expression of CD20 by Vα7.2+CD161+ T cells

Next, t-distributed stochastic neighbour embedding (tSNE), was used to assess the phenotype of CD20+ T cells and to compare between CD20+ and CD20- T cells. First, memory CD3+CD19-CD8+ were used for tSNE under normal optimised conditions, where learning configuration selection in FlowJo were selected and used the standard literation, preplixibility and literation rate. The pre-gated memory, naïve, CD20+ and CD20- cells were applied to the generated tSNE plot. The tool allows for the separation of the cells into islands according to the expression of the markers that has been used for the separation **(Table 2.7.1.1)**. Each island shows a homogenous phenotype based on the selected markers from the panel. Interestingly, no distinct islands in the CD20+ cells were absent from the CD20- population. However, a distinct population was identifiable and also showed the presence of Tem, Tcm

and Temra **(Fig 4.2.2A)**. The separated island showed higher expression of Vα7.2 and CD161, and comprised a high percentage of the CD20+ T cells **(Fig 4.2.2B)**. Usually the expression of Vα7.2+ CD161+ is enriched with MAIT cells (Dias et al., 2018).

4.2.3 Vα7.2+CD161+ population comprises more of the CD20+ compartment

Vα7.2+ CD161+ within CD20+ and CD20- populations have been further investigated and compared to the CD20+ or CD20- Vα7.2- population. First, CD20+ and CD20- CD8+ populations have been used to gate the Vα7.2+CD161+ and Vα7.2- (CD161+ and CD161-) **(Fig 4.2.3A)**. Interestingly, Vα7.2+CD161+ comprised a higher percentage of the CD20+CD8+ population in compared to the CD20-CD8+ population. However, the Vα7.2- population showed higher percentage among the CD20-CD8+ population in compared to the CD20+CD8+ population **(Fig 4.2.3B)**. Using CD45RA and CCR7, naïve, Tcm, Tem and Temra populations were examined within the Vα7.2+CD161+ and Vα7.2- populations from the CD20+CD8+ and CD20-CD8+ cells. In both CD20+ and CD20-CD8+ populations, Vα7.2+CD161+ cells showed predominantly Tem phenotype through the loss of CD45RA and CCR7. However, the Vα7.2- population showed different phenotype, where naïve, Tcm, Tem and Temra populations were found within both CD20+ and CD20- Vα7.2- populations. Even though, CD20-Vα7.2- population showed the highest percentage of naïve population followed by Tem. However, CD20+Vα7.2- showed significantly higher percentages of naïve, where naïve CD20+Vα7.2- population represent the lowest percentages within this population **(Fig 4.2.3C,D)**. Indeed, comparing the naïve to the memory CD20+Vα7.2- populations revealed significantly higher percentage of memory cells than naïve cells within the CD20+Vα7.2- **(Fig 4.2.3E)**.

.

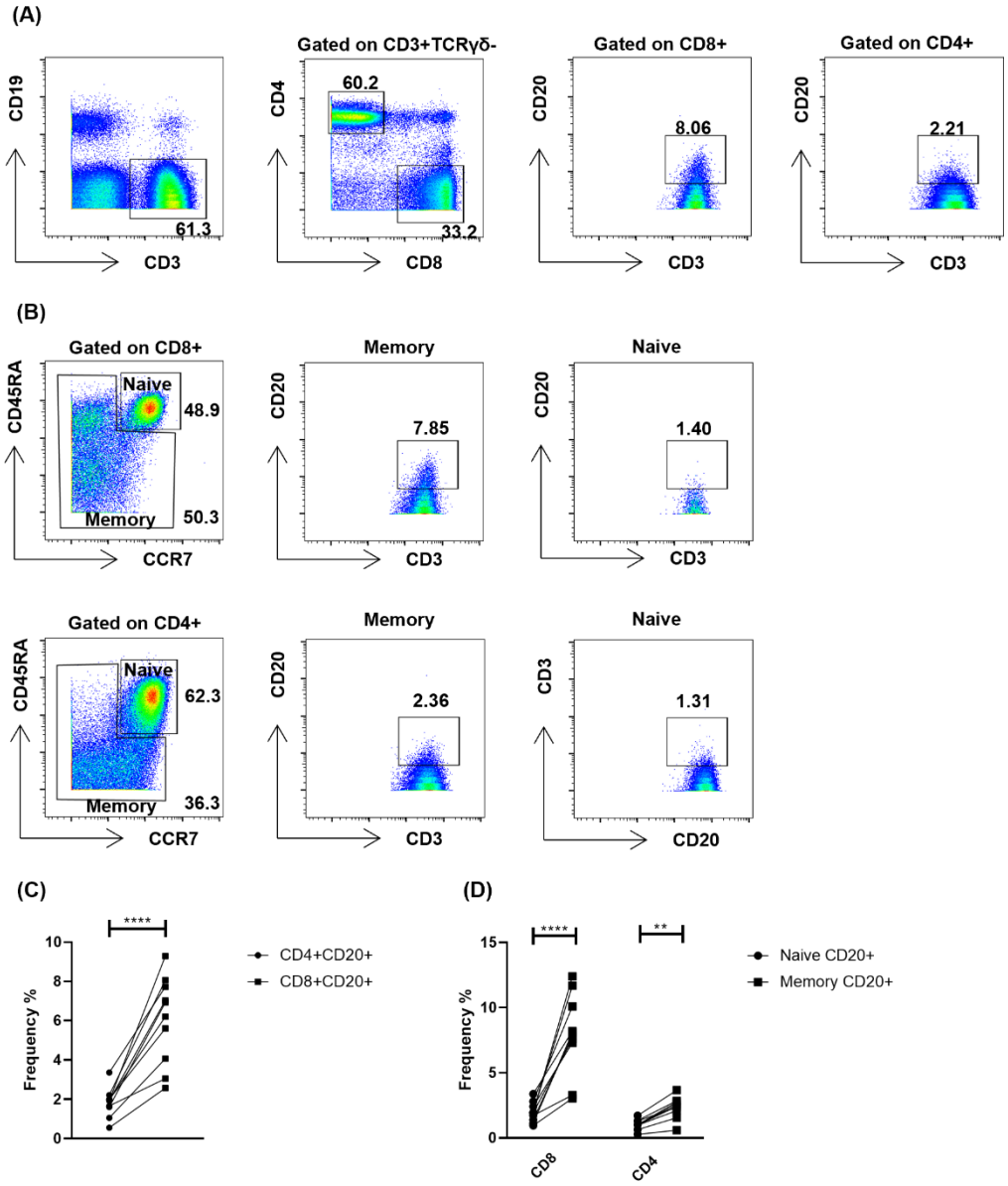

Figure 4.2.1 Mass cytometry data replicate the results from flow cytometry.

Gating strategy to assess CD20+ T cells presence within CD4+ and CD8+ compartments using PBMCs isolated from healthy donors (A). Representative of the memory phenotype of the CD8+/CD4+ CD20+ T cells (n=10) (B). Mann-Whitney test. ** P < 0.005, **** P < 0.0001.

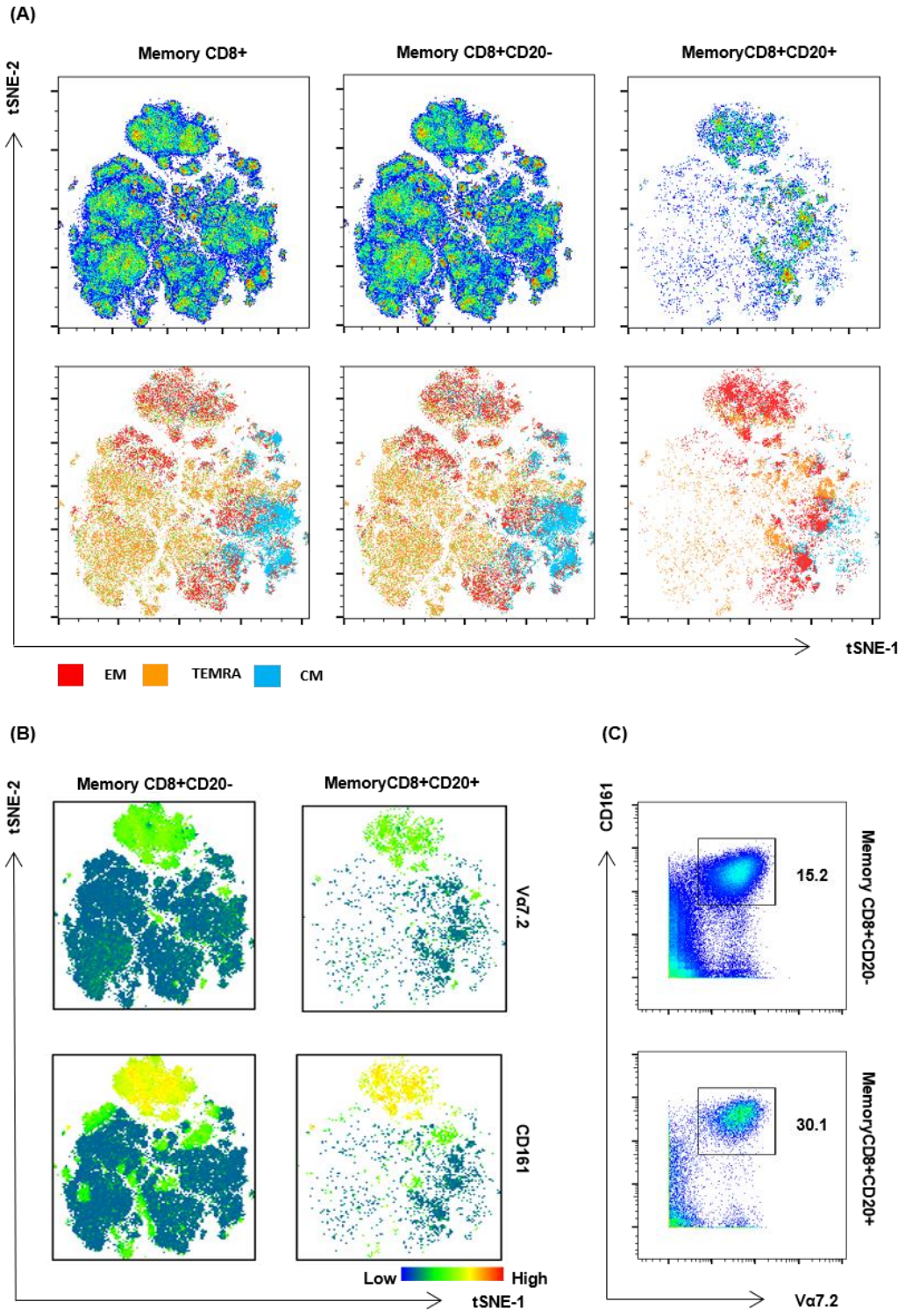

Figure. 4.2.2 Expression of CD20 by Vα7.2+CD161+ T cells.

CD8+CD20+/- cells concatenated from all the donors were analysed using tSNE and pre-gated Tem, Temra and Tcm were applied to the generated plots **(A).** Representative of the CD20 expression intensity on tSNE generated plots **(B).** Representative of Vα7.2+CD161+ percentages among memory CD20+/- pre-gated cells **(C).** tSNE; t-distribute stochastic neighbour embedding, Vα7.2; TCRAV7S2.

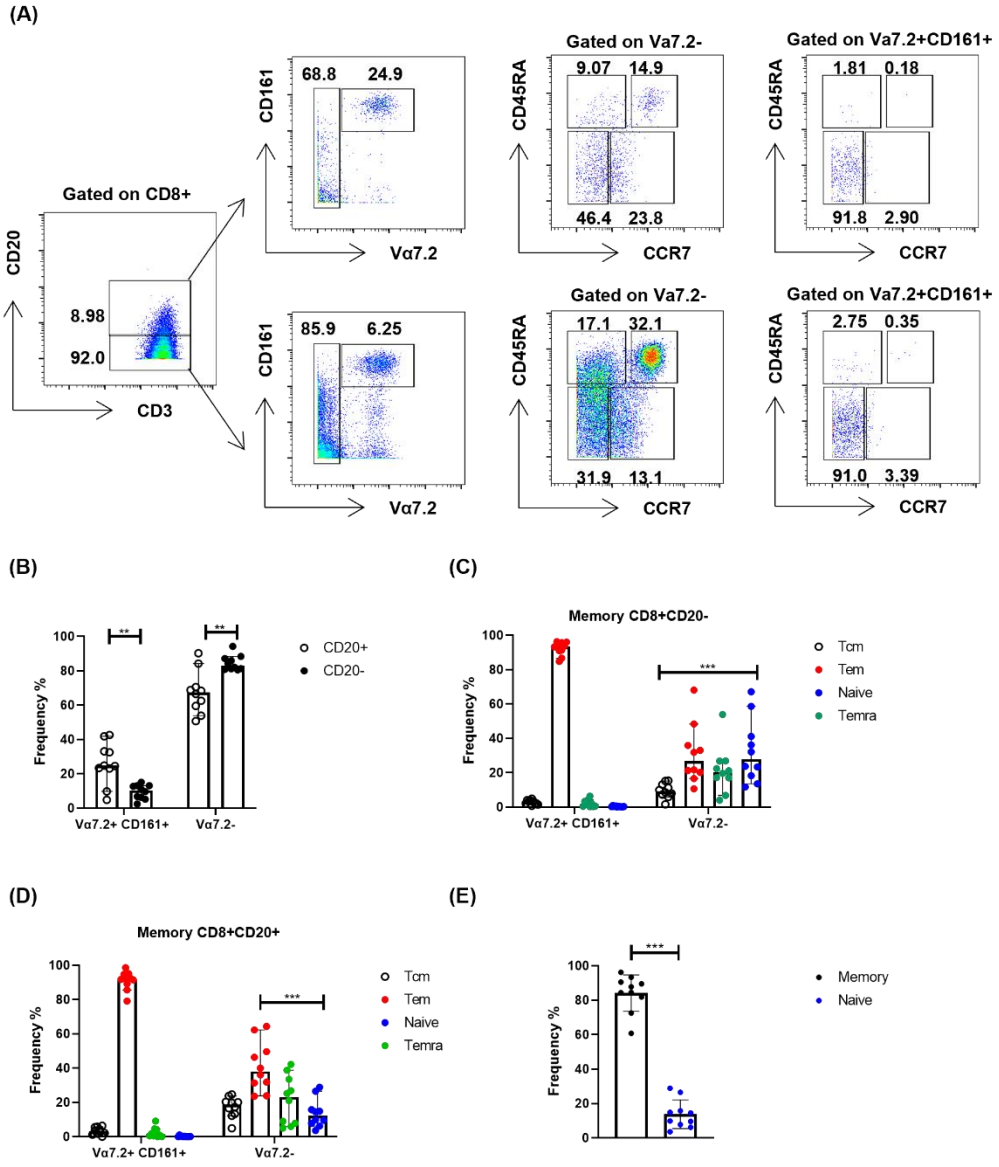

Figure 4.2.3 Vα7.2+CD161+ population comprise more of the CD20+ compartment.

CD8+CD20+/- cells divided into Va7.2+CD161+and Vα7.2- (CD161+/-) and the memory phenotype were analysed using CD45RA and CCR7 **(A).** The percentages of Vα7.2+CD161+CD20+/- were used to show the difference between Vα7.2+ CD161+ CD20+/- cells **(B).** Pere-gated Vα7.2+CD161+ and Vα7.2- (CD161+/-) were used to show their memory phenotype from CD20- **(C)** and CD20+ **(D).** CD8+CD20+Vα7.2- cells were used to show that CD20+ mainly show memory phenotype (n=10) **(E).** Mann-Whitney test. ** P < 0.005, *** P < 0.0005. Vα7.2; TCRAV7S2.

4.2.4 Vα7.2+ CD161+comprise more CD8+ and show low frequency of CD20

Next, a gating strategy was established to assess the expression of CD20 by the Vα7.2+ CD161+ cells. First, single live CD3+CD19-TCRγδ- cells were gated, and from this population the Vα7.2+CD161+ cells were gated. The Vα7.2+ CD161+ cells were used to assess the expression of CD4 and CD8 within the Vα7.2+ CD161+ gated cells **(Fig 4.2.5A)**. About 80% of these Vα7.2+ CD161+ cells were CD8+ followed by less than 15% double negative (CD4-CD8-) and finally almost zero % of CD4+ **(Fig 4.2.5B)**.

4.2.5 Vα7.2+ CD161+ CD20- cells express more CD4 than the Vα7.2+ CD161+CD20+ population

Similar to the Vα7.2- CD20+ population, Vα7.2+ CD161+CD20+ cells showed more CD8+ cells than CD4+ and double negative (CD8-CD4-) cells **(Fig 4.2.5A)**. In fact, comparing the percent of CD8+, CD4+ and double negative cells between the Vα7.2+ CD161+CD20+ and the Vα7.2+ CD161+CD20- populations revealed similar percentages of CD8+ and double negative cells. However, Vα7.2+ CD161+CD4+ cells were found within the CD20- population and only a few within the CD20+ subset **(Fig 4.2.5B,C,D)**.

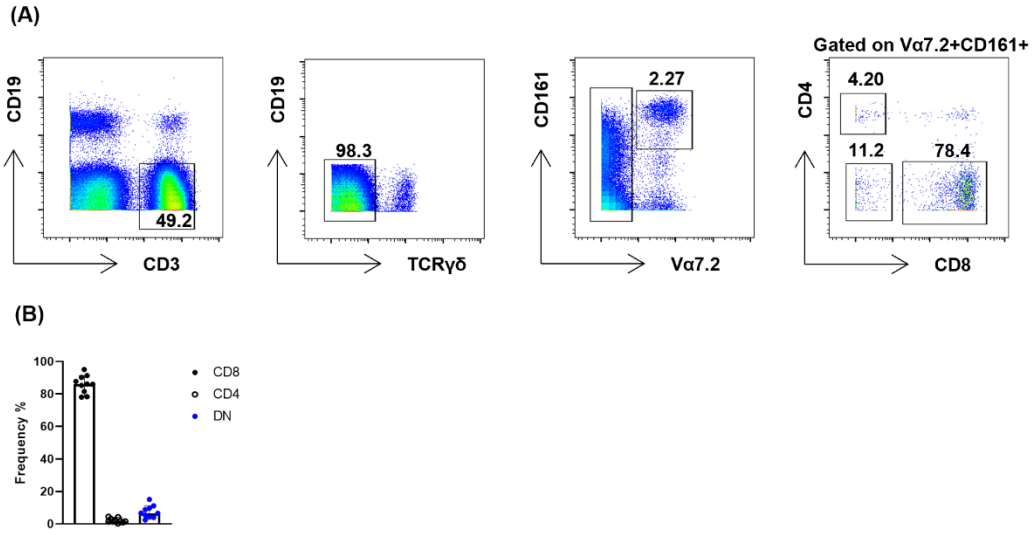

Figure 4.2.4 Vα7.2+ CD161+ comprise more CD8+ and show low frequency of CD20.

Vα7.2+ CD161+ cells (Vα7.2+CD161+) cells were gated by gating CD3+CD19-TCRγδ-Vα7.2+CD161+ population and assessed for the expression of CD4 and CD8 **(A).** The percentages CD8+, CD4+ and double negative (CD8-CD4-) were calculated **(B).** Mann-Whitney test. * $P < 0.05$ (n=10). TCRγδ; TCR-gamma delta, Vα7.2; TCRAV7S2.

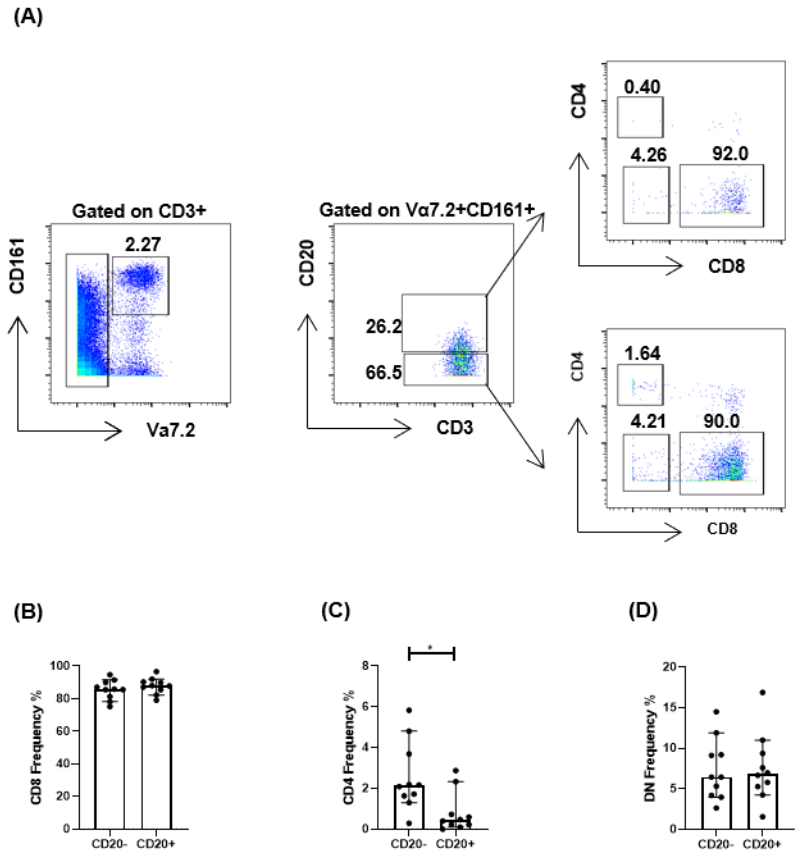

Figure 4.2.5 Vα7.2+ CD161+ CD20- population express more CD4 than the CD20+ population.

CD3+CD19-TCRγδ- population were divided into Va7.2+CD161+and Vα7.2- (CD161+/) and the Vα7.2+ CD161+ cells phenotype were assessed in the CD20+ and CD20- populations using CD8 and CD4 markers **(A).** The frequencies of CD8+ **(B),** CD4+ **(C),** and double negative (CD8-CD4-) **(D)** were assessed (n=10)**.** Mann-Whitney test. * P< 0.05. Vα7.2; TCRAV7S2.

4.2.6 Vα7.2+ CD161+ CD8+CD20+ show similar phenotype to the CD20- compartment

Since Vα7.2+CD161+CD8+CD20+ cells constitute a higher percentage of the Vα7.2+ CD161+CD20+ cells, further investigation was needed through comparing Vα7.2+ CD161+CD8+CD20+ cells with Vα7.2+ CD161+CD8+CD20- cells using different markers. Using the available markers, we found that the expression of CD56, CD27 and CD127 were similar between Vα7.2+ CD161+CD8+CD20+ and CD20- populations and no significant differences were detected **(Fig 4.2.6A,B,C)**.

4.2.7 Vα7.2+ CD161+ CD20+ cells show similar PD-1 and CD57 levels to the CD20- compartment

Further to CD27, CD127 and CD56, PD-1 and CD57 expression were assessed for Vα7.2+ CD161+CD8+CD20+/- populations. The Vα7.2+ CD161+ cells showed similar expression of both markers within either CD20+ or CD20- compartments **(Fig 4.2.7A,B)**.

4.2.8 Memory CD20+ T cells express more longevity and suppression markers than memory CD20- T cells

To further investigate the phenotyping of the different memory subsets phenotype within the CD20+ and CD20- T cells, Tcm, Tem and Temra were gated to assess the expression of a number of aditional markers. First, CD27 was used to assess the longevity of generated memory within both CD20+ and CD20- populations. Despite the similar levels between CD20+ Tcm and CD20- Tcm, the Tem and the Temra subsets showed significantly higher levels of CD27 within the CD20+ population as compared to CD20- Tem and Temra **(Fig 4.2.8A)**. Furthermore, similar results were observed for CD127 **(FIG 4.2.8B)**. Although memory CD20+ showed higher expression of the longevity markers, they showed significantly higher expression of the exhaustion markers PD-1 and CD57 compared to memory CD20- cells, including Tcm, Tem and Temra **(Fig 4.2.8C,D)**.

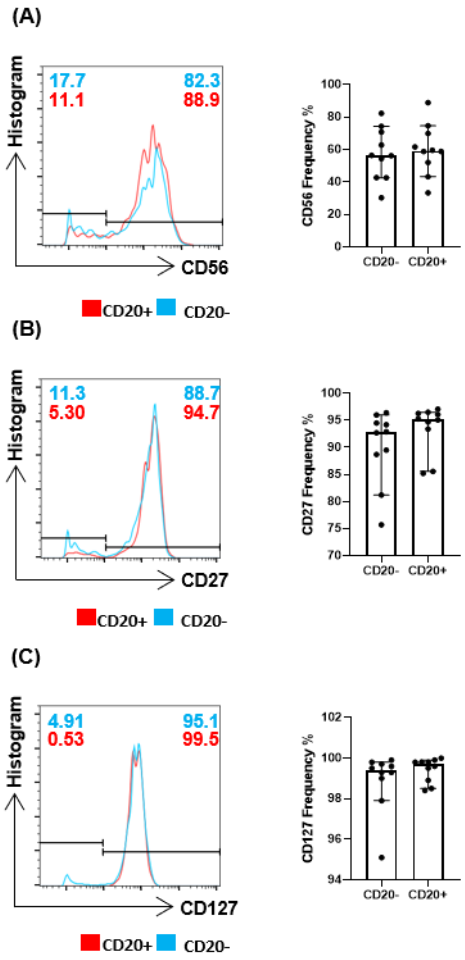

Figure 4.2.6 Vα7.2+ CD161+ CD8+CD20+ show similar phenotype to the CD20- compartment.

Vα7.2+ CD161+CD8+CD20-/+ population were assessed for the expression of CD56 **(A),** CD27 **(B),** and CD127 **(C)** (n=10)**.**

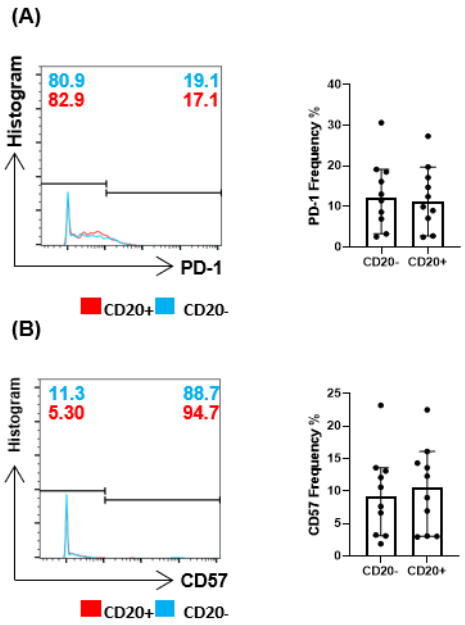

Figure 4.2.7 Vα7.2+ CD161+ CD20+ show similar PD-1 and CD57 levels to the CD20- compartment.

Vα7.2+ CD161+CD8+CD20-/+ population were assessed for the expression of PD-1 **(A) and** CD57 **(B)** (n=10)**.**

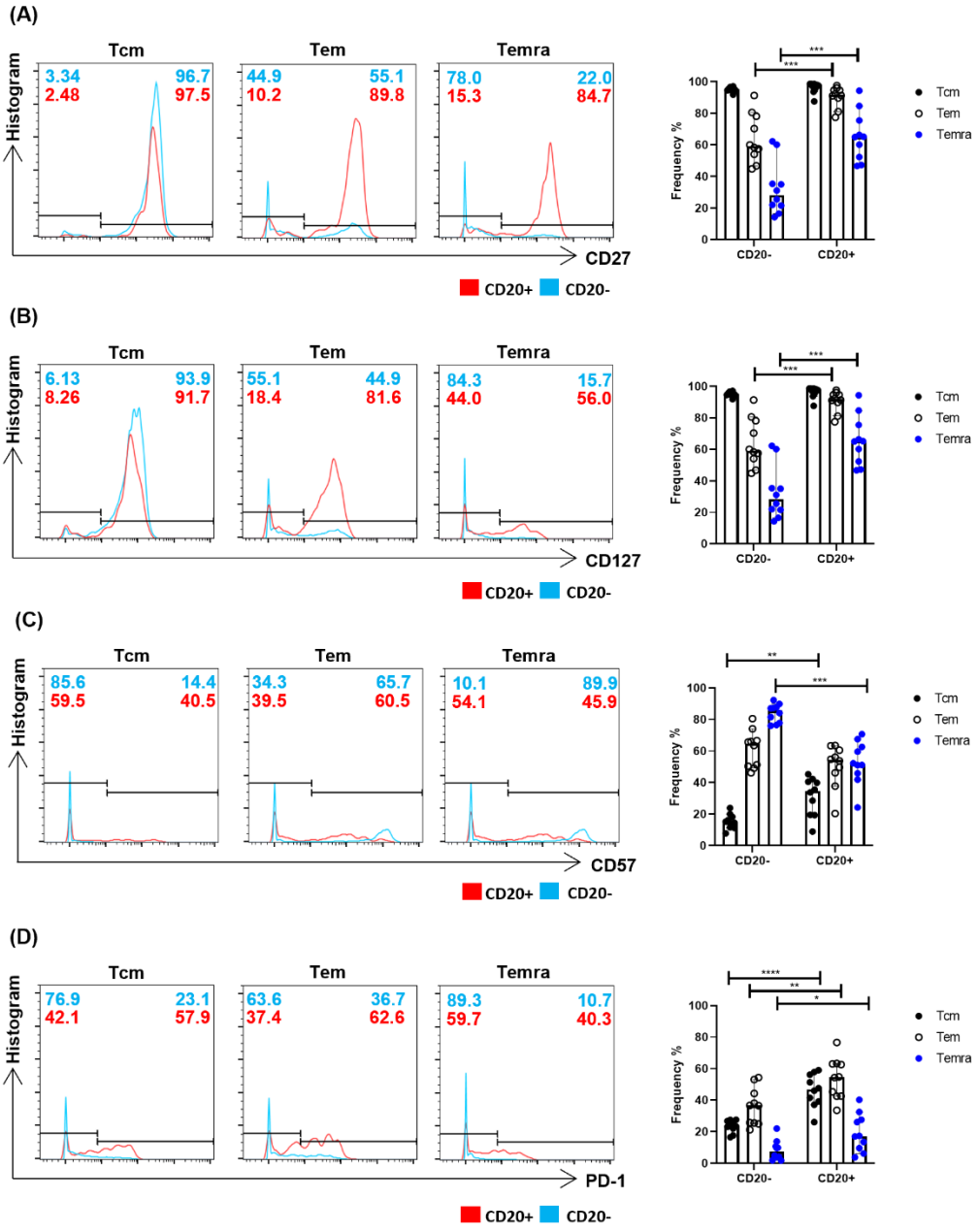

Figure 4.2.8 Memory CD20+ T cells express more longevity and suppression markers than memory CD20- T cells.

CD8+CD20+/- were divided using CD45RA and CCR7 into Tcm (CD45RA+CCR7+), Tem (CD45RA+CCR7-) and Temra (CD45RA-CCR7-). The expression of CD27 **(A)** CD127 **(B)** CD57 **(C)** PD-1 **(E)** were assessed in the CD20+ and CD20- from each population (n=10) **.** Mann-Whitney test. * $P < 0.05$, ** $P < 0.005$, *** $P < 0.0005$, **** $P < 0.0001$. Tcm; central memory, Tem; effector memory, Temra; effector memory CD45RA revertant.

4.2.9 Assessment of cytotoxic markers for CD20+ and CD20- compartments from both Vα7.2+ CD161+ and Vα7.2- populations

In addition to the memory phenotype, we assessed the cytotoxic markers from the Vα7.2+CD161+ cells and the Vα7.2-CD20+/- T cells through the assessment of perforin, granzyme-A and granzyme-B expression. Comparing Vα7.2-CD20- and CD20+ cells revealed variation in the expression of perforin and granzymes-A and B. The Vα7.2-CD20+ showed the highest percent of perforin expression, while the Vα7.2- CD20- expressed significantly more granzyme A and B **(Fig 4.2.9A)**. On the other hand, both the Vα7.2+ CD161+CD20+ and CD20- show similar pattern of expression, where over than 80% of them express perforin and granzyme-A. Granzyme-B showed very low levels of expression, where less than 10% of them express granzyme-B **(Fig 4.2.9B)**.

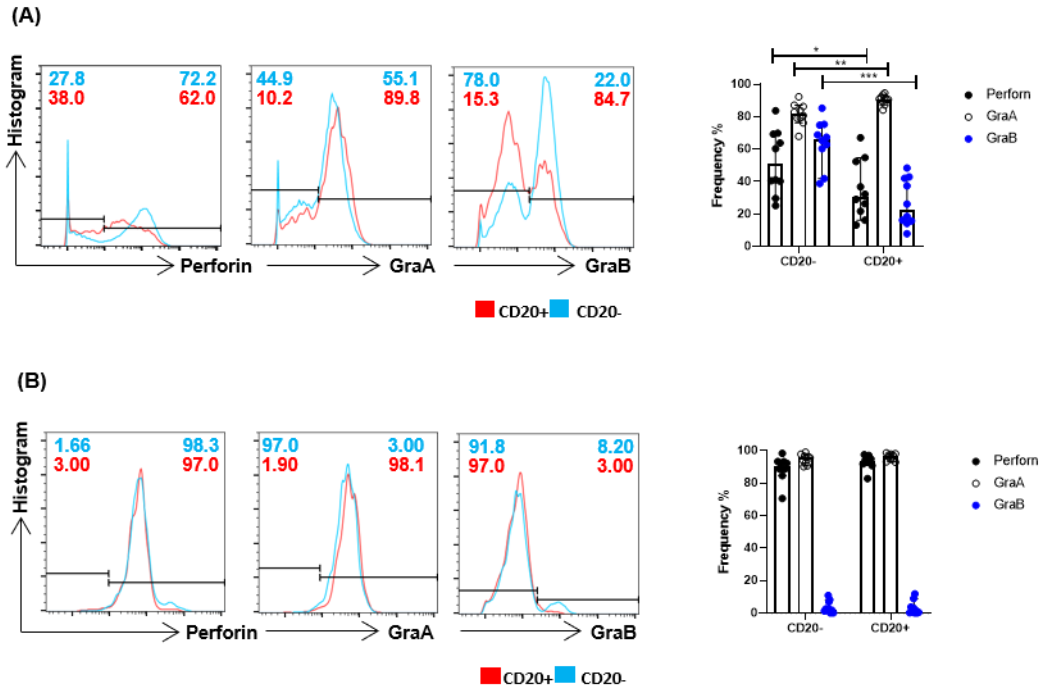

Figure 4.2.9 Assessment of cytotoxic marker for CD20+ and CD20- compartments form both Vα7.2+ CD161+ and Vα7.2- populations.

Memory CD8+CD20-/+ populations were assessed for the expression of Perforin, GraA and GraB from Vα7.2- (CD161+/-) CD20+/- **(A),** and Vα7.2+ CD161+CD20+/- **(B)** (n=10)**.** Statistical difference was measured using Mann-Whitney test. * $P < 0.05$, ** $P < 0.005$, *** $P < 0.0005$. Vα7.2; TCRAV7S2.

4.3 Discussion

The phenotype of CD20+ T cells remains unclear; however, it has been shown by others and our data in chapter one, using flow cytometry, that most of the CD20+ T cells are CD8+ with more memory phenotype over naïve cells (Schuh et al., 2016, von Essen et al., 2019). Mass cytometry allows for the use of up to 60 different markers in a single panel and the ability to use tSNE and other logarithmic tools to analyse the phenotype of those cells. In this study the tSNE analysis was performed using all of the T cell markers in the panel **(Table 2.7.1.1)**. Due to the COVID-19 pandemic, we decided to use mass cytometry data from a previously published study where they used 10 PBMCs isolated from healthy donors for the mass analysis using 38 different mass cytometry antibodies (Toghi Eshghi et al., 2019). However, the sensitivity of this technique can be lower than flow cytometry and the ability to detect rare subsets of cells, such as CD20+ T cells, can be problematic. Therefore, we chose to compare data from mass cytometry to the flow data and use the previous shown findings about the CD20+ T cells to add another internal control to the selected data. In agreement with flow data, CD20+ T cells tended to be more within the memory CD8+ compartment **(Fig 4.2.1C,B)**. Hence, CD20+ T cells from flow cytometry resemble the data from mass cytometry, allowing further investigation of these cells by mass cytometry.

The presence of different antibodies in the staining panel used for this dataset and especially the presence of Vα7.2 and CD161, which can be used to gate MAIT cells, allowed us to detect a novel MAIT-like cell subset that expresses CD20+ **(Fig 4.2.2B,C)**. MAIT cells are characterised by the expression of TCRα Vα7.2 and their higher expression of CD161. It has been shown that they develop in the thymus and are able to detect non-peptide antigens through an MHC-like protein MR-1. Due to the abundance of these cells within the gut and their responses against different bacteria, they have been named mucosal-associated invariant T cells (Godfrey et al., 2019).

Similar phenotypic and functional features were observed between MAIT and CD20+ T cells. First, MAIT cells resembled a Tem phenotype, while CD20+ T cells showed significantly higher overall memory cells than naïve; which would support the possibility of MAIT cells being CD20+ **(Fig 4.2.3 C,D,E)**. Second, like CD20+ T cells, more than 80% of the total MAIT cells were CD8+, which can highlight the similarities between CD20+ T cells and MAIT cells **(Fig 4.2.4B,D)**. Third, the ability of these cells to produce IL-17, express CCR6 and acquire a memory phenotype links to a potential CD20+ phenotype (Dusseaux et al., 2011, Martin et al., 2009). Like MAIT T cells, CD20+ T cells usually show a memory phenotype **(Fig 4.2.3C,D)**, and many CD20+ T cells expressed CCR6 (von Essen et al., 2019) Finally, upon stimulating sorted CD20+ T cells, they were able to produce IL-17 (Schuh et al., 2016).

Further analysis to compare the differences between CD20+ and CD20- MAIT-like cells revealed no difference in terms of the expression of either; CD27, CD127, CD56, PD-1 orCD57 **(Fig 4.2.6 and 4.2.7)**. However, comparing the non-MAIT (Va7.2-CD161+/-) CD20+ and CD20- different memory subsets revealed differences in the expression of other markers. First, CD27 and CD127 showed significantly higher expression on CD20+Tem and Temra compared to the CD20- subsets.

Although, CD27 and CD127 levels are usually reduced on highly differentiated cells, especially Tem and Temra, CD20+ cells showed significantly higher levels of both markers compared with CD20- cells within both Tem and Temra populations (Romero et al., 2007, Hamann et al., 1999) (**Fig 4.2.8A,B)**. In fact, CD27 is a co-stimulatory molecule and the expression of that marker, in addition to CD28 may indicate the ability of the CD20+ cells to proliferate (Mojumdar et al., 2012), while CD127, which is an IL-7 receptor molecule, can promote the survival of the T cells (Joshi et al., 2007). The loss of CD27 expression can be

used to indicate poor telomerase activity resulting in terminally differentiated cells which can be highly senescent (Hamann et al., 1999).

T cell senescence refers to the status of cells that differentiate towards the end stage of differentiation and demonstrate higher cytotoxic ability with significant low proliferation compared to other cells. It has been proposed that Temra in humans are senescent cells that can be more cytotoxic with low proliferative activity (Larbi and Fulop, 2014). CD45RA+CD27- cells display a senescent phenotype through the expression of p38 MAPK (Callender et al., 2018). CD27 and CD127 have been used to indicate effector CD8+ that would survive to become long-lived memory cells, where the expression of those markers can promote the formation of memory cells following effector CD8+ contraction (Joshi et al., 2007, Kaech et al., 2003). Therefore, the higher expression of these markers by Tem and Temra CD20+ T cells may indicate the higher proliferation ability of these cells and a better survival rate over equivalent CD20- T cells. The low proliferation ability of CD20+ T cells has been reported previously (Wilk, Witte et al. 2009). However, another study showed that post-CNS antigenic stimulation, the CD20+ T cells showed higher proliferative capacity over the CD20- T cells (von Essen, Ammitzbøll et al. 2019).

It is well known that PD-1 can be a suppressor marker that can inhibit the pro-inflammatory responses and eventually lead to cell exhaustion. Moreover, it has been approved by the Food and Drug Administration (FDA) as a target for immunotherapy checkpoint blockade in cancer patients to minimise the immune escape mechanisms by which cancer cells can survive immunological responses of cytotoxic cancer-specific CD8+ (Gong et al., 2018). Although PD-1 has been known as a suppressive marker, there is strong evidence that it can be used as an activation marker. To illustrate, upon naïve T cell activation, PD-1 is up-regulated alongside CD69 and CD25, which are well known as activation markers (Ahn et al., 2018). Therefore, PD-1 can be assessed according to the context of the immune response.

The up-regulation of PD-1 during contexts such as cancer can be an indication of T cell exhaustion, while during a normal physiological context it might be an immune tolerance mechanism by which the immune system can avoid autoimmunity. Therefore, the higher expression of PD-1 by the CD20+ T cells **(Fig 4.2.8D)** could be a control mechanism to prevent any damage by these high cytokine producing cells.

Finally, we assessed the cytotoxicity of both CD20+ and CD20- from the MAIT-like and the non-MAIT cells using perforin, GraB and GraA. Although, the ability of CD20+ T cells to produce more cytotoxic molecules compared to the CD20- T cells has been shown before, we found that the non-MAIT memory CD20+ T cells expressed significantly less perforin and GraB compared to the non-MAIT memory CD20- T cells (Schuh et al., 2016, von Essen et al., 2019). Perforin and granzymes, both A and B, are preserved proteins within granules inside the cytotoxic CD8+ which can be released at the immunological synapse causing cell lysis of the infected cells (Voskoboinik et al., 2015).

Interestingly, low perforin producing memory CD8+ T cells have been shown to be CD27+CD28+CCR5+CCR7-IFNγ+ cells. The proposed differentiation stages starts from GraA+GraB-GraK+ to GraA+GraB+GraK+ and finally the terminally differentiated GraA+GraB+GraK- (Bratke et al., 2005). Due to the absence of CD28, CCR5 and GraK from the mass cytometry panel used, testing the same differentiation stages was not possible. However, the presence of CD27 and low GraB expression could be an indication of the stage of differentiation of the CD20+ T cells. Another study using human CD8+ T cells from recipients of the smallpox vaccine have shown that a year after the vaccination, the virus specific CD8+ T cells developed a memory phenotype able to produce Gra A and not Gra B and with low perforin (Rock et al., 2005). Therefore, taking previous results into consideration, both surface markers and cytotoxicity molecules, the memory cells within the CD20+ T cells subset, especially Tem and Temra, showed a less differentiated phenotype

compared to both populations within the memory CD20- T cells. Further experiments measuring the proliferation and function of sorted CD20+ and CD20- T cells will be required to reveal more functional properties of each subset.

Chapter Five: Investigating the phenotype of CD20+ T cells in colorectal cancer

5.1 Introduction

Colorectal cancer (CRC) represents a common cancer and is considered to be the third most diagnosed cancer worldwide (Favoriti et al., 2016). Although, standard treatments can involve surgical resection of the affected tissues, new immunotherapy treatments have been approved including anti-PD1, an immune checkpoint blockade therapy. The target of these blockade treatments includes CD8+ T cells that can mount anti-tumour responses to clear cancerous cells (Farhood et al., 2019). In fact, the number of tumour-specific CD8+ T cells infiltrating tumour microenvironments enhances survival in colorectal cancer (Chiba et al., 2004). Furthermore, cancer associated lymph nodes can be used as a prognostic tool to estimate the metastasis and survival rate of cancer patients (Onitilo et al., 2013).

The presence of CD20+ T cells within lymph nodes has been reported previously (Schuh et al., 2016). A single report in the literature explored the role of CD20+ T cells in ovarian cancer. They found an increase of the CD20+ T cells within ascitic fluid of the ovarian cancer patients over PBMCs isolated from cancer patients and healthy volunteers. The phenotyping of these cells revealed a tendency to have a CD8+ EM memory phenotype able to produce more Th1/Tc1 cytokines, including IFNγ. Although the phenotype of these cells can be promising for anti-tumour responses and tumour regression, the presence of the CD20+ T cells within the ascitic fluid of those patients did not corelate with the response to therapy or disease stages (de Bruyn et al., 2015). Therefore, the original aim of this chapter was to assess the presence of CD20+ T cells within different types of tumour, including breast cancer, colon cancer and CRC. Due to the COVID-19 pandemic, my own analysis was restricted to breast and colon cancers. We used an online mass cytometry data set using tumour associated lymph nodes and PBMC isolated from patients with CRC to carry out a more detailed phenotypic analysis (de Vries et al., 2020).

5.1.1 Aims

1- Check the presence of CD20+ T cells within tumour and adjacent tissues of colon cancer and breast cancer, and matched blood and lymph nodes of CRC patients.

2- Characterize the phenotype of CD20+ T cells within those patients.

3- Determine the differences between CD20+ and CD20- T cells through the assessment of the CD20+ T cell phenotype within CRC patients.

5.2 Results

5.2.1 CD20+ T cells can be detected within tumour and adjacent breast tissue

The presence of CD20+ T cells within cancer patients was previously reported in ascitic fluid from ovarian cancer patients (de Bruyn et al., 2015). However, their presence within solid tumours has not been reported. Therefore, we used single cell suspensions from tumour and adjacent tissue and PBMCs (isolated from matched obtained blood before the operation from the same patient). A gating strategy was established to identify CD8+ and CD8- T cells (gated from single cells CD3+CD19- T cells) **(Fig 5.2.1A)**. Interestingly, CD20+ T cells were detected in both tumour and adjacent tissue from both CD8+ and CD8- T cells, although the percent of CD20+ T cells in the adjacent tissue was slightly higher than the tumour tissue. On the other hand, matched blood showed a very low percentage of the CD20+ T cells below the level of isotype control **(Fig 5.2.1B)**.

5.2.2 CD20+ T cells can be detected within tumour and adjacent colon tissue

To further expand the analysis of the role of CD20+ T cells within the tumour microenvironment, samples from colon tumour patients were used. The same gating strategy in **Fig 5.2.1A** was used for the determination of CD20+ T cells in these patients. CD20+ T cells were detected in both tumour and adjacent tissue. However, the percentages of the CD20+ T cells was higher on the adjacent tissue than the tumour tissue **(Fig 5.2.2B)**.

5.2.3 The relation between CD20 and CD39 expression on T cells

Recently, CD39 was reported as a bystander marker that can be used to assess tumour specific CD8+ T cells, where CD39- tumour infiltrated cells are enriched with tumour-specific T cells (Simoni et al., 2018b). Therefore, we studied the possible correlation between CD20 expression and CD39 within T cells from matched blood, adjacent and tumour tissues. A gating strategy was developed to assess CD20 and CD39 expression within pre-gated

CD3+CD19-CD8+ and CD8- populations **(Fig 5.2.3A)**. In both CD8+ and CD8- populations, CD20+ CD39+ cells showed a similar percentage to the CD20-CD39+ population within the tumour tissue. However, in adjacent tissue the CD8-CD20+ CD39+ population was more than the CD8-CD20-CD39+ population **(Fig 5.2.3B)**. Due to the COVID-19 pandemic, it was not possible to complete further analysis of the breast and colon cancer tissues.

5.2.4 CD20+ T cells can be found in tumour and adjacent tissue of colorectal cancer patients

We next used publicly available online previously published data to analyse the tumour CD20+ T cells. Mass cytometry datasets from CRC patients, including tumour associated lymph nodes, normal tissue, tumour tissue and matched blood from the same patients, were analysed **(Table 2.7.2.1) (Table 2.7.2.2)** (de Vries et al., 2020). A gating strategy was developed to assess the presence of CD20+ T cells within the tumour and the adjacent tissue by gating CD3+TCRγδ-CD8+CD20+ or CD4+CD20+ population **(Fig 5.2.4A)**. CD20+ T cells were found within both tumour tissue and normal adjacent tissue at similar levels **(Fig 5.2.4B)**. However, both CD4+ and CD8+ T cells had CD20+ cells among both populations. As expected the tissues showed more memory phenotype compared to the naïve population. Using CCR7 and CD45RO, four different populations can be gated, where CCR7+CD45RO- represent naïve, CCR7+CD45RO+Tcm, CCR7-CD45RO- Temra and CCR7-CD45RO+ Tem. Although CD20+ T cells can be enriched within Tcm, Tem and Temra, they were not present within naïve subset from either CD4+ and CD8+ cells **(Fig 5.2.4C,D)**.

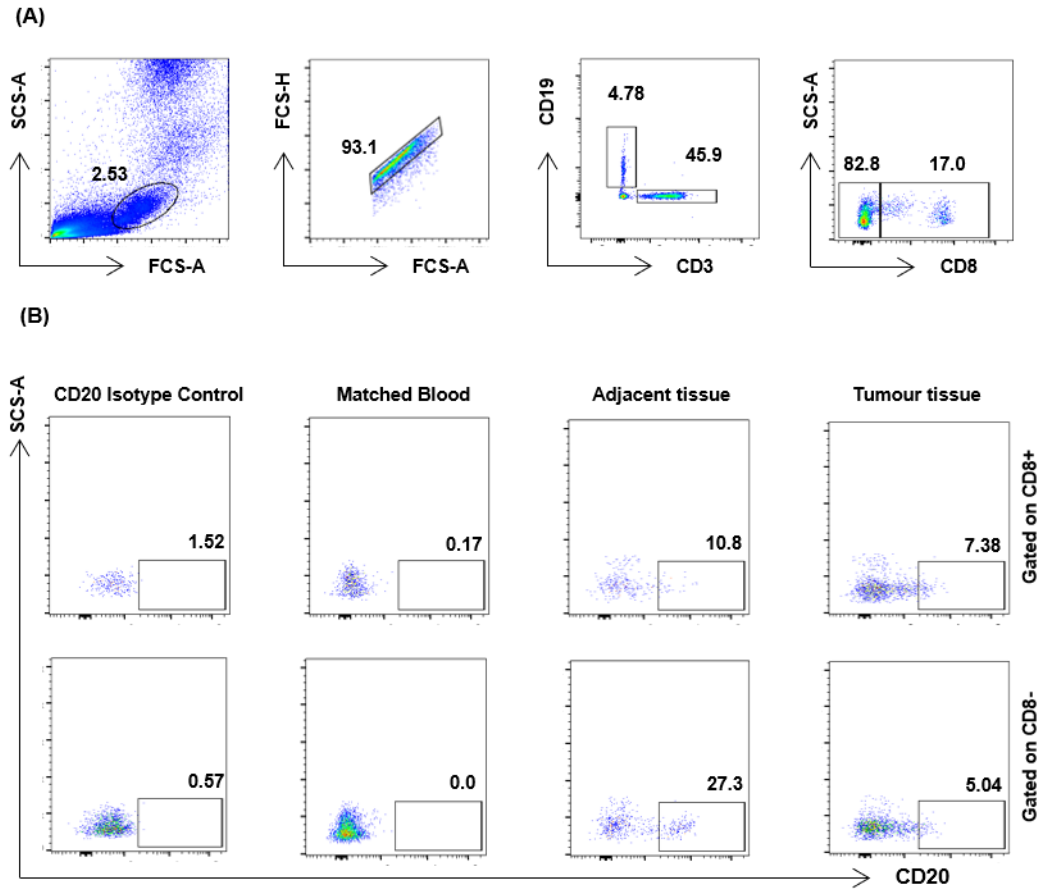

Figure 5.2.1 CD20+ T cells can be detected within tumour and adjacent breast tissue.

Tumour and normal tissues and matched blood (pre-operational blood from the same patient) from a patient with breast cancer were used for flow cytometry analysis. CD8+/- were gated from the singlet cell CD3+CD19- population **(A)**. CD20+ T cells within the CD8+ and CD8- compartments were gated according to the isotype control for CD20 (n=1) **(B)**.

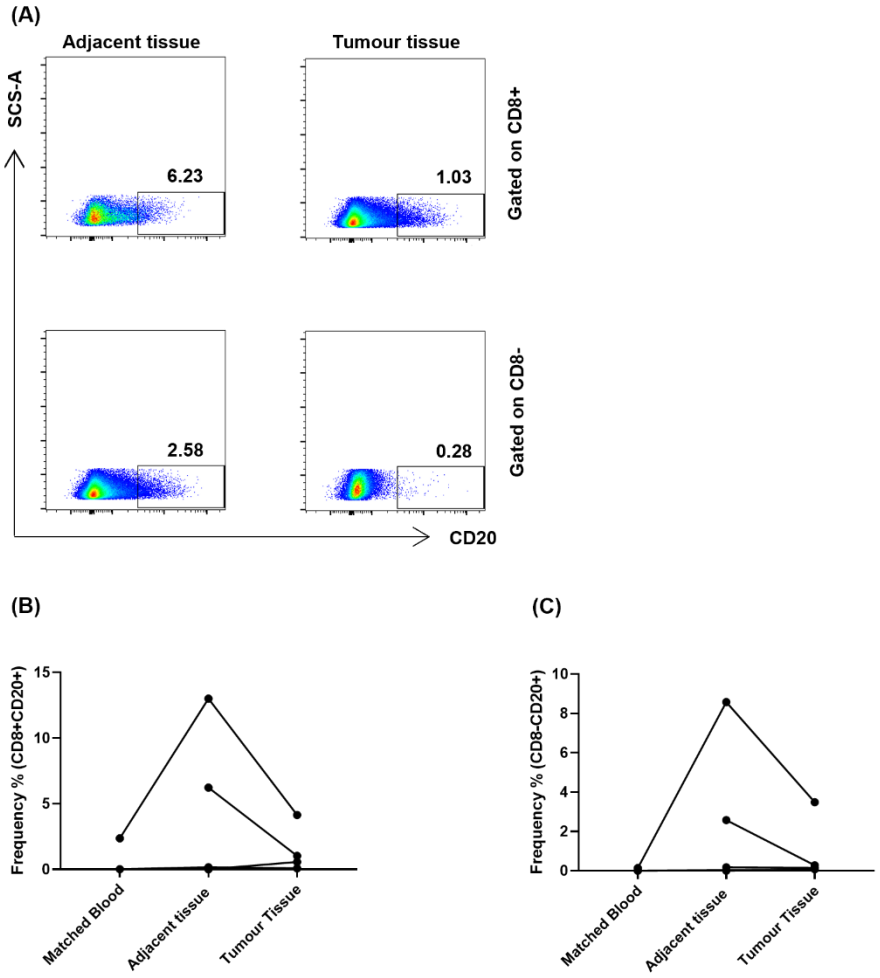

Figure 5.2.2 CD20+ T cells can be detected within tumour and adjacent colon tissue.

Colon tumour and adjacent tissues were used to obtain single cell suspension for flow analysis. Representative dot plots to show the percentage of CD20+ cells within CD8+/- T cells subsets (gated on CD19- CD3+ CD8+/-) **(A)**. The percentages of CD20+ CD8+ **(B)** and CD8- **(C)**cells were compared between adjacent tissue and tumour tissue from three patients **(B), (C)** (n=3); each line represents a separate patient.

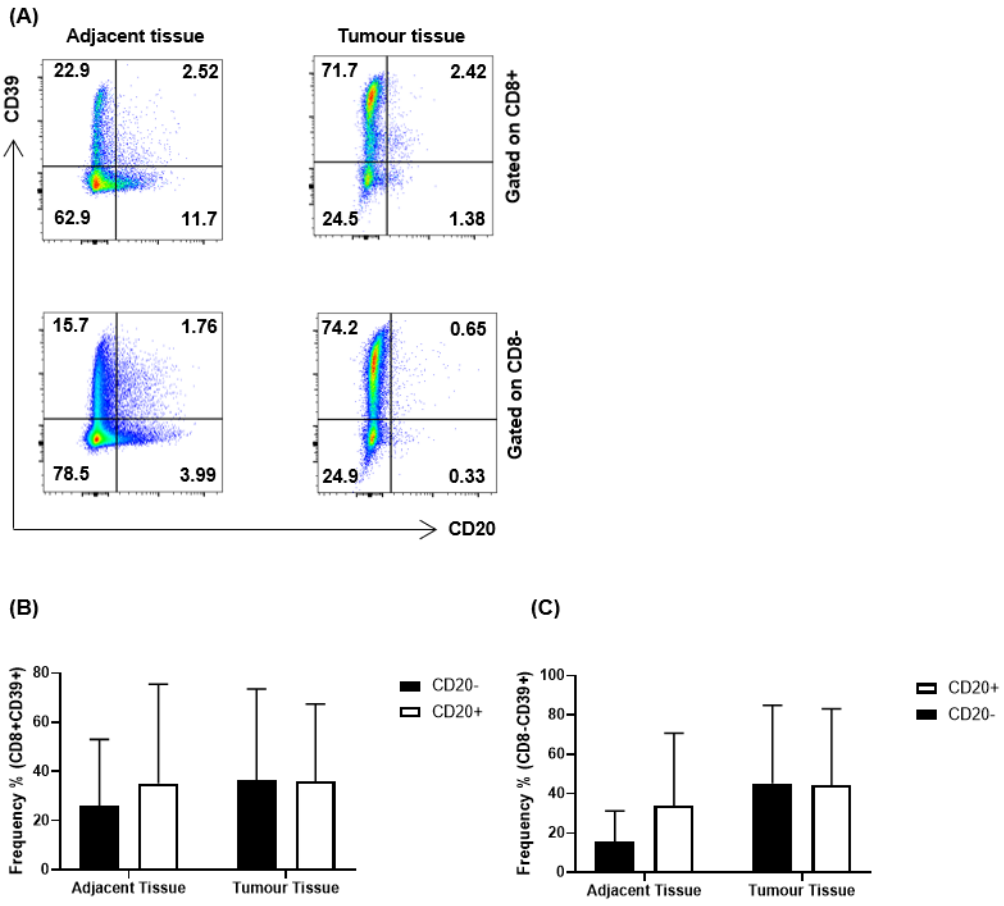

Figure 5.2.3 The relation between CD20 and CD39 expression on T cells.

Representative dot plots to show the correlation between CD20 and CD39 expression on CD8+/- populations (gated from CD3+CD19- cells from colon adjacent and tumour tissues) **(A)**. The cells expressing CD20, CD39, or both, from the CD8+ population **(B)** and CD8- population **(C)** were assessed using three colon cancer patient's adjacent and tumour tissues (n=3).

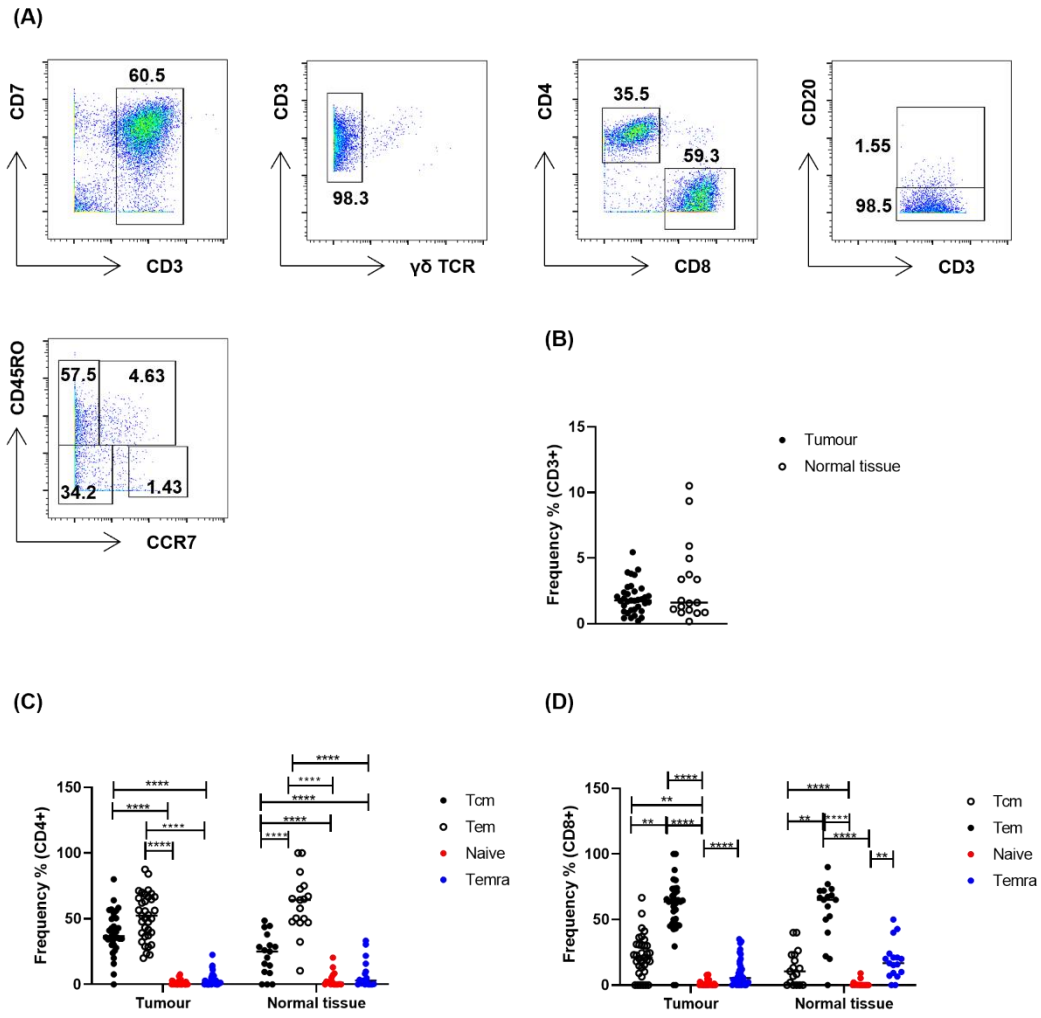

Figure 5.2.4 CD20+ T cells can be found in tumour and adjacent tissue of colorectal cancer patients.

Gating strategy to assess CD20+ T cells within different tissues using cells isolated from tumour and adjacent tissues of colorectal cancer patients **(A).** The percentage of CD3+TCRgd-CD8+CD20+ cells from adjacent and tumour tissues **(B).** CD8+CD20+/- memory phenotype was assessed using CCR7 and CD45RA to gate Tcm, Tem, naïve, Temra and Tstm **(C)**. Percentages of each memory population from CD8+CD20+ population within adjacent and tumour tissues of all patients (adjacent tissue n=17, tumour tissue n=35). Mann-Whitney test. * $P < 0.05$, *** $P < 0.0005$, **** $P < 0.0001$.

5.2.5 CD20+ T cells can be found in blood and lymph nodes of Colorectal cancer patients

In order to assess the presence of CD20+ T cells within the lymph nodes and the blood of these CRC patients, live CD3+TCRγδ-CD8+ T cells were gated followed by CD20+ and CD20- gates **(Fig 5.2.5A)**. CD20+ T cells were detected within the lymph nodes and the blood of CRC patients. Indeed, there was no significant difference between PBMCs and lymph node CD20+ T cells, however the lymph node percentages showed slightly higher percentages in some patients but not others **(Fig 5.2.5B)**. As in previous analyses, CD20+ T cells comprised more memory cells than naïve in both lymph nodes and PBMCs; Tcm, Tem and Temra showed significantly higher levels within CD20+ T cells compared to naïve **(Fig 5.2.5D)**. The same results were observed in lymph nodes, although Temra showed significantly lower levels than in the blood. As expected, Tcm and naïve both showed significantly higher levels within lymph nodes compared to blood **(Fig 5.2.5E)**.

5.2.6 Assessing the memory phenotype of CCR6+CD161+, MAIT-like, cells

Due to the absence of Vα7.2 from the panel used for this study, and following the previous finding in Chapter 4 where a proportion of the CD20+ T cells expressed Vα7.2 and CD161, we assessed the presence of MAIT-like cells in these samples using the combination of CCR6 and CD161. By gating the CCR6+CD161+ population from CD8+ T cells, it can be noticed that, within the represented sample, they showed a memory phenotype, with the remainder of the cells showing 28.1% naïve cells, 30% Tcm, 27.6% Tem and 12.3% Temra **(Fig 5.2.6 A)**. Furthermore, using the t-SNE visualizing tool, a population that expresses CCR6 and high CD161 could be separated from other populations **(Fig 5.2.6B)**.

5.2.7 CCR6+CD161+ cells represent a higher percentage of CD8+CD20+ T cells compared with CCR+CD161- T cells

We next analysed the abundance of CCR6+CD161+ cells from the total CD20+ and CD20- T cells **(Fig 5.2.7A)**., The CCR6+CD161+ population constituted a higher percentage of the total CD20+ T cells in blood. On the other hand, CCR6+CD161+ cells within the CD20- population were of a lower percentage as compared to the CD20+ population. CCR6+CD161+ and CCR6+CD161- cells showed no significant difference within the CD20- compartment **(Fig 5.2.7B)**.

In the lymph nodes there was a significant higher percentage of CCR6+CD161- than CCR6+CD161+ cells in both CD20+ and CD20- populations **(Fig 5.2.7C)**.

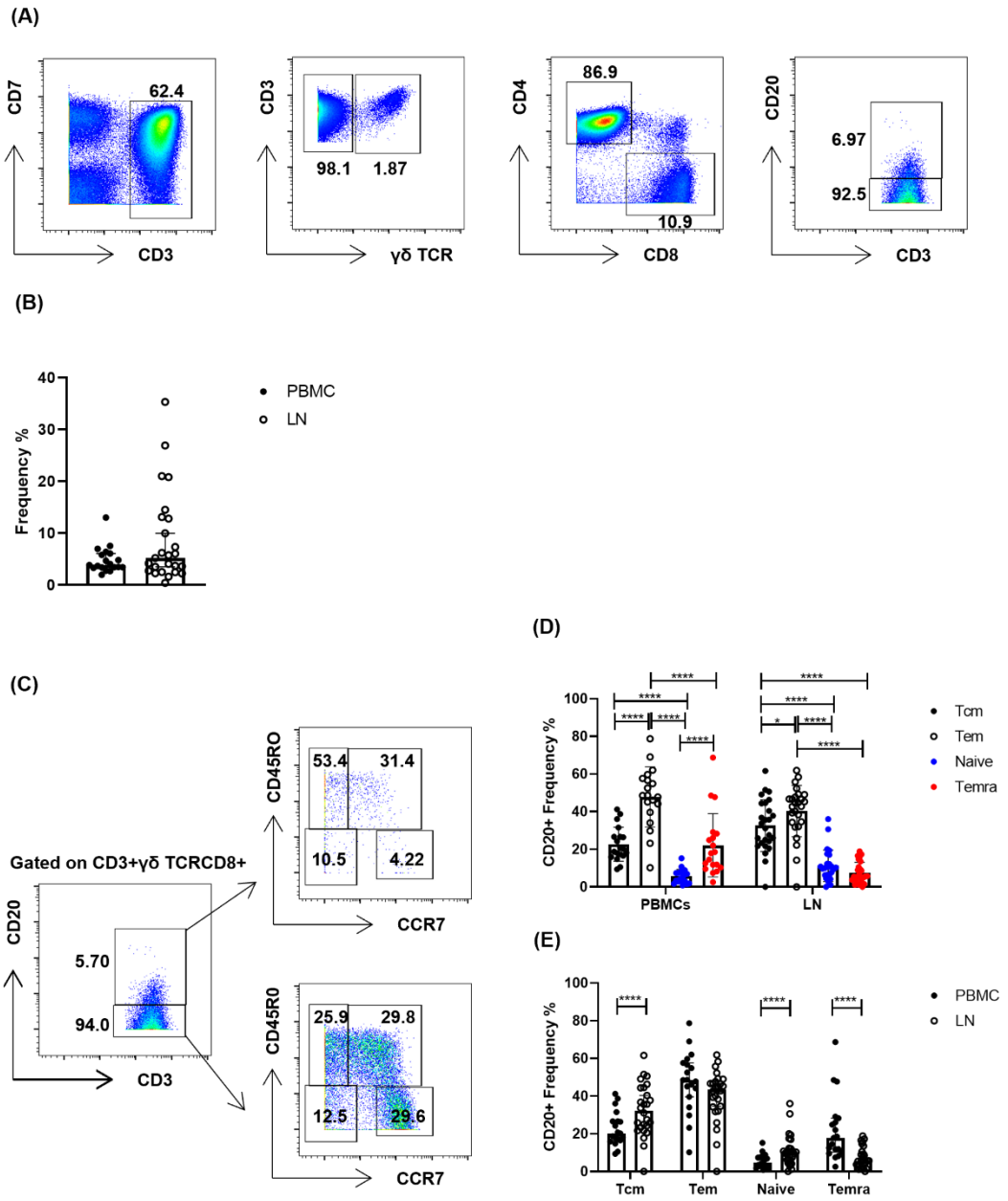

Figure 5.2.5 CD20+ T cells can be found in blood and lymph nodes of colorectal cancer patients.

Gating strategy to assess CD20+ T cells using PBMCs isolated from matched blood and lymph nodes (LN) of colorectal cancer patients **(A).** The percent of CD3+ TCRγδ- CD8+CD20+ cells from PBMCs and lymph nodes **(B).** CD8+CD20+/- memory phenotype was assessed using CCR7 and CD45RO **(C,D)**. Percentages of each memory population from the CD8+CD20+ population within PBMCs and lymph nodes of all patients **(E)** (PBMCs n=19, lymph nodes n=26). Mann-Whitney test. * $P < 0.05$, ** $P < 0.005$, *** $P < 0.0005$, **** $P < 0.0001$.

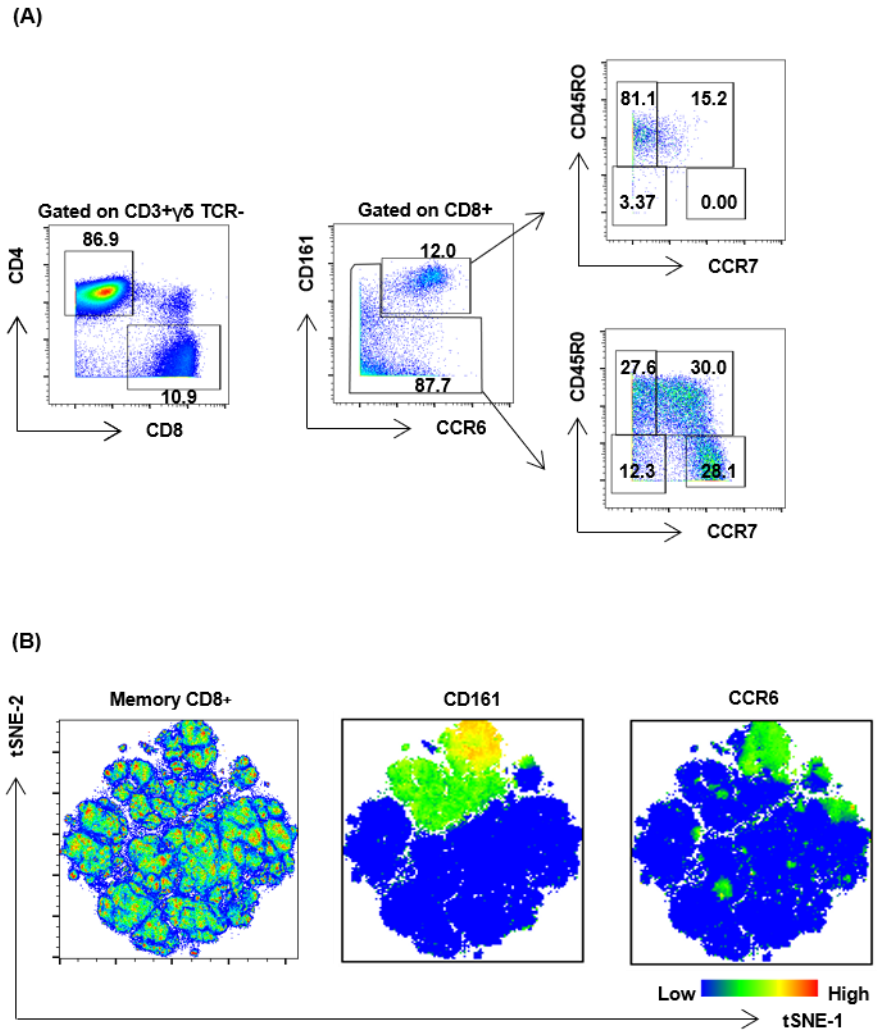

Figure 5.2.6 Assessing the memory phenotype of CCR6+CD161+, MAIT-like, cells.

Representative gating strategy to assess memory phenotype of MAIT-like cells using PBMCs isolated from matched blood of colorectal cancer patients **(A).** tSNE plots using concatenated file (all the PBMC samples from all the CRC patients pooled in one file) to show the segregation of the CCR6+CD161+ cells in one island; through showing CD161 and CCR6 expression within the generated tSNE plot (PBMCs n=19, lymph nodes n=26) **(B).** tSNE; t-distribute stochastic neighbour embedding.

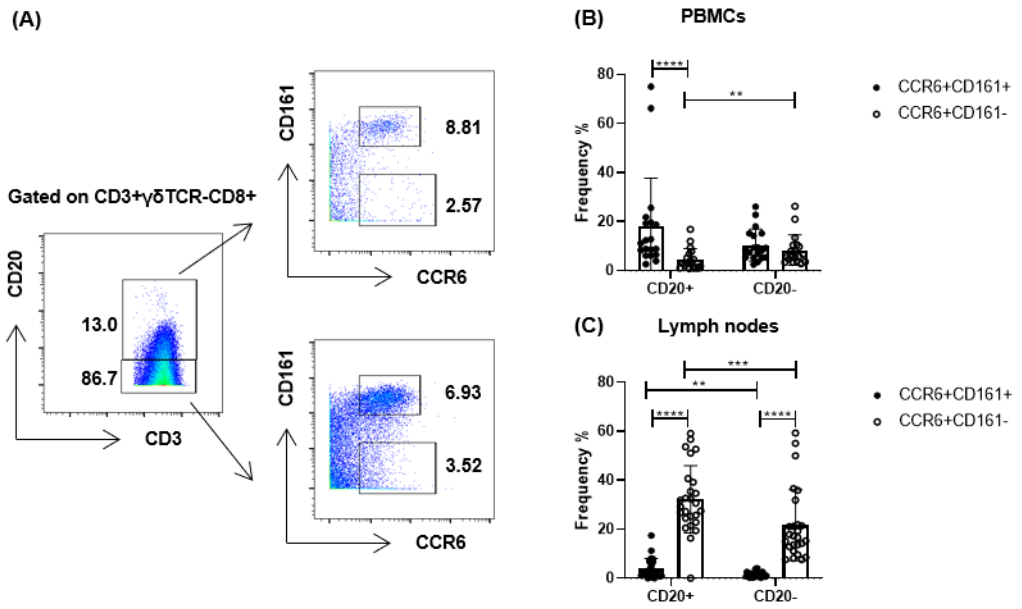

Figure 5.2.7 CCR6+CD161+ cells represent a higher percentage of CD8+CD20+T cells compared with CCR6+CD161 T cells.

CD20+ and CD20- T cells from CD3+TCRγδ-CD8+ were used to assess the presence of CCR6+CD161+ and CCR6+CD161- cells **(A).** The expression of CD20 on each population was determined across all donors, both PBMCs **(B)** and lymph nodes **(C)** (PBMCs n=19, lymph nodes n=26). Mann-Whitney test. ** $P < 0.005$, *** $P < 0.0005$, **** $P < 0.0001$**.**

5.2.8 CCR6+CD161+ cells express higher levels of CD56 and CD69 than other CD20+ T cells

In order to evaluate the differences between the CCR6+CD161+ and other CD20+ T cells, CCR6+CD161+ cells were gated from CD20+CD8+ T cells and other cells were gated into a second gate, which includes CCR6+CD161-, CCR6-CD161- and CCR6-CD161+ populations, from lymph node and PBMCs. There was a significant increase of CD56 levels within the CCR6+CD161+ population as compared to others within both lymph nodes and PBMCs **(Fig 5.2.8A,B)**. However, CD69 showed significantly higher levels by the CCR6+CD161+ population within PBMCs, whereas, other cells showed similar CD69 levels to the CCR6+CD161+ within lymph nodes **(Fig 5.2.8C,D)**. The CD69 pattern of expression was not mirrored by CD38, where the CCR6+CD161+ cells showed significantly lower expression within lymph nodes and slightly lower within PBMCs **(Fig 5.2.8E,F)**.

5.2.9 CCR6+CD161+ cells express higher levels of CD127 and CD28

CCR6+CD161+CD20+CD8+ T cells showed significantly higher levels of CD127 and CD28 than other cells **(Fig 5.2.9A,B,C,D)**, but lower levels of PD-1 within PBMCs with similar PD-1 levels within the lymph nodes **(Fig 5.2.9E,F)**. Finally, KLRG-1 levels were higher among the CCR6+CD161+ within PBMCs and showed similar levels within lymph nodes **(Fig 5.2.9G,H**

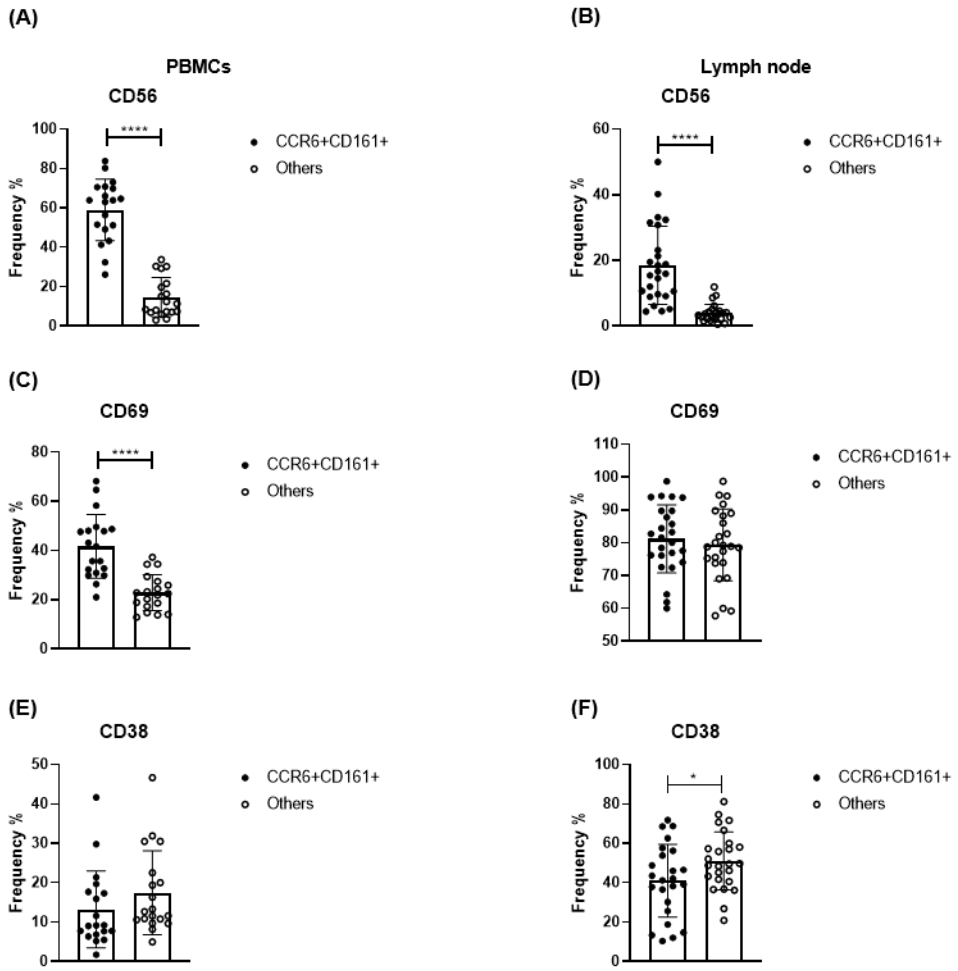

Figure 5.2.8 CCR6+CD161+ cells express higher levels of CD56 and CD69 than other CD20+ T cells.

Pre-gated Gated CD3+TCRγδ-CD8+CD20+ T cells were used to gate CCR6+CD161+ and other cells (CCR6+CD161-, CCR6-CD161+ and CCR6-CD161-). The two populations were used to assess the expression of CD56, CD69 and CD38 in PBMCs **(A,C,E)** and lymph nodes **(B,D,F)** (PBMCs n=19, lymph nodes n=26). Mann-Whitney test. * $P < 0.05$, **** $P < 0.0001$**.**

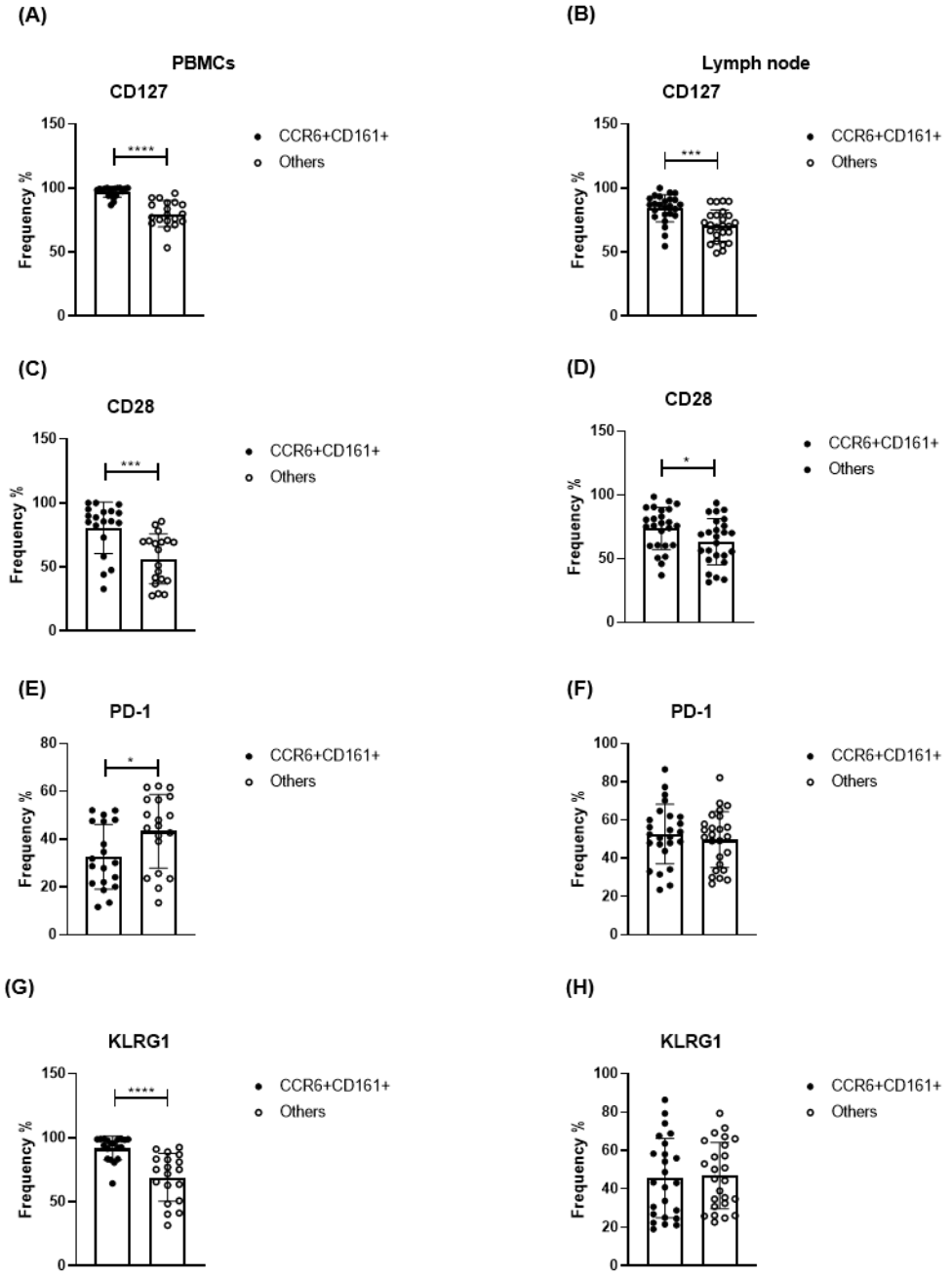

Figure 5.2.9 CCR6+CD161+ cells express higher levels of CD127 and CD28.

Pre-gated Gated CD3+TCRγδ-CD8+CD20+ T cells were used to gate CCR6+CD161+ and other cells (CCR6+CD161-, CCR6-CD161+ and CCR6-CD161-). The two population were used to assess the expression of CD127, CD28, PD-1 and KLRG1 in PBMCs **(A,C,E,G)** and lymph nodes **(B,D,F,H)** (PBMCs n=19, lymph nodes n=26). Mann-Whitney test. * $P < 0.05$, *** $P < 0.0005$, **** $P < 0.0001$**.**

5.2.10 CCR6+CD161+ cell activation status is similar between CD20+ and CD20- populations

The activation status of the CCR6+CD161+ subset within CD20+ and CD20- population was assessed through the analysis of CD56, CD69 and CD38 expression. First CD69 has been used as an early activation marker, while CD38 and CD56 have been found to be upregulated on activated CD8+ T cells (Caruso et al., 1997, Glaría and Valledor, 2020, Van Acker et al., 2016). Similar levels of CD56 were observed within both lymph nodes and PBMCs, with no significant difference to the CD20- CCR6+CD161+ subset **(Fig 5.2.10A,B)**. Similar findings were observed when comparing CD69 and CD38 expression levels between the CCR6+CD161+ cells from the CD20+ and the CD20- populations in the lymph nodes and the blood **(Fig 5.2.10C,D,E,F)**. Therefore, the activation status of both populations, as determined by these markers, were similar.

5.2.11 CCR6+CD161+CD20+CD8+ T cells upregulate markers of inhibition over the CCR6+ CD161+ CD20-CD8+ population

CD127 and CD28 levels were similar on the CCR6+CD161+ cells within the CD20+ and the CD20- population in both lymph nodes and PBMCs **(Fig 5.2.11A,B,C,D)**. Although PD-1 expression on the CCR6+CD161+ cells from the CD20+ and the CD20- populations in blood was similar, in lymph nodes the expression of PD-1 was higher on CCR6+CD161+ cells **(Fig 5.2.11E,F)**. Furthermore, KLRG1 levels were significantly higher on the CD20+CCR6+CD161+ cells over the CD20- cells in both lymph nodes and PBMCs **(Fig 5.2.11G,H)**. PD-1 has been well known as an inhibitory molecule, while KLRG1 is a co-inhibitory molecule that is upregulated in late differentiated T cells (Greenberg et al., 2019, Paley et al., 2012). Hence, the CCR6+CD161+ from the CD20+ population would be more inhibited over the CD20- population through the higher expression of PD-1 and KLRG1.

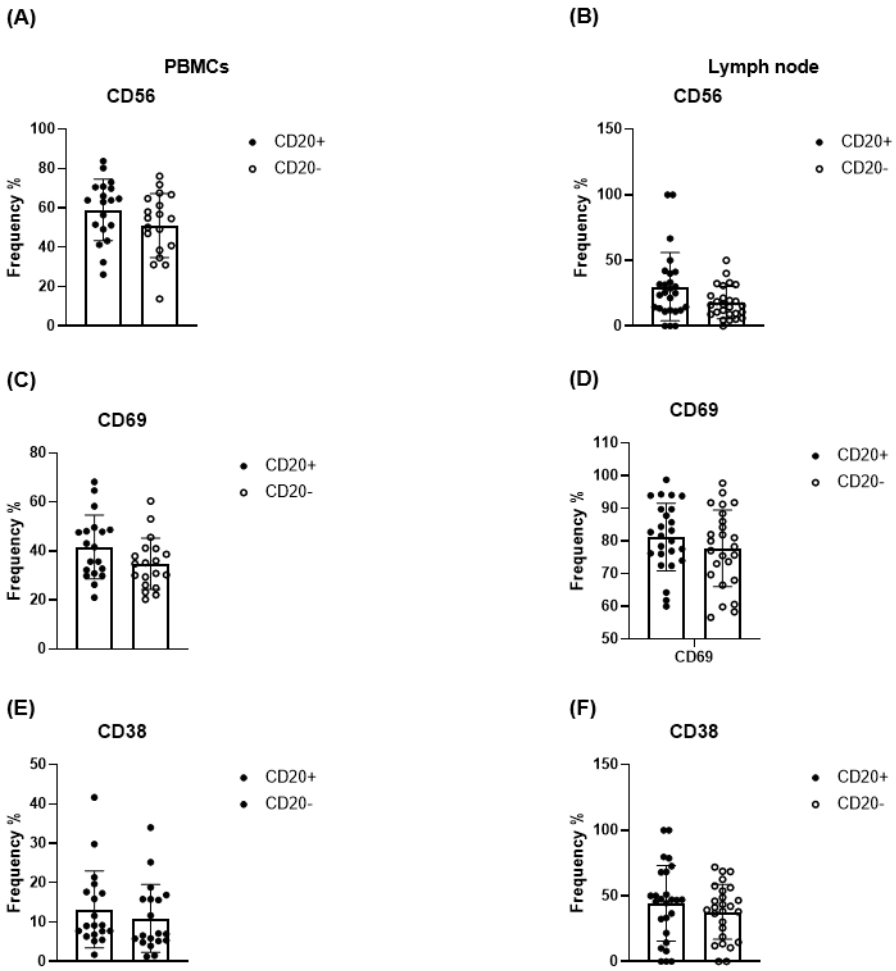

Figure 5.2.10 CCR6+CD161+ cell activation status is similar between CD20+ and CD20- populations.

Pre-gated CD3+TCRγδ-CD8+CCR6+CD161+ cells were used to gate CD20+ and CD20- T cells. The two population were used to assess the expression of CD56, CD69 and CD38 in PBMCs **(A,C,E)** and lymph nodes **(B,D,F)** (PBMCs n=19, lymph nodes n=26).

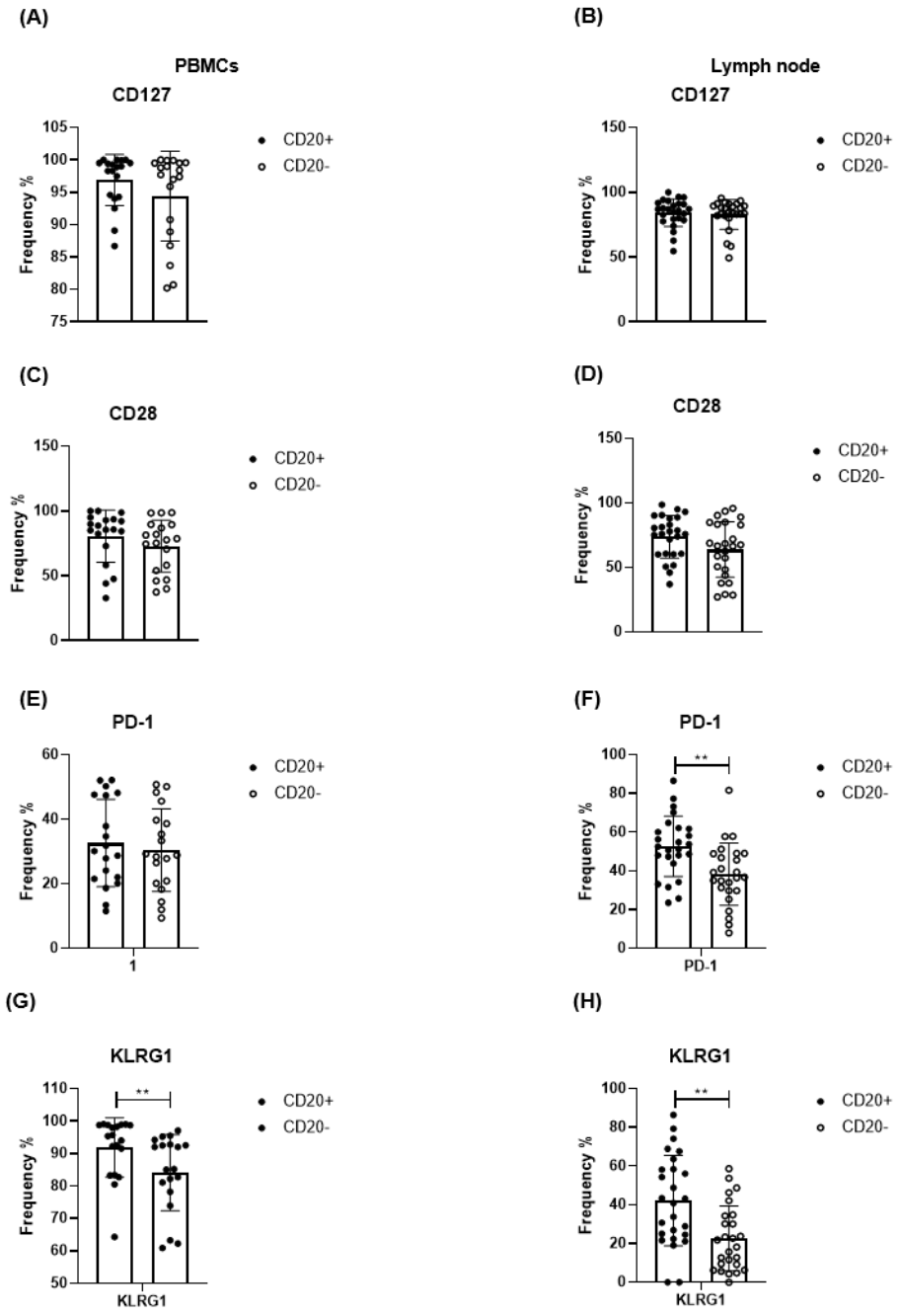

Figure 5.2.11 CCR6+CD161+CD20+CD8+ T cells upregulate markers of inhibition over the CCR6+CD161+CD20- population.

Pre-gated Gated CD3+γδTCR-CD8+CCR6+CD161+ were used to gate CD20+ and CD20- T cells. The two population were used to assess the expression of CD127, CD28, PD-1 and KLRG1 in PBMCs **(A,C,E,G)** and lymph nodes **(B,D,F,H)** (PBMCs n=19, lymph nodes n=26). Mann-Whitney test. ** $P < 0.005$.

5.2.12 CD20+,CCR6+CD161+ excluded, CD8+ T cells simulate a long-lived memory phenotype

By excluding CCR6+CD161+ from the analysis, the other populations (CCR6+CD161-, CCR6-CD161+ and CCR6-CD161-) from the CD20+ and CD20- T cells were compared using different markers. Like the phenotype of memory CD20+ T cells in healthy volunteers, memory CD20+, CCR6+CD161+ excluded, T cells from colorectal cancer patients showed higher levels of CD127 by Tem and Temra within PBMCs **(Fig 5.2.12A)**. However, no significant difference was detected within the memory populations in lymph nodes **(Fig 5.2.12B)**. Like CD127, CD28 was significantly increased by Tem and Temra within CD20+ compared to the CD20- population in both PBMCs and lymph nodes **(Fig 5.2.12C,D)**. On the other hand, CD27 showed higher levels within the Tem and Temra from the CD20+, CCR6+CD161+ excluded, T cells compared to CD20- T cells within PBMCs isolated from these patients **(Fig 5.2.12E)**. Although CD28 expression was higher on the CD20+ Temra population within lymph nodes, CD27 expression on CD20+ Temra showed a slightly lower level than on CD20- Temra within lymph nodes and was not significantly different from the CD20+ counterpart. CD27 is still expressed at a high significant level on Tem CD20+ compared to Tem CD20- within lymph nodes **(Fig 5.2.12F)**.

5.2.13 CD20+, CCR6+CD161+ excluded, T cells express a more inhibitory phenotype

CD20+ T cells, excluding the CCR6+CD161+ population. Were analysed using three different markers; PD-1, Killer cell lectin like receptor G1 (KLRG1) and CD69. CD20+ T cells showed higher levels of PD-1, especially within Tem and Tcm in the blood of these patients **(Fig 5.2.13A)**. PD-1 showed higher levels on CD20+ Tem and Tcm, and in lymph nodes CD20+ Tcm showed significantly higher levels compared to CD20- Tcm **(Fig 5.2.13B)**. Tem and Temra from both CD20+ and CD20- populations showed similar levels of PD-1, however, Tem overall showed higher expression of PD-1 compared to Temra. KLRG1

was highly expressed by CD20+ Tcm compared to CD20- Tcm, while Tem and Temra showed similar levels between the two populations in blood **(Fig 5.2.13C)**. However, lymph node CD20+ memory cells showed higher expression of KLRG1 on all memory subsets compared to CD20- memory cells **(Fig 5.2.13D)**. To exclude the possibility of transient activation, we analysed the expression of CD69. Only CD20+ Temra showed significant high expression of CD69 compared to CD20- Temra within PBMCs, but not in lymph nodes. Tem and Tcm within lymph nodes showed similar levels of CD69 **(Fig 5.2.13E,F)**. Therefore, upregulation of PD-1 and KLRG1 and similar levels of CD69 indicate a potentially inhibited phenotype of the CD20+, CCR6+CD161+, T cells over the equivalent CD20- T cells within these CRC patients.

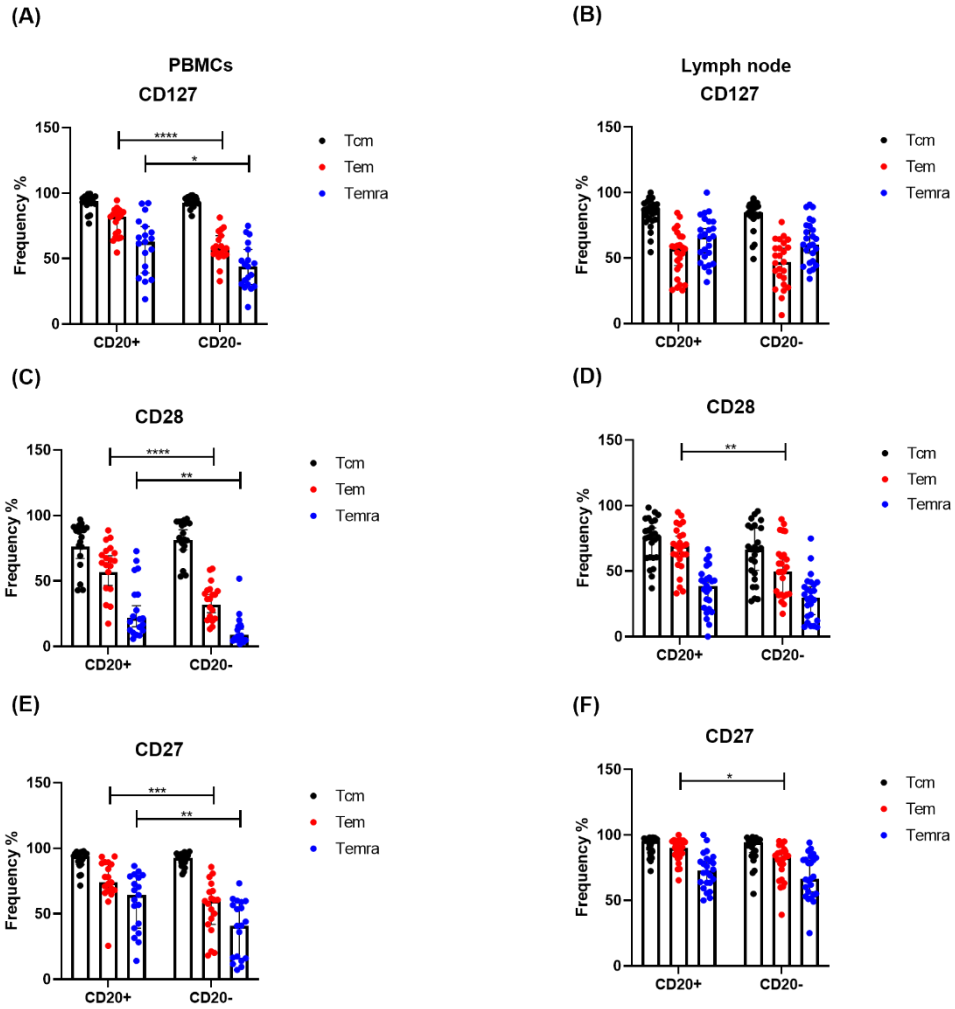

Figure 5.2.12 CD20+, CCR6+CD161+ excluded, CD8+T cells simulate long-lived memory phenotype.

Pre-gated CD3+TCRγδ-CD8+CD20+ and CD20- T cells, CCR6+CD161+, excluded cells assessed for the expression of CD127, CD28, PD-1 and KLRG1 in PBMCs **(A,C,E,G)** and lymph nodes **(B,D,F,H)** (PBMCs n=19, lymph nodes n=26). Mann-Whitney test. * P < 0.05, ** P < 0.005, *** P < 0.0005, **** P < 0.0001**.**

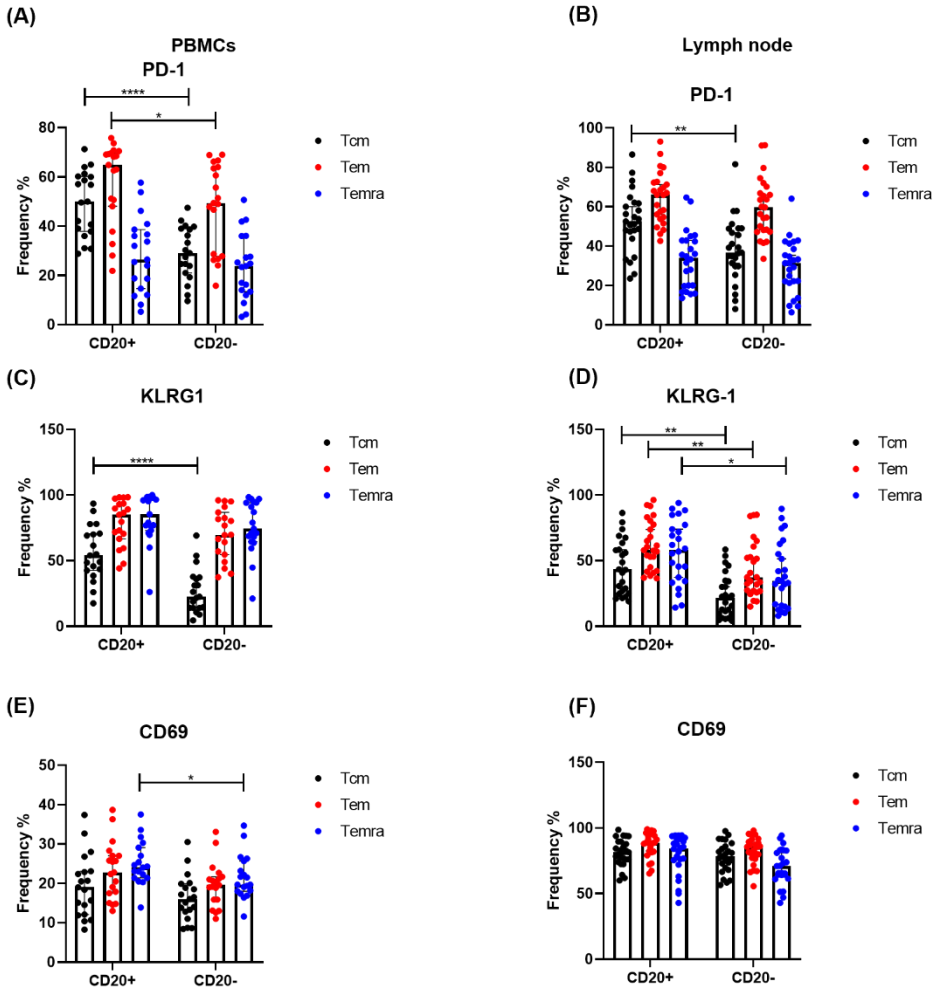

Figure 5.2.13 CD20+, CCR6+CD161+ excluded, CD8+ T cells express a more inhibitory phenotype**.**

Pre-gated Gated CD3+TCRγδ-CD8+CD20+ and CD20- T cells. The CCR6+CD161+ cells were excluded from this analysis. The two population were used to assess the expression of CD127, CD28, PD-1 and KLRG1 in PBMCs **(A,C,E,G)** and lymph nodes **(B,D,F,H)** (PBMCs n=19, lymph nodes n=26). Mann-Whitney test. * $P < 0.05$, ** $P < 0.005$, *** $P < 0.0005$, **** $P < 0.0001$**.**

5.3 Discussion

The presence of CD20+ T cells within the tumour microenvironment was investigated using three types of tissue; tumour tissue, adjacent tissue and matched blood from patients with colon and breast cancer. The tumour and adjacent tissue were checked by a pathologist from the Tissue Biobank at the University of Birmingham, where the normal and tumour tissue were determined.

In general, flow analysis revealed the presence of CD20+ T cells within both tumour and adjacent tissue. However, CD20+ T cells were frequently absent from the matched patients' blood **(Fig 5.2.1B, 5.2.1C,D)**. This could be due to the assigned treatment for the patients, for example, chemotherapy and radiotherapy, which may affect the presence of those cells within matched blood. Another theory is that the absence of these cells from the matched blood is due to the recruitment of these cells to the tumour tissues. Chemotherapy and radiotherapy are considered as immunosuppressive agents and in fact the total lymphocytes, including CD4+ and CD8+ T cells, can be decreased after the treatment (Van Meir et al., 2017). CD20+CD8+ T cells were however detected within the tissue, although with a slightly higher percentage in the adjacent tissue over the tumour tissue in both breast and colon cancer **(Fig 5.2.1B, 5.2.2B,C)**. This mirrors the results from the healthy donors and other publications findings (de Bruyn et al., 2015, Schuh et al., 2016).

Recently, CD39 has been proposed as possible marker to help identify the tumour-specific CD8+ infiltrated T cells. This was explained by the absence of CD39 expression on tumour infiltrated lymphocytes from colon and lung cancer patients, that were able to respond to tumour non-specific antigens and were not stimulated by the tumour antigens (Simoni et al., 2018a).

We sought to investigate any possible correlation between CD39 and CD20 expression on the tumour infiltrated lymphocytes from colon cancers. The expression of CD39 was high on CD20+ cells in both CD8+ and CD8- T cells **(Fig 5.2.3B,C)**. However, the data represent the analysis of only 3 different colon tumours, and it may need further investigation to detect any possible relationship between CD39 and CD20 expression **(Fig 5.2.3B,C)**.

Due to the impact of the COVID-19 pandemic, we decided to use uploaded data from public resources and previously published data. The data used in this chapter were from colorectal cancer patients' blood, tumour tissue, adjacent normal tissue and tumour-associated lymph nodes (de Vries et al., 2020). Scanning for the presence of CD20+ T cells revealed that they were found in tumour and normal adjacent tissue **(Fig 5.2.4B)**. The phenotype of the CD20+ T cells within both tissues revealed their persistence within the memory compartment **(Fig 5.2.4C,D)**. However, further phenotyping of those cells was difficult due to the total low number of lymphocytes within tumour tissue. The CD20+ T cells were found in the blood and the lymph nodes of these patients, which has been reported before in healthy donors (Murayama et al., 1996). These authors demonstrated a similar phenotype of being more within the memory CD8+ population **(Fig 5.2.5)**.

Although, naïve CD20+ T cells can be found at significantly higher level in lymph nodes than blood, memory CD20+ T cells showed a significantly higher percentage of the total CD8+CD20+ T cells within lymph nodes **(Fig 5.2.5F)**. In agreement with previous findings, CD20+ T cells maintained a memory phenotype rather than naïve. It is worth noting that the lymph nodes analysed in this dataset are tumour-associated lymph nodes, and may show differences to lymph nodes from healthy individuals.

The expression of CCR6 on high CD161 expressing cells has been reported before on MAIT cells (Wong et al., 2013, Walker et al., 2012). Although the Vα7.2 marker was not included

in the panel used for this published dataset, a distinct population within the t-SNE analysis that express high CD161 and CCR6 was found within the CD20+CD8+ T cells population. The presence of CD161+CD8+ T cells that are present in various tissues through their ability to express CCR6 and mimic the CD4+ T helper 17 phenotype has been previously reported in patients with chronic inflammatory diseases (Billerbeck et al., 2010). CD161+ CD8+ T cells can be classified into three different populations: MAIT cells, Tc17 and stem cell like memory cells (Konduri et al., 2021). Each of these populations have been reported to express CCR6, affecting their tissue homing ability and potential to have more innate based characteristics (Fergusson et al., 2014). Based on the expression of CCR7 and CD45RA, cells expressing high levels of CD161 usually have a Tem phenotype, while CD161 intermediately expressing cells show both Tem and Temra phenotypes (Fergusson et al., 2016). This can be seen in our data, where about 80% of the CCR6+CD161+ were Tem **(Fig 5.2.6A)**. Further phenotyping of the CCR6+CD161+ cells within CD20+ T cells and compare them to other populations; including CCR6+CD161-, CCR6-CD161+ and CCR6-CD161-, revealed substantial differences.

These differences can be seen in the expression of the NK cells marker CD56; which were higher on the CCR6+CD161+ cells as compared to others within both blood and lymph nodes **(Fig 5.2.8A,B)**. It has been shown that CD56 expression can be found on activated CD8+ T cells; which can enhance the cytotoxicity of those cells to acquire NK like killing mechanisms and cytokine production (Chan et al., 2013, Poonia and Pauza, 2014).

CD69 is a co-stimulatory marker that has been used as an early activation marker and can be up regulated after hours of T cells activation (Caruso et al., 1997). CCR6+CD161+ cells showed higher percentages of CD69 over other cells in blood (**Fig 5.2.8C,E)**. The higher expression of CD56 and CD69 within the blood of these patients may indicate an activated state of the CCR6+CD161+ population over other populations. Besides, the presence of the

CCR6 and CD69 may indicate higher ability of those cells to migrate toward tissues, where both markers are used to predict tissue homing resident markers (Fergusson et al., 2016). Thus, tissue homing abilities of those may indicate the ability of those cells to migrate to the tumour tissues over other cells. In fact, the presence of CD161+CD8+ T cells within tumour infiltrating cells can enhance survival and be a favourable prognosis for tumour regression (Welters et al., 2018).

A study on hepatocellular carcinoma showed that the presence of CD161+PD-1+CD8+ T cells can indicate better survival, where those cells demonstrate higher cytotoxicity and IL-7Ra expression (Li et al., 2020b). Our data showed that CCR6+CD161+ cells within the CD20+ population showed higher expression of CD127 and CD28 in both lymph nodes and blood compared to other populations **(Fig 5.2.9A,B,C,D)**. The presence of these two markers can estimate the potential long-lived memory status of these cells. To illustrate, CD28 is a co-stimulatory molecule while CD127 can be used to estimate the terminally differentiation of memory cells, where memory cells lose the expression of both markers by differentiation towards terminally differentiated cells (Thome et al., 2014). Surprisingly, the CCR6+CD161+ population showed significantly lower PD-1 expression than other populations in the blood **(Fig 5.2.9E)**. However, the presence of significantly high KLRG1 on the CCR6+CD161+ cells over other populations of CD20+ T cells in blood, may indicate a poor anti-tumour response through reduced proliferation capacity and cytokine production (Li et al., 2016), **(Fig 5.2.9G)**. Although PD-1 is usually considered as a co-inhibitory molecule that marks exhausted cells, while KLRG1 can be used as a senescence marker to determine over stimulation that results in terminally differentiation state of the cell, both can result in low anti-tumour immune responses. Therefore, the high expression of KLRG1 by the CCR6+CD161+ cells could indicate a possible senescent phenotype of the CD20+ T cells.

In conclusion, CD20+ T cells can be found in tumour associated lymph nodes of colorectal cancer patients, as well as in blood. Interestingly, the CCR6+CD161+ population was found within CD20+ and CD20- T cell subsets. The CCR6+CD161+ population showed the possibility for more effector functions through the high expression of CD56, CD69, CD127 and CD28, whereas other (CCR6+CD161+ excluded) memory CD20+ T cells showed up-regulation of PD-1 and KLRG1 that may result in a more inhibited phenotype. Further investigating the expression of Vα7.2 and MR-1 tetramer by the CCR6+CD161+ population would be required to determine the presence of CD20+ MAIT cells within this population. Besides, further investigating the presence of CD20+ T cells within the tumour-specific T cells would be required to assess the role of CD20+ T cells in anti-tumour immune responses.

Chapter Six: Investigating CD20+ T cells in melanoma patients receiving anti-PD-1 and anti-CTLA-4

6.1 Introduction

Melanoma is a skin cancer that arises from melanin producing cells and is often curable at the early stages of the cancer. However, metastatic melanoma can cause serious life threating symptoms that eventually can cause the death of the patient. Anti-PD-1 or anti-CTLA-4, or a combination of both, immunotherapeutic treatments are known as immune checkpoint blockade therapies. They are approved by the FDA and show excellent results in increasing survival rate (Larkin et al., 2015, Robert et al., 2015). PD-1 and CTLA-4 are two inhibitory molecules that used by the normal immune system to maintain the balance between pro-inflammatory and anti-inflammatory responses contributing to immune tolerance (Rotte, 2019).

The using of immune checkpoint blockade in melanoma patients can enhance the anti-tumour immune responses by T cells. This has been shown through the increase of different pro-inflammatory cytokines including IL-2 and IFN-γ that resulted in lesion regression (Das et al., 2015). CD20+ T cells have been shown to produce more cytokine as compared to CD20- T cells following *in vitro* activation and they express higher levels of PD-1 (Rathbone, 2018). This suggests that CD20+ T cells might be a good target for therapy. A single report in the literature investigated the role of CD20+ T cells within ovarian cancer; CD20+ T cells expanded in the ascitic fluid of those patients and showed more anti-tumour abilities via acquiring a TC1 like phenotype (de Bruyn et al., 2015). Therefore, the aim of my study is to investigate the role of CD20+ T cells in melanoma patients and their role in the response to the treatment. As I was unable to access the laboratories for these experiments, I have re-analysed published data sets from melanoma patients receiving anti-PD-1 or anti-CTLA-4 **(Table 2.7.3.1)** (Subrahmanyam et al., 2018).

6.1.1 Aims

1. Investigate the presence of CD20+ T cells presence in the blood of melanoma cancer patients.

2. Determine the phenotype of CD20+ T cells within those patients.

3. Investigate the cytokine production profile of the CD20+ T cells.

4. Assess the effects of anti-PD-1 or anti-CTLA-4 therapy on the phenotype of CD20+ T cells.

5. Investigate the relation between response to the therapy and CD20+ T cells.

6.2 Results

6.2.1 CD20+ T cells show similar percentages in treatment responders and non-responders

A gating strategy was developed to assess the presence of CD20+ T cells in PBMCs from melanoma patients. The patients had received pembrolizumab which is a monoclonal antibody that blocks PD-1 from interacting with either PD-L1 or PD-L2. Other patients received another type of treatment to inhibit CTLA-4 interaction called ipilimumab. First, beads were excluded by gating the DNA+ cells, which are the cells that have DNA and to prevent any interference by the calibration beads, and the single cells followed by live cells. Live cells were used to gate the CD3+CD19-TCRγδ-CD8+ population for the assessment of CD20+ T cells. CD20+ T cells were detectable in the blood of these patients **(Fig 6.2.1A)**. Analysing the percentages of the CD20+ T cells within both responders and non-responders patients to the treatment showed no significant difference **(Fig 6.2.1B)**. There are also no differences between genders or the type of treatment received **(Fig 6.2.1C,D)**. It is important to note that the published data sets contained blood from melanoma patients and lacked normal healthy controls, which limits the comparisons that can be made.

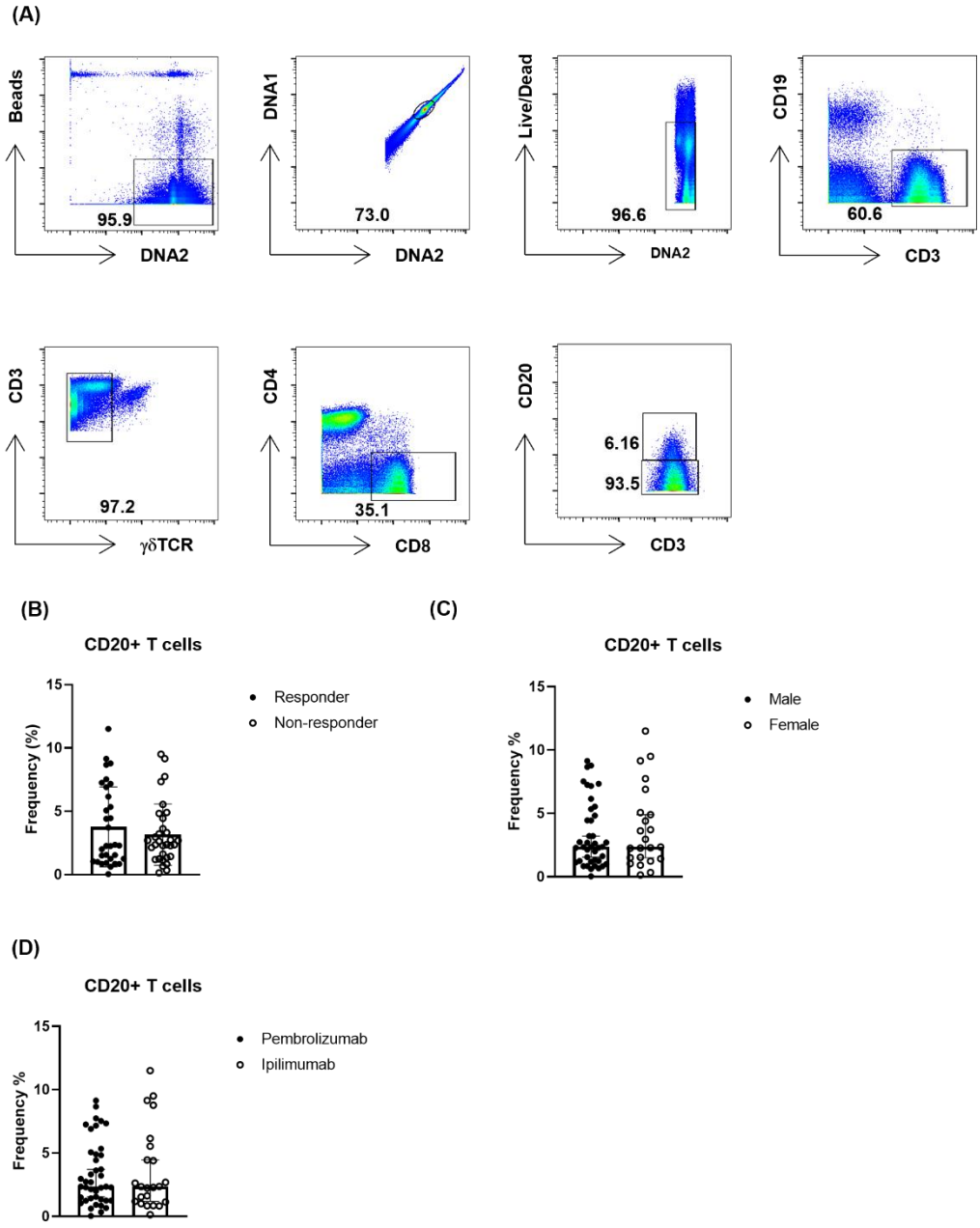

Figure 6.2.1 CD20+ T cells show similar percentages in treatment responders and non-responders.

Gating strategy to assess CD20+ T cell percentages using PBMC isolated from peripheral blood of melanoma patients receiving Ipilimumab or Pembrolizumab **(A).** The percent of CD3+CD19-TCRγδ-CD8+CD20+ cells in responders and non-responders **(B),** male and female **(C)** and in patients receiving Ipilimumab or Pembrolizumab **(D)** (n=64) **.** Mann-Whitney test and results were non-significant ($p > 0.05$). TCRγδ; gamma-delta T cells.

6.2.2 The majority of CD20+ T cells are Tem and Temra

Using CCR7 and CD45RA expression, cells were divided into naïve (CCR7+CD45RA+), Tcm (CCR7+CD45RA-), Tem (CCR7-CD45RA-) and Temra (CCR7-CD45RA+) **(Fig 6.2.2A)**. For the CD20+ T cells, the naïve population was significantly lower than memory populations. Tcm showed similarly low levels to the naïve population. On the other hand, Tem constitute significantly higher levels compared to naïve and Tcm, with Temra showing the highest percentage **(Fig 6.2.2B)**. CD20- T cells showed a different profile to the CD20+ T cells. The naïve population was present within the CD20- T cells and was significantly higher than Tcm. However, Tem and Temra showed significantly higher levels than naïve cells with no significant difference between the Tem and Temra levels **(Fig 6.2.2C)**.

6.2.3 Responders show significantly higher Temra levels

Responder and non-responder patients were assessed for the memory phenotype of the CD20+ and CD20- T cells in their blood. Similar levels of Tcm and Tem were observed within CD20+ T cells. However, Temra showed significantly higher levels within responders over non-responders **(Fig 6.2.3A)**. The same observation was observed within the CD20- memory phenotype, where Tcm and Tem showed similar levels between responders and non-responders, while CD20- Temra showed significantly higher levels within responder patients to treatment over non-responders **(Fig 6.2.3B)**. The Temra population within CD20- T cells in non-responder patients showed slightly lower percentage as compared to the Temra within CD20+ T cells from non-responder patients. Overall, Temra from both populations were higher in responders to the treatment comparing to non-responders.

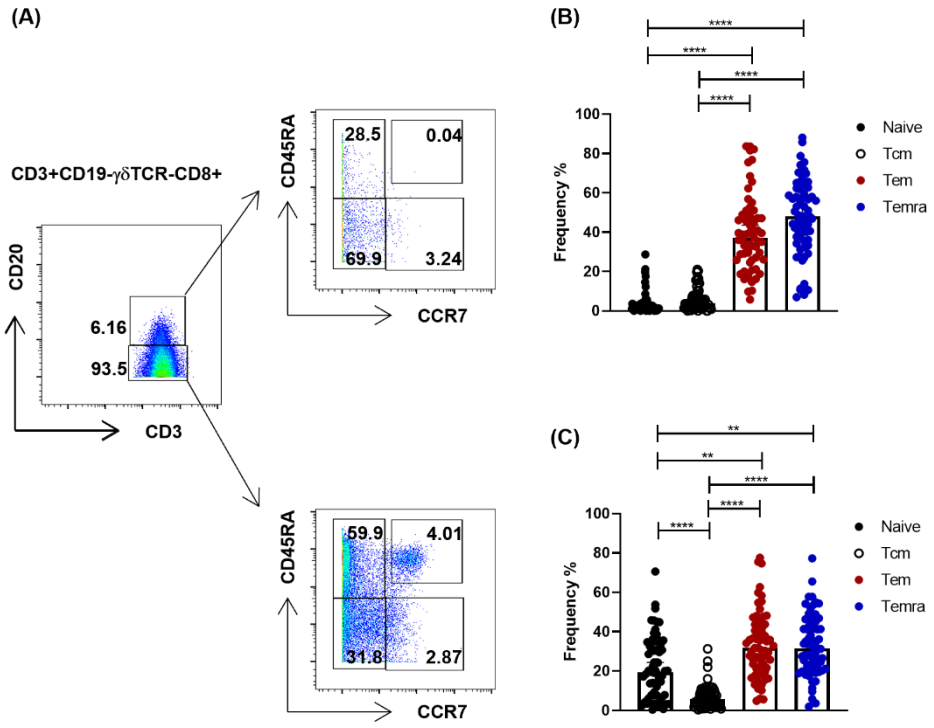

Figure 6.2.2 The majority of CD20+ T cells are Tem and Temra.

Gating strategy to assess the memory phenotype of CD20+ T cells in the melanoma patients **(A).** Naive, Tcm, Tem and Temra percentages of the total CD8+CD20+ T cells **(B)** and CD20- T cells **(C)** were assessed across all patients (n=64). Statistical difference was measured using Kruskal-Wallis test. ** P < 0.005, **** < 0.0001**.**

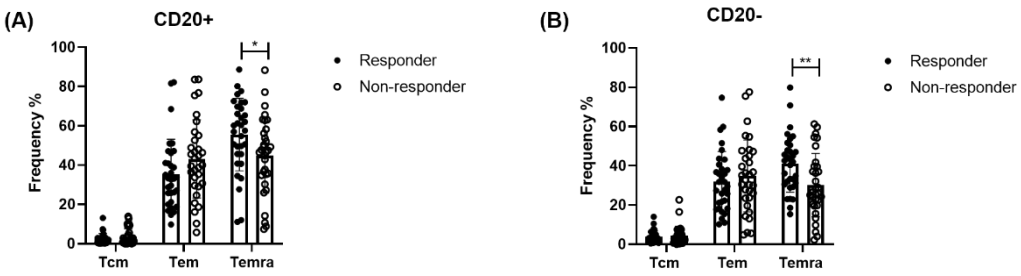

Figure 6.2.3 Responders shows significantly higher Temra levels.

Tcm, Tem and Temra percentages of the total CD8+CD20+ T cells **(A)** and CD20- T cells **(B)** were assessed across responder and non-responder patients (n=64). Statistical difference was measured using Mann-Whitney test. * $P < 0.05$, ** $P < 0.005$.

6.2.4 Phenotyping memory CD20+/- T cells

Further analysis of the memory phenotype of the CD20+ T cells and comparison to the CD20- T cells revealed differences in the expression of a number of markers. The CD20+ Tcm showed significantly higher expression of CD57, CD28, CD127 and CD27 compared to the CD20- Tcm, while CD25 showed higher expression on the CD20- Tcm compared to the CD20+ Tcm **(Fig 6.2.4A)**. On the other hand, Tem showed significantly higher expression of CD28, CD69, CD127 and CD27 on the CD20+ T cells compared to the CD20- T cells, whereas CD57 was slightly higher on the Tem from the CD20- T cells over the CD20+ T cells **(Fig 6.2.4B)**. The Temra CD20+ population showed higher expression of CD57, CD28, CD127 and CD27, however, CD25 was significantly higher on Temra from the CD20- population **(Fig 6.2.4C)**. Overall CD25 expression was slightly lower on all memory subsets from both CD20+ and CD20- populations and less than 20% of these cells expressed CD25.

5.2.5 Responders and non-responders show a similar phenotype

In order to determine any link between response to treatment and phenotype, we have assessed the possible difference in the phenotype of Temra cells within CD20+ and CD20- T cells between responders and non-responders. By comparing the expression of CD25, CD57, CD28, CD69, CD127 and CD27, Temra showed a similar phenotype in both CD20+ and CD20- T cells in responders and non-responders **(Fig 6.2.5A,B)**.

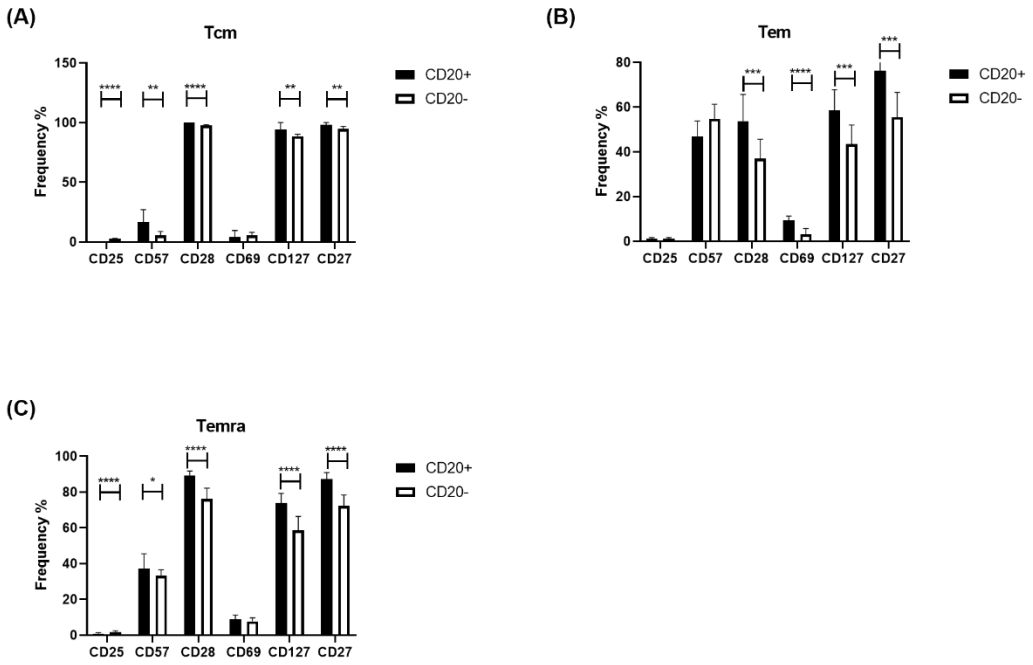

Figure 6.2.4 Phenotyping Memory CD20+/- T cells.

CD3+CD19-TCRγδ-CD8+CD20+/- were used to gate Tcm, Tem and Temra using CCR7 and CD45RA. The expression of each marker was assessed in the CD20+/- Tcm **(A),** Tem **(B)** and Temra (n=64) **(C).** Statistical difference was measured using Mann-Whitney test.* $P < 0.05$, ** $P < 0.005$, *** $P < 0.0005$, **** $P < 0.0001$**.**

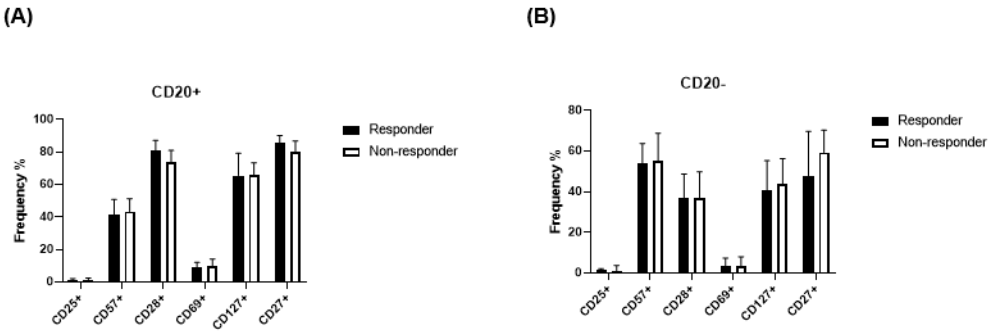

Figure 6.2.5 Responders and non-responders show a similar phenotype.

CD3+CD19-γδTCR-CD8+CD20+/- were used to gate all memory subsets (Tcm+Tem+Temra) using CCR7 and CD45RA, and used Temra population for further analysis. The expression of each marker was assessed in the CD20+ compartment **(A)** and CD20- **(B)** (n=64). Mann-Whitney test and results were not significant.

6.2.6 CD20+ T cells express more PD-1 than CD20- T cells

To evaluate the PD-1 expression by CD20+ and CD20- T cells, memory cells were gated from the CD8+ compartment; using CCR7 and CD45RA. This was followed by gating CD20+ and CD20- memory CD8+ to assess PD-1, PD-L1, PD-L2 and CTLA-4 expressions on each population **(Fig 6.2.6A)**. CD20+ memory cells showed higher expression of PD-1 over CD20- memory cells in all patients. Although patients received an anti-PD-1 monoclonal antibody, more than 50% of the total CD20+ memory cells still expressed PD-1. PD-L1 showed very low expression in both CD20+ and CD20- memory cells, whereas PDL-2 showed higher expression among the CD20- memory cells. In addition to PD-1, CD20+ memory cells showed higher expression of CTLA-4 as compared to CD20- memory cells **(Fig 6.2.6B)**.

6.2.7 Responders show similar checkpoints level to non-responders from CD20+ and CD20- T cells

Although, PD-1 levels were higher within CD20+ memory cells as compared to CD20- memory cells, the same results were observed in both responders and non-responders **(Fig 6.2.7A)**. In addition, PD-L1, PD-L2 and CTLA-4 also showed similar levels between responder and non-responder patients from both CD20+ and CD20- T cells **(Fig 6.2.7B,C,D)**. Therefore, expression of immune checkpoint molecules was similar between responders and non-responders.

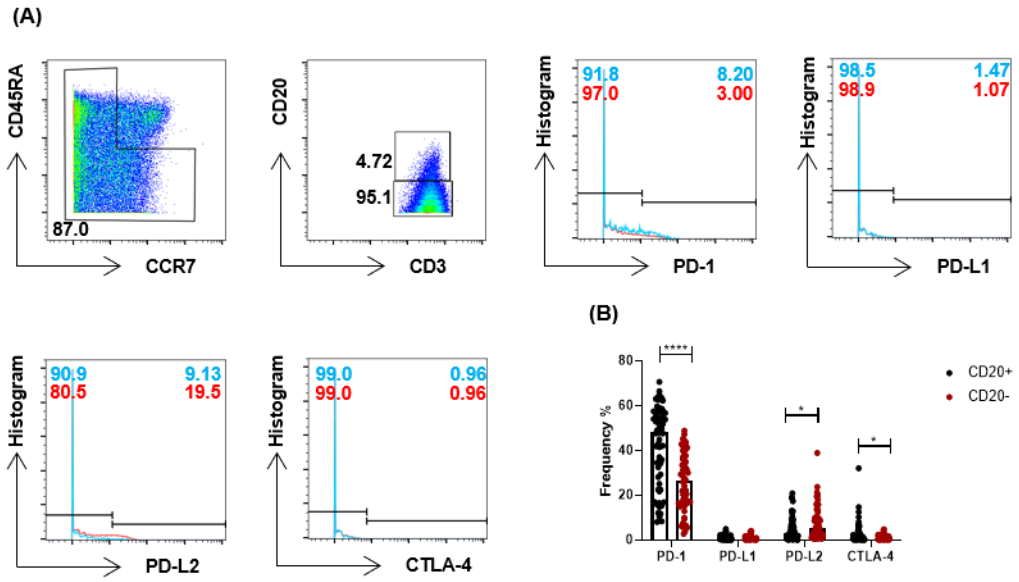

Figure 6.2.6 CD20+ T cells express more PD-1 than CD20- T cells.

CD3+CD19-TCRγδ-CD8+ were used to gate all memory subsets (Tcm, Tem and Temra) using CCR7 and CD45RA. Memory gated cells were used to gate CD20+ and CD20- memory cells **(A)**. The expression of PD-1, PDL-1, PD-L2 and CTLA-4 in the CD20+ and CD20- memory cells **(B)** (n=64)**.** Statistical difference was measured using Mann-Whitney test. * $P < 0.05$, **** $P < 0.0001$**.**

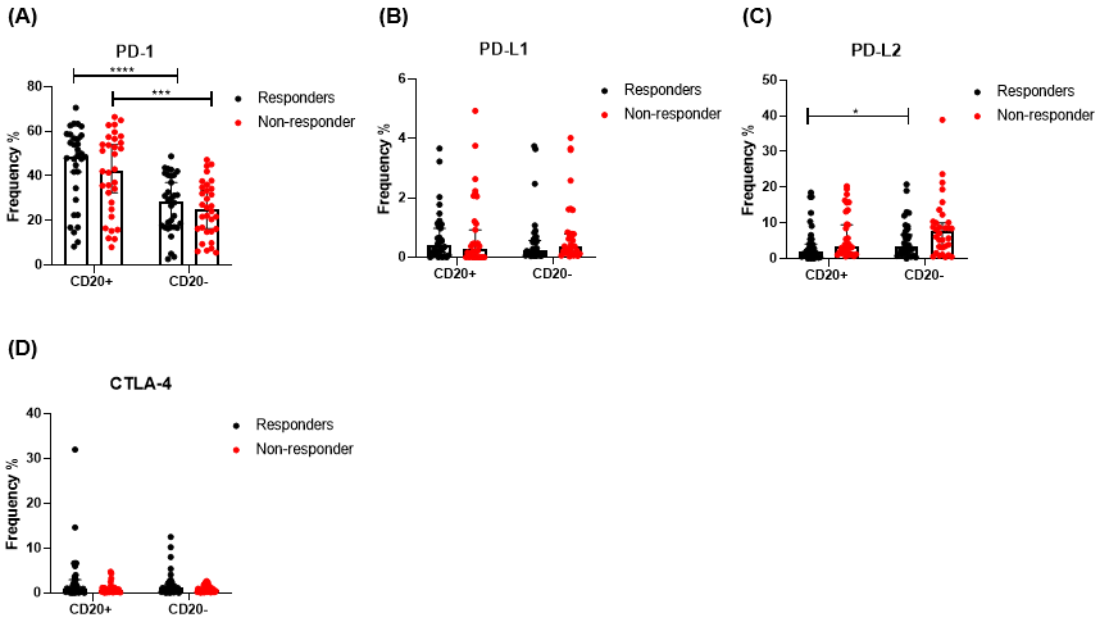

Figure 6.2.7 Responders shows similar checkpoint levels to non-responders from CD20+ and CD20- T cells.

Memory CD20+/- T cells were used to assess checkpoints levels in responders and non-responder patients. The expression of PD-1, PDL-1, PD-L2 and CTLA-4 in the CD20+ memory cells **(A)** and the CD20- memory cells **(B)** (n=64). Statistical difference was measured using Mann-Whitney test. * $P < 0.05$, *** $P < 0.0005$, **** $P < 0.0001$**.**

6.2.8 Stimulated CD20+ T cells produce more cytokines compared to CD20- T cells

In the published data that was re-analysed, the authors isolated cells from melanoma patients receiving anti-PD-1 or anti-CTLA-4 and stimulated them in vitro using PMA and ionomycin with the addition of brefeldin and monensin, as described in the methods chapter **(section 2.7.3)**. Cytokines were measured from the stimulated CD20+ and CD20- T cells to compare the level and the cytokines profile of each population. Stimulated CD20+ T cells showed the ability to produce more cytokines, including IL-10, IL-4, macrophage inflammatory protein β (MIP-1β), TNF-α, IFN-γ and IL-2, as compared to stimulated CD20- T cells. Indeed, more than 90% of the CD20+ T cells were able to produce MIP-1β, IFN-y and TNF-α. Although the production of IL-10 was low in both populations, stimulating CD20+ T cells resulted in more IL-10 production than stimulating CD20- T cells. The same result was seen for IL-4 and IL-17 production, where approximately 20% of the CD20+ T cells were able to produce IL-4 and IL-17. On the other hand, the levels of the cytotoxic markers perforin and GraB for both populations showed similar levels, where less than 40% were able to produce GraB and about 20% produced perforin. Granulocyte-macrophage colony stimulating factor (GM-CSF) production was similar by both populations. In addition, CD20+ T cells showed significantly more degranulation through the expression of CD107a as compared to CD20- T cells. Overall, CD20+ T cells were able to produce more pro-inflammatory cytokines compared to stimulated CD20- T cells, but with similar cytotoxic marker expression but more degranulation by the CD20+ T cells **(Fig 6.2.8A)**.

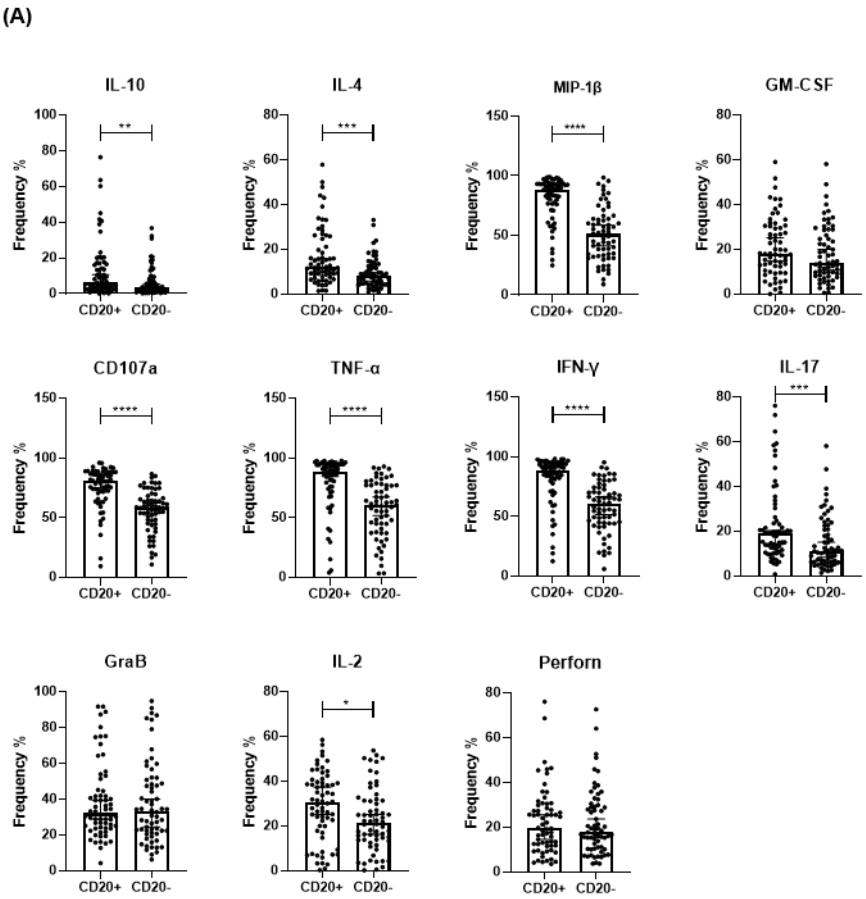

Figure 6.2.8 Stimulated CD20+ T cells produce more cytokines compared to CD20- T cells.

CD20+/- T cells were used to assess cytokine production after stimulation with 10ng/ml PMA and 1 µg/ml Ionomycin **(A)** (n=64). Statistical difference was measured using Mann-Whitney test. ** P < 0.005, *** P < 0.0005, **** P < 0.0001**.** GraB; granzyme B.

6.2.9 Responder and non-responder patients cells produce similar levels of cytokines from CD20+ and CD20- T cells

Further analysis of the differences between treatment responder and non-responder patients revealed no differences in the cytokines produced by the CD20+ T cells or the CD20- T cells. Stimulated CD20+ T cells were able to produce more IL-10 compared to CD20- T cells, however, non-responder patients showed similar levels of IL-10 by both populations. Stimulated CD20+ T cells from both responders and non-responders were able to produce more MIP-1β, IL-4, CD107a, TNF-a, IFN-γ and IL-17 compared to CD20- T cells. However, unlike IL-10, IL-2 was produced significantly more by the CD20+ T cells within non-responder patients compared to CD20- T cells. GM-CSF, perforin and GraB showed similar levels between CD20+ and CD20- T cells in both responders and non-responders. Overall, the cytokine profile of the responder patients was similar to non-responders for both CD20+ and CD20- T cells **(Fig 6.2.9A)**.

(A)

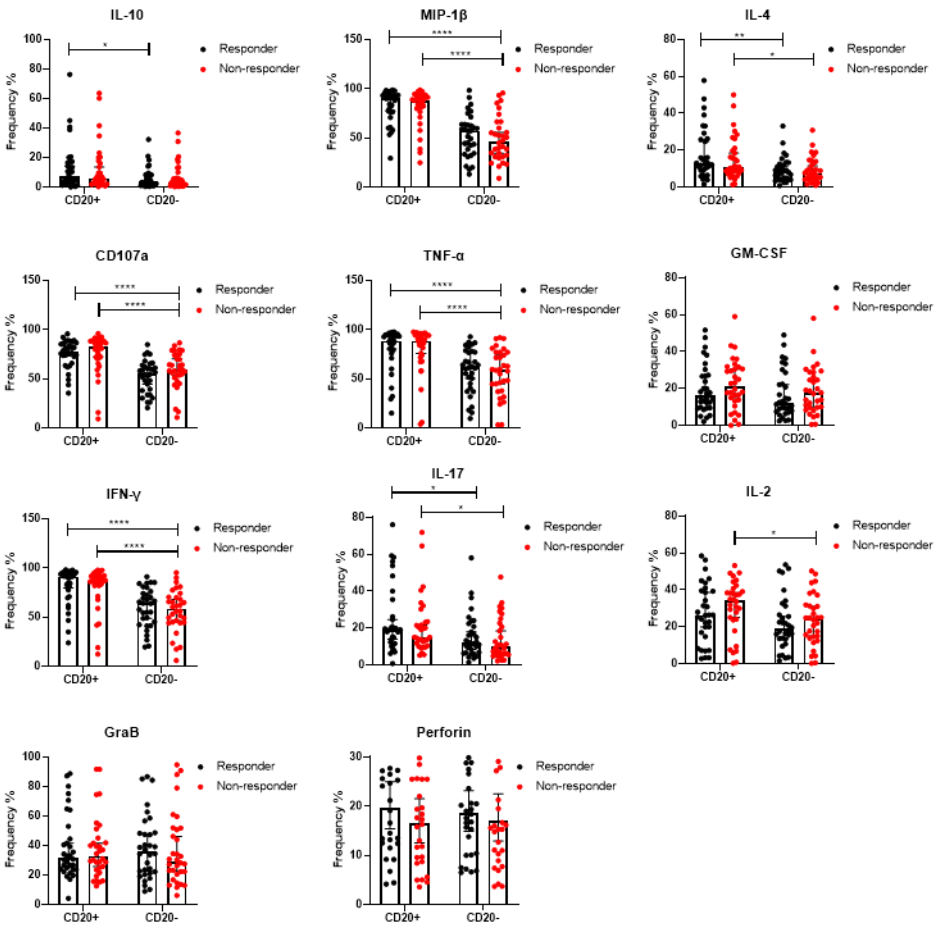

Figure 6.2.9 Responder and non-responder patients cells produce similar levels of cytokines from CD20+ and CD20- T cells.

CD20+/- T cells were used to assess cytokine production after stimulation with 10ng/ml PMA and 1 μg/ml Ionomycin in responders and non-responders **(A)** (n=64). Statistical difference was measured using Mann-Whitney test. * $P < 0.05$, **** $P < 0.0001$**.** GraB; granzyme B.

6.2.10 Anti-PD-1 or anti-CTLA-4 generate similar cytokine profile by the CD20+ T cells

To investigate the possible effect of the type of treatment on the cytokine profile of the CD20+ T cells, patients receiving anti-PD-1 (Pembrolizumab) or anti-CTLA-4 (Ipilimumab) were grouped into responders and non-responders to the treatment. Next, the cytokines released from the pre-gated CD20+ T cells isolated from those patients that were stimulated with PMA and ionomycin were measured. The cytokine profile of the CD20+ T cells from patients receiving both treatments showed similar cytokines levels. To illustrate, IL-4, MIP-1β, TNF-a, GM-CSF, IFN-γ, IL-17 and IL-2 released by CD20+ T cells showed similar levels between patients received anti-PD-1 or anti-CTLA-4 from responders and non-responders. Although a slight reduction in GM-CSF and IL-2 in patients with anti-CTLA-4 compared to patients receiving anti-PD-1 were observed, this reduction was not significantly different. However, IL-10 from non-responder patients receiving anti-PD-1 was significantly higher than non-responder patients to anti-CTLA-4. Degranulation through the measurement of CD107a, perforin and GraB showed similar levels. Therefore, the type of treatment was not affecting the cytokine profile by the CD20+ T cells from either responders or non-responder patients **(Fig 6.2.10A)**.

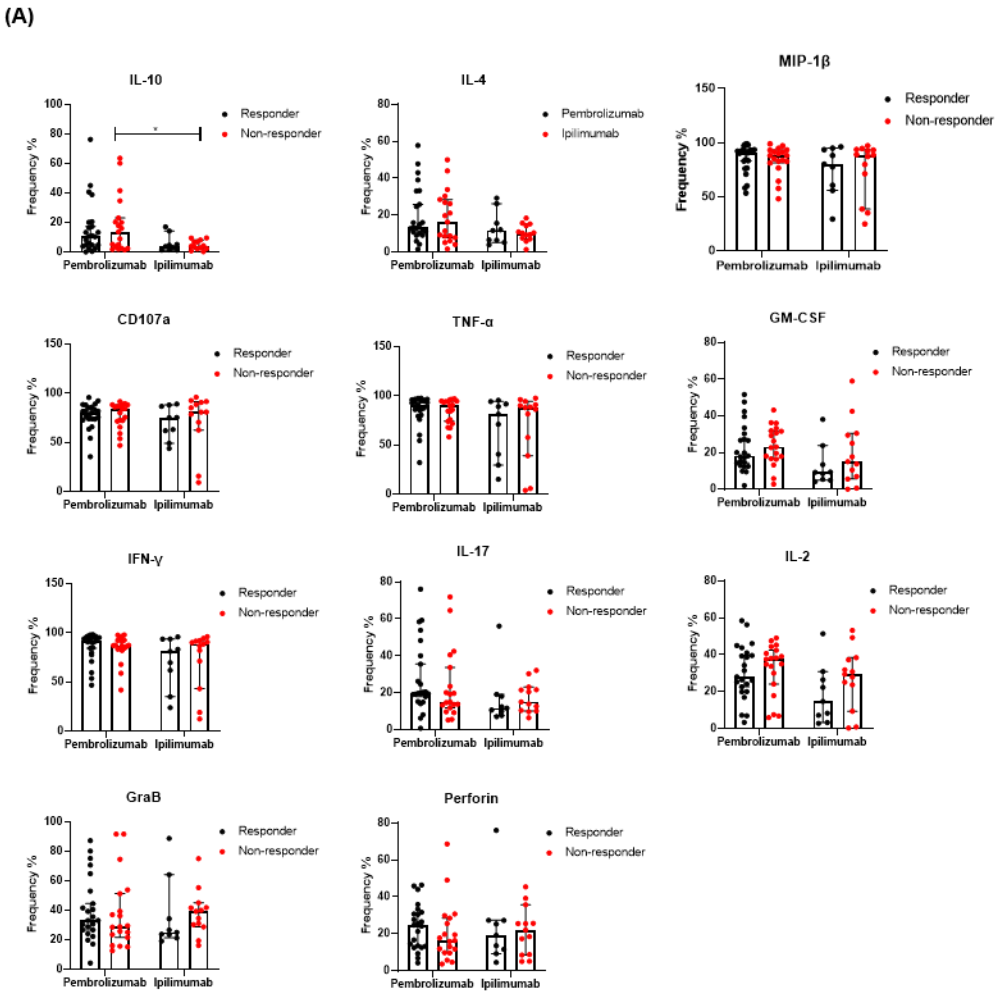

Figure 6.2.10 Anti-PD-1 or anti-CTLA-4 generate similar cytokine profile by the CD20+ T cells.

CD20+ T cells were gated to assess cytokine production from responder and non-responder patients to anti-PD-1 (Pembrolizumab) or anti-CTLA-4 (Ipilimumab) therapy. The cells were stimulated with 10ng/ml PMA and 1 μg/ml Ionomycin **(A)** (n=64). Statistical difference was measured using Mann-Whitney test. * $P < 0.05$**.** GraB; granzyme B.

6.3 Discussion

The datasets I have used in this chapter are from melanoma patients receiving anti-PD-1 or anti-CTLA-4 that are known as checkpoint blockade immunotherapy (Subrahmanyam et al., 2018). The presence of CD20+ T cells was observed by gating of CD3+CD19-TCRγδ-CD8+CD20+ cells **(Fig 6.2.1A)**. Although these cells could be detected in melanoma patients, the percentages of were similar in both responder and non-responder patients with either anti-PD-1 or anti-CTLA-4 **(Fig 6.2.1B,C,D)**.

These results may indicate that the role of CD20+ T cells in the response to treatment is minimal. However, CD20+ T cells showed a more differentiated memory phenotype with the presence of high levels of Temra and Tem (Schuh et al., 2016). Indeed, in the same study, using multivariate analysis techniques, the authors demonstrated that Temra cells from the CD8+ compartment showed a higher frequency within patients responding to anti-CTLA-4 over non-responders (Subrahmanyam et al., 2018). In parallel with these findings, Temra levels were higher in responding patients over non-responders from the CD20+ and CD20- T cells subsets **(Fig 6.2.3A,B)**. This specific type of memory cell has been proposed to be highly differentiated with lower proliferation ability and a senescent like phenotype, although, they show higher cytotoxicity over other memory subsets (Henson et al., 2012). Further investigation of the phenotype of all memory subsets within the CD20+ and CD20- T cells from these patients revealed differences in additional markers, including CD28, CD27 and CD127.

It is well known that CTLA-4 compete with CD28 signalling by binding to CD80 and CD86 on APC and the presence of high CD28 may result in a lower inhibition effect of the CTLA-4 (Collins et al., 2002). Indeed, CD28 signalling has been shown to be crucial for an effective PD-1 blockade therapy, especially in rescuing exhausted virus-specific CD8+ in mice

(Kamphorst et al., 2017b). The higher expression of CD27 and CD127 may indicate a better response by these memory cells over the CD20- memory cells, because the downregulation of these markers has been shown to be associated with exhaustion or senescence (Dong et al., 2019), **(Fig 6.2.4A,B,C)**.

Overall, memory CD20+CD8+ T cells showed the potential to be more effective through the higher expression of CD28, CD27 and CD127, however, responders and non-responders showed a similar memory phenotype within both CD20+ and CD20- memory cells. Therefore, no marker was identified that might influence the response to the treatment.

Anti-PD-1 can result in the accumulation of exhausted PD-1+CD8+ T cells in the blood of melanoma patients and in the lung of lung cancer patients (Huang et al., 2017, Kamphorst et al., 2017a). The higher expression of PD-1 by the CD20+ T cells might be unfavourable for the response to the anti-PD1 therapy, as the CD8+ intermediate PD-1 expressing cells have been suggested to be the most responsive to the treatment (Wherry, 2011). The reasons for this variation in responses might be related to the exhaustion status of the cells, where a number of the irreversible exhausted T cells could not be recovered with the anti-PD-1 therapy (Lei et al., 2020).

The level of PD-1 was similar between responders and non-responders, which may influence another mechanism of anti-PD-1 in responder patients that resulted in tumour regression **(Fig 6.2.7A)**. Generally, CD20+ memory cells within the blood of those patients showed higher expression PD-1, but higher expression of CD28, CD27 and CD127 as well. This could indicate a possible activated status rather than an exhaustion phenotype. Resistance to anti-PD-1 therapy has been reported before, where not all patients responded to the therapy. The anti-PD-1 resistance could be due to a number of different factors including the lower immunogenicity of the tumour, irreversible exhausted state of the T cells, IFN-γ resistance,

dysfunctional MHC molecule expression and a highly immunosuppressive tumour microenvironment (Lei et al., 2020).

The cytokine profile secreted by the stimulated CD20+ T cells revealed a higher expression of several cytokines over the stimulated CD20- T cells. To illustrate, CD20+ T cells showed higher expression of IL-2, IFN-γ, TNF-α and MIP-1β that are known to drive proinflammatory responses through activating, recruiting and promoting the survival of other immune subsets. This can be beneficial in terms of tumour clearance, however it can also increase the risks of developing autoimmunity as a side effect of the treatment (Lim et al., 2019). CD20+ T cells showed higher degranulation through higher CD107a, which reflects the cytotoxic ability of the cells to kill the targeted cells, in this scenario the tumour cells (Aktas et al., 2009).

CD20+ T cells showed the ability to secrete high IL-17 and IL-10, which might enhance tumour immunosurveillance. It has been shown that targeting IL-17 in melanoma murine models resulted in tumour regression and prevented the cells becoming tumour cells *in vitro* (Chen et al., 2019). IL-10 has been well known for the ability to suppress immune responses and can be used by Treg to protect tumour from anti-tumour responses (Sawant et al., 2019). Interestingly, the amount of GraB and perforin released by the cells was similar. GraB and perforin represent the cytotoxic granules by which cytotoxic CD8+ can directly kill the targeted cells through different cell death mechanisms (Voskoboinik et al., 2015).

Overall, CD20+ T cells showed the ability to secrete more cytokine than CD20- T cells, except for GM-CSF and showed similar cytotoxic markers level **(Fig 6.2.8A)**. Further investigation of the cytokine profile between responders and non-responders showed similar cytokine profiles from both stimulated CD20+ and CD20- T cells. Both types of treatment, anti-PD-1 or anti-CTLA-4, showed similar cytokine profiles by the CD20+ T cells and no

difference was detected in responders and non-responders. Screening isolated cells from the tumour tissue, rather than peripheral blood might reveal the possible role of these cells in anti-tumour responses, and would benefit from analysis of antigen-specific compartment.

Chapter Seven: General Discussion

7. Discussion

7.1 The origin of CD20+ T cells

The origin of CD20+ T cells is debatable and two different proposals have been suggested. First, CD20 might be acquired from B cells in a process known as trogocytosis. This was proposed due to the increased CD20 expression on leukemic T cells after co-culturing with a B cell line and the expression of CD20 having been maintained for up to 46 hours in culture (de Bruyn et al., 2015). However, more recent papers show that CD20 can be transcribed on pre-sorted CD20+ T cells in addition to CD3 and the existence of CD20+ T cells could be the result of the transcription of CD20, not trogocytosis (Schuh et al., 2016). Our data support the second proposal, not trogocytosis, as the results show the existence of CD20+ T cells that have unique TCRβ CDR3 amino acid sequences that were absent in the CD20- compartment **(Fig. 3.2.5)**. Acquiring CD20 would most likely result in similar repertoires between the CD20- and CD20+ T cells; however, the opposite was found. The presence of unique amino acid sequences in the CD20+ compartment may suggest that those cells have been matured in the thymus. However, naïve CD20+ T cells were extremely low in healthy blood **(Fig. 3.2.3C)** and the lymph nodes of CRC patients **(Fig. 5.2.1D)**. This would suggest an alternative maturation process for those cells, where CD20 is expressed following T cell activation in a microenvironment that has yet to be defined.

In addition, further analysis of thymic CD20+ T cells is required to understand their maturation process. The presence of CD20+ T cells within the thymus has been reported before (Schuh et al., 2016). However, the specific phenotype of these cells and whether they have been through negative or positive selection has not been shown. Therefore, further experiments would be required to determine the origin of CD20+ T cells and to confirm whether the reported thymic CD20+ T cells have been through negative or positive selection or have simply migrated back through the thymus. This can be achieved through enzymatic

digestion of human thymus tissue and using the isolated cells for further phenotyping using flow cytometry.

The panel should include CD44 and CD25 to define the maturation stages of these cells within the thymus (Dudley et al., 1994). In addition, single-cell RNA sequencing would be a valuable technique in assessing the similarities between CD20+ and CD20- T-cell genes, to accept or refute the trogocytosis theory.

7.2 CD20+ MAIT cells

Our data revealed the novel presence of CD20 on a proportion of the MAIT cells by gating on the Vα7.2+CD161+ cells **(Fig. 4.2.3A,B)**. Two methods can be employed to detect MAIT cells: the use of MR-1 tetramers and gating the Vα7.2+CD161+ population. Although the Vα7.2+CD161+ population is enriched with MAIT cells, using MR-1 tetramers revealed that not all those cells are MAIT cells (Dias et al., 2018, Gherardin et al., 2018). This would open a new area for investigation to assess the expression of CD20 by MR-1 tetramer+ MAIT cells. The using of MR-1 tetramer would confirm the presence of CD20+ MAIT cells, where PBMCs isolated from healthy donors can be examined for the presence of CD20+MR-1 tetramer+ cells.

CD20+ and CD20- MAIT cells showed similar phenotypes, including cytotoxic markers, and no differences could be detected **(Fig. 4.2.7,9)**. However, this novel finding in respect of the presence of CD20+ MAIT cells could be valuable for further investigations. The similarity between CD20+ and CD20- MAIT cell phenotypes raises a question about the role of CD20 in those cells and could be used as a direction for further research. CD20+ T cells showed the ability to secrete more cytokines than the CD20- T cells and the ability to assess the cytokine secretion between the CD20+ and CD20- MAIT cells would determine if the source of the higher cytokine production within the CD20+ T cells is the CD20+ MAIT cells.

In CRC patients, the CCR6+CD161+ population resembled the phenotype of MAIT cells. The expression of CCR6 and CD161 has been well known in respect of MAIT cells (Lee et al., 2018). However, the absence of Vα7.2 from the panel prevented the accurate gating of MAIT cells. Despite this, it was clear that the CCR6+CD161+ population can be found within the CD20+ T cells in PBMCs and lymph nodes isolated cells from CRC patients **(Fig. 5.2.2)**.

Again, using MR-1 tetramers would help in detecting the presence of CD20+ MAIT cells within cancer patients and could be used to assess possible differences between CD20+ and CD20- MAIT cells.

7.3 CD20+ T cells represent antigen-experienced cells

In line with other publications, our data confirmed the persistence of the memory phenotype of the CD20+ T cells in blood, lymph nodes, tumour tissue and normal tissues. Using two EBV-specific lytic antigen tetramers, EBV-specific CD8+ T cells showed a higher percentage of CD20+ T cells compared with CD20- T cells **(Fig. 3.2.9)**. The phenotyping of CD20+ T cells showed their enrichment within memory cells that have been developed from previously activated T cells; which increases the possibility of B cells being the APC that presented the antigen to T cells and therefore, CD20 could be trogocytosed from those B cells. The presence of a higher frequency of EBV-specific CD20+ T cells compared to the CD20- T cells would indicate higher possibilities of previous interaction with B cells, as B cells are target for EBV (Delecluse et al., 2019). However, EBV-specific CD20+ T cells were less than 3% of the total CD20+ T cells, which may indicate another source for the CD20 **(Fig 3.2.9)**, including *de novo* expression.

Memory CD20+ T cells showed a tendency to express higher levels of CD27, CD127 and CD28, especially within PBMCs isolated from healthy donors and CRC patients **(Fig. 4.2.4, 5.2.8)**. They also showed higher expression of PD-1 than memory CD20- T cells **(Fig. 4.2.4, 5.2.9)**. This expression profile was observed in both healthy donors and CRC patients; which may indicate that cancer has no effect on the phenotype of these cells.

As discussed in chapter 4, the upregulation of CD127, CD27 and CD28, especially by Tem and Temra T cells, could indicate a higher proliferation ability and survival rate of these cells (Kaech et al., 2003, Joshi et al., 2007), whereas a higher expression of PD-1 could be an indication of exhausted cells (Gong et al., 2018). It is also possible that the higher expression of PD-1 could be a physiological mechanism to control the activity of these cells. However, the proliferation ability of CD20+ T cells has been debated. For example, it was shown that the proliferation of CD20+ T cells was low in RA patients receiving rituximab (Wilk et al., 2009), while in MS patients, the *in vitro* stimulation of CD20+ T cells resulted in a higher proliferation than CD20- T cells (von Essen et al., 2019). Therefore, further assessment of the proliferation ability of those cells and RNA-sequencing analysis would be needed to explain the significance of the upregulation of these markers.

7.4 CD20+ T cells in cancer

The role of the CD20+ T cells in cancer has been addressed in a single report, in which they were investigated in ovarian cancer patients (de Bruyn et al., 2015). CD20+ T cells were expanded in the ascitic fluid of those patients and were able to secrete higher amount of IFNγ over CD20- T cells. The same report proposed trogocytosis as the origin of those cells.

However, the role of CD20+ T cells in different types of cancer has not been investigated before. Our data revealed the presence of CD20+ T cells within different tissues isolated from cancer patients with diagnoses that included breast cancer, colon cancer and CRC. They could also be found in blood obtained from the same patient and in the lymph nodes of CRC patients. Their presence was at a lower percentage than normal adjacent tissue and investigating their phenotype and functions was difficult. However, investigating blood and lymph nodes for CD20+ T cells revealed different results. To illustrate, in colon cancer patients, the majority of CD20+ T cells were CD39- **(Fig. 3.2.6)**, and CD39 has been used to differentiate between tumour-specific and bystander infiltrating CD8+ (Simoni et al., 2018b). The lack of CD39 expression on CD20+ infiltrating T cells in colon cancer may indicate that these cells are among the bystander infiltrating CD8+ T cells.

Further investigation of the CD20+ T cells within the matched blood of CRC patients showed an enriched CCR6+CD161+ population **(Fig. 5.2.3)**. The CD161 gene has been shown to be a predictive marker of survival in different types of cancer, including prostate, colon and bladder cancers, melanoma and other types of cancer (Konduri et al., 2021). In humans, CD161 can be expressed by NK cells and CD161 high CD8+ cells share some NK-like functions. These cells are usually proposed as having innate functions (Kurioka et al., 2018). Further phenotyping of CCR6+CD161+CD20+ T cells showed a higher expression of CD56, which is known as an NK cell marker **(Fig. 5.2.8A,B)** (Poli et al., 2009).

The CD56+CD8+ population was shown to be a high cytokine producer population with a lower ability to proliferate and a higher tendency towards apoptosis (Ohkawa et al., 2001). Hence, the CD161+ population would be a good survival marker in cancer patients and their enrichment within CD20+ T cells could be used for further investigation of those cells within different types of cancer. CCR6+CD161- cells were found to be the highest population among the CD20+ T cells within the lymph nodes isolated from CRC patients. However, in

both blood and lymph nodes, CD20+ T cells showed a higher expression of CCR6, which is known as a tissue homing marker (Fergusson et al., 2016). This would suggest the ability of CD20+ T cells to migrate to different types of tissue, including the tumour microenvironment. However, the loss of CD39 among CD20+ T cells within tumour-infiltrating T cells could lead to categorising those cells among tumour-infiltrating polyclonal T cells, and thus not tumour-reactive T cells. The antigen specificity of those cells needs to be further investigated, as they showed a higher response to EBV tetramers and the presence of MAIT cells could indicate their possible roles in responses against pathogens, not cancer.

7.5 CD20+ T cell response to checkpoint blockade therapy

Using dataset from melanoma patients receiving anti-PD-1 or CTLA-4 inhibitors, the analysis of CD20+ T cell percentages revealed no significant difference between responders and non-responders to treatment **(Fig. 5.2.1B) (Table 2.7.3.1)**. This includes both phenotypic differences and cytokine release profile post *in vitro* stimulation **(Fig. 5.2.5A, 5.2.9)**.

However, in agreement with an observation in the same published paper of the dataset, CD20+ T cells showed a significantly higher percentage of Temra T cells within responders than non-responders **(Fig. 5.2.3A)** (Subrahmanyam et al., 2018). This could be necessary for responses to the treatment, where it has been shown that most tumour-reactive cells are found within a highly exhausted population of tissue-infiltrating lymphocytes (Gros et al., 2014, Inozume et al., 2010).

Temra cells represent highly differentiated memory T cells that show a more exhausted phenotype (Callender et al., 2018). Overall, no significant difference was found between responders and non-responders, except for Temra levels, which could also be noted in the CD20- T cells **(Fig. 5.2.3B)**. However, *in vitro* stimulation of PBMCs isolated from those

patients resulted in a significantly higher production of different cytokines by CD20+ T cells than CD20- T cells **(Fig. 5.2.8)**.

Among these cytokines, TNF-α, MIP-1β, IL-2 and IFNγ are known as pro-inflammatory cytokines (Murphy and Weaver, 2016). In addition, CD20+ T cells showed higher amount of the degranulation marker CD107a. Surprisingly, the amounts of perforin and Granyzme B were similar for the two populations, which may indicate that they have similar cytotoxic activities **(Fig. 5.2.8)**. Further investigation of the functionality of the CD20+ T cells is needed to determine the ability of these cells to elicit an immune response and kill the target. Although anti-PD-1 was administered to those melanoma patients, more than 50% of these cells expressed PD-1 **(Fig. 5.2.6)**. No relation between CD20+ T cells and response to the treatment could be found. This might indicate a higher exhausted phenotype among the CD20+ T cells which needs further investigation of the proliferation ability of those cells. The higher expression of PD-1 can indicate a possible higher activation state of the CD20+ T cells over the CD20- T cells, which can be further investigated through, for example, using cytotoxic and killing assays.

Generally, these observations can be found in both normal healthy donors and cancer patients. The constant expression of PD-1 by these cells could be a physiological mechanism by which these higher cytokine producer cells could be controlled to prevent excessive activation. Therefore, further investigation of the functionality of those cells would be needed to examine their capability to function normally and to determine their antigen specificity.

7.6 Limitations

There are a number of limitations to my studies described in this thesis. First in chapter 3 the main limitation was the number of the samples used in this study. This was due to two main reasons; first the budget and the expensive cost of the TCR-sequencing analysis experiment

and second, the difficulty in successfully sorting adequate numbers of the CD20+ T cells. For the EBV tetramer staining, HLA-A*02-positive donors were needed for the experiment and three donors only were obtained before the COVID-19 pandemic. The same issue can be noticed in the data I generated in chapter 5, where only one sample was used from breast cancer and 3 samples from colon cancer, where the COVID-19 pandemic prevented further phenotyping of CD20+ T cells on those types of cancer. Second, the other results in chapters 4, 5 and 6, were based on previously published mass cytometry datasets, therefore the methodology design was already determined and I needed to use the available uploaded data. The main issue would be the absence of an anti-CD20 isotype control or CD20 mass minus one. Data used in chapter 5 were from cancer-associated lymph nodes and PBMCs isolated from CRC patients, which may show the systematic phenotype of the CD20+ T cells and not the actual tumour-infiltrated CD20+ T cells. Thus, increasing the number of the baseline stained cells or pre-sorting of the CD20+ T cells prior to the staining would emphasise the possibility of assessing the tumour-infiltrated CD20+ T cells. Finally, in chapter 6, the dataset included the PBMCs isolated from melanoma patients who had received anti-PD-1 or anti-CTLA-4 without normal healthy isolated PBMCs nor PBMCs isolated from those melanoma patients before starting the treatment to compare with. This prevented the proper comparison between CD20+ T cells in the normal healthy state and in melanoma cancer patients. Tracking the changes caused by the anti-PD-1 or anti-CTLA-4 treatment would be difficult without the sample from the same patients before receiving the treatment. However, overall, the generated data would indicate the direction for further researching the biology of the CD20+ T cells, for example, the origin of the cells, their exhaustion status and the presence of novel CD20+ MAIT cells.

7.7 Future work

Various questions about the biology of CD20+ T cells remain unanswered. Although the results from TCR sequencing may not have favoured the trogocytosis theory, further investigations might show the possible origin of thymic CD20+ T cells, where both induced and generic expression of CD20 can possibly be the origin of the CD20 on those cells. Hence, investigating the presence and the phenotype of the CD20+ T cells within human thymus would reveal the possible presence of CD20+ double positive (CD4+CD8+) cells within the thymus. Besides, this would help to assess the presence of naïve CD20+ T cells or whether the CD20+ T cells are generated more in the periphery as result of trogocytosis or activation. Furthermore, assessing the methylation of CD20 across naïve T cells would indicate if there is an on and off switching mechanism; by which specific stimuli can induce the expression of the CD20 on CD20+ T cells.

The antigenic specificity of CD20+ T cells clearly requires further investigation. To illustrate, identifying if the CD20+ T cells are specialized cells against EBV, where the higher interaction of those cells with B cells resulted in more trogocytosis and thus acquiring the CD20 from those cells. Indeed, this may explain the presence of unique TCRβ CDR3 amino acid sequences in the CD20+ T cells population, which theoretically may result from a bias toward EBV responses and the more diverse CD20- T cells repertoire. Antigen specificity should also be examined in the cancer samples. As only a small percentage of tumour-infiltrating T cells are cancer-specific, it remains possible that CD20+ T cells do indeed play a significant role in the anti-tumour responses.

Furthermore, two different observations in this study could be used for further examination: first, the presence of MAIT CD20+ T cells could be further confirmed using MR-1 tetramers; and second, it would be interesting to use the higher expression of CD27, CD28 and CD127,

especially by Temra T cells, to assess the proliferation ability of the cells and their ability to function normally, by performing killing assays and *in vitro* functional assays.

Finally, the higher cytokine production by these cells would emphasise the need to investigate the role of CD20, and whether CD20 acts as a stimulatory receptor that boosts the activation of the CD20+ T cells over the CD20- T cells. Different techniques, such as, CRISPR gene editing, to knock out the CD20 from the CD20+ T cells could be used to assess the role of CD20 on these cells.

In summary, pre-sorted CD20+ and CD20- memory CD8+ T cells showed the presence of unique TCRβ CDR3 amino acid sequences of the CD20+ T cells, which may indicate that the trogocytosis theory is highly unlikely to be supported. In addition, memory CD20+ T cells showed a higher expression of CD27, CD28 and CD127 and, therefore, indicated a higher survival and proliferation ability. However, the persistence ability of the CD20+ T cells to commit within the antigen-experienced cells through the higher percentages of memory cells and a greater ability to respond to EBV tetramers would emphasise the need for further investigations of the thymic CD20+ T cells, in order to determine the origin and the development of those cells. The presence of novel CD20+ MAIT cells has been demonstrated through the presence of Vα7.2+CD161+CD20+ T cells. However, this would need further confirmation using MR-1 tetramers.

On the other hand, CD20+ T cells lack the expression of CD39 in colon cancer. Moreover, no link could be detected between a response to anti-PD-1 and CTLA-4 inhibitors in melanoma patients. The phenotype of those cells would influence their potential as possible effective cells in cancer patients. This can be demonstrated through their ability to secrete higher pro-inflammatory cytokine levels than CD20- T cells **(Fig 7.6.1)**. However, the antigenic specificity of those cells is still being debated and their ability to respond to EBV tetramers

and the presence of MAIT cells within CD20+ T cells may influence their roles in bacterial and viral immunity. Therefore, further investigation of possible tumour-reactive cells among CD20+ T cells would be critical to assess the potential use of those cells as a therapeutic approach and to understand their biology.

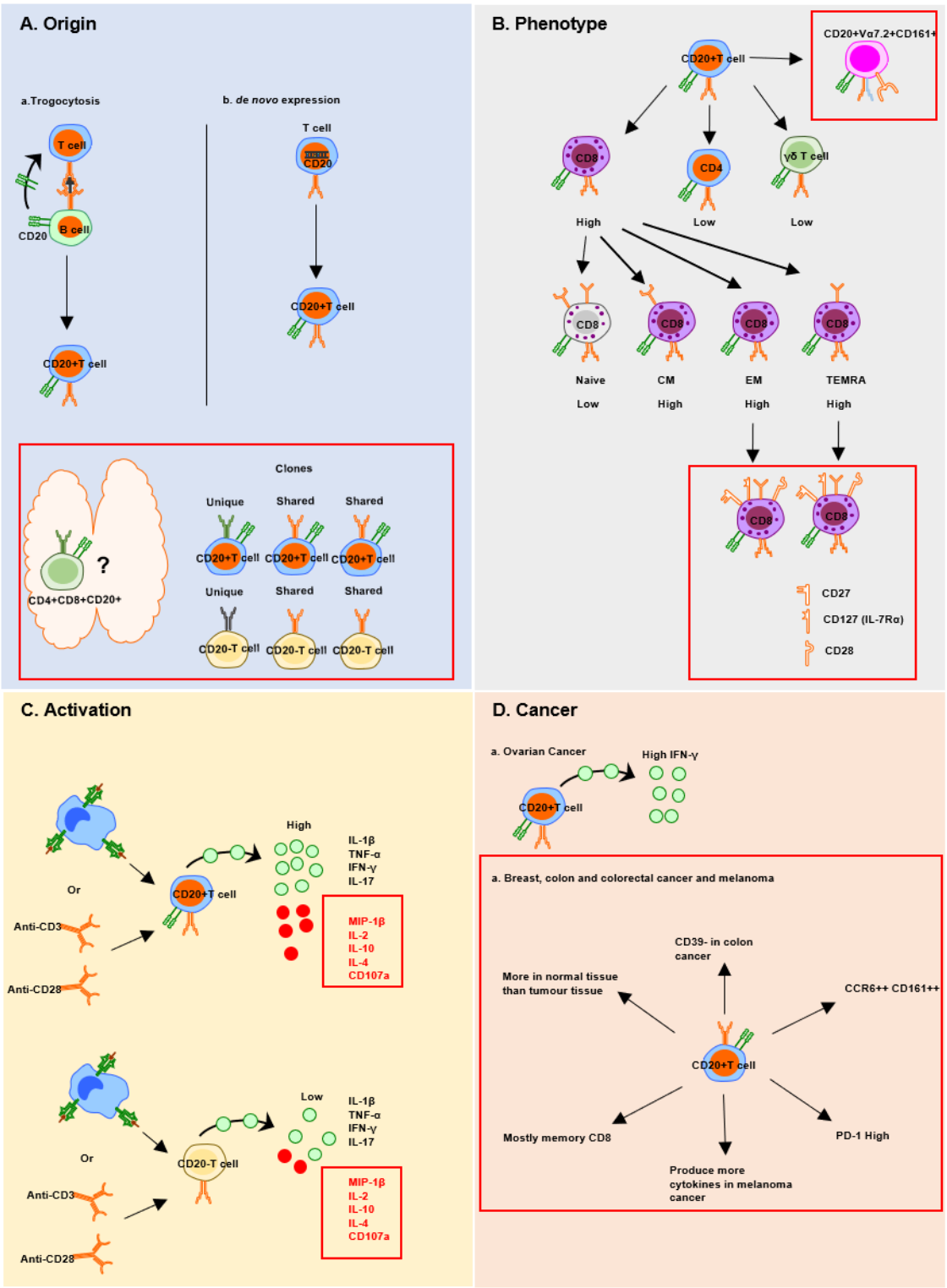

Figure 7.6.1 Summary of the previous and new findings about CD20+ T cells.

The possible explanations of the presence of CD20+ T cells **(A).** Reported and new findings about CD20+ T cells phenotype **(B)**. Cytokines produced upon activation, new cytokines reported (**C)**. The reported functions of CD20+ T cells in cancer environment **(D)**. New findings from the studies in my thesis are contained within the red boxes.

Chapter Eight: References

List of references

AHN, E., ARAKI, K., HASHIMOTO, M., LI, W., RILEY, J. L., CHEUNG, J., SHARPE, A. H., FREEMAN, G. J., IRVING, B. A. & AHMED, R. 2018. Role of PD-1 during effector CD8 T cell differentiation. *Proceedings of the National Academy of Sciences,* 115**,** 4749-4754.

AKTAS, E., KUCUKSEZER, U. C., BILGIC, S., ERTEN, G. & DENIZ, G. 2009. Relationship between CD107a expression and cytotoxic activity. *Cellular immunology,* 254**,** 149-154.

ANDERSEN, M. H., SCHRAMA, D., THOR STRATEN, P. & BECKER, J. C. 2006. Cytotoxic T cells. *Journal of Investigative Dermatology,* 126**,** 32-41.

ANDERSON, M. S., VENANZI, E. S., KLEIN, L., CHEN, Z., BERZINS, S. P., TURLEY, S. J., VON BOEHMER, H., BRONSON, R., DIERICH, A. & BENOIST, C. 2002. Projection of an immunological self shadow within the thymus by the aire protein. *Science,* 298**,** 1395-1401.

ARNOLD, D. M., DENTALI, F., CROWTHER, M. A., MEYER, R. M., COOK, R. J., SIGOUIN, C., FRASER, G. A., LIM, W. & KELTON, J. G. 2007. Systematic review: efficacy and safety of rituximab for adults with idiopathic thrombocytopenic purpura. *Annals of internal medicine,* 146**,** 25-33.

ATTAF, M., LEGUT, M., COLE, D. K. & SEWELL, A. K. 2015. The T cell antigen receptor: the Swiss army knife of the immune system. *Clinical & Experimental Immunology,* 181**,** 1-18.

BENNETT, F., LUXENBERG, D., LING, V., WANG, I.-M., MARQUETTE, K., LOWE, D., KHAN, N., VELDMAN, G., JACOBS, K. A. & VALGE-ARCHER, V. E. 2003. Program death-1 engagement upon TCR activation has distinct effects on costimulation and cytokine-driven proliferation: attenuation of ICOS, IL-4, and IL-21, but not CD28, IL-7, and IL-15 responses. *The Journal of Immunology,* 170**,** 711-718.

BENZ, C., MARTINS, V. C., RADTKE, F. & BLEUL, C. C. 2008. The stream of precursors that colonizes the thymus proceeds selectively through the early T lineage precursor stage of T cell development. *Journal of Experimental Medicine,* 205**,** 1187-1199.

BERENZON, D., SCHWENK, R. J., LETELLIER, L., GUEBRE-XABIER, M., WILLIAMS, J. & KRZYCH, U. 2003. Protracted protection to Plasmodium berghei malaria is linked to functionally and phenotypically heterogeneous liver memory CD8+ T cells. *The Journal of Immunology,* 171**,** 2024-2034.

BEST, J. A., BLAIR, D. A., KNELL, J., YANG, E., MAYYA, V., DOEDENS, A., DUSTIN, M. L. & GOLDRATH, A. W. 2013. Transcriptional insights into the CD8+ T cell response to infection and memory T cell formation. *Nature immunology,* 14**,** 404-412.

BHATTACHARYYA, N. D. & FENG, C. G. 2020. Regulation of T helper cell fate by TCR signal strength. *Frontiers in immunology,* 11**,** 624.

BILLERBECK, E., KANG, Y.-H., WALKER, L., LOCKSTONE, H., GRAFMUELLER, S., FLEMING, V., FLINT, J., WILLBERG, C. B., BENGSCH, B. & SEIGEL, B. 2010. Analysis of CD161 expression on human CD8+ T cells defines a distinct functional subset with tissue-homing properties. *Proceedings of the National Academy of Sciences,* 107**,** 3006-3011.

BLACKBURN, S. D., SHIN, H., HAINING, W. N., ZOU, T., WORKMAN, C. J., POLLEY, A., BETTS, M. R., FREEMAN, G. J., VIGNALI, D. A. & WHERRY, E. J. 2009. Coregulation of CD8+ T cell exhaustion by multiple inhibitory receptors during chronic viral infection. *Nature immunology,* 10**,** 29-37.

BOUILLET, P., PURTON, J. F., GODFREY, D. I., ZHANG, L.-C., COULTAS, L., PUTHALAKATH, H., PELLEGRINI, M., CORY, S., ADAMS, J. M. & STRASSER, A. 2002. BH3-only Bcl-2 family member Bim is required for apoptosis of autoreactive thymocytes. *Nature,* 415**,** 922-926.

BOUTROS, C., TARHINI, A., ROUTIER, E., LAMBOTTE, O., LADURIE, F. L., CARBONNEL, F., IZZEDDINE, H., MARABELLE, A., CHAMPIAT, S. & BERDELOU, A. 2016. Safety profiles of anti-CTLA-4 and anti-PD-1 antibodies alone and in combination. *Nature reviews Clinical oncology,* 13**,** 473-486.

BRATKE, K., KUEPPER, M., BADE, B., VIRCHOW JR, J. C. & LUTTMANN, W. 2005. Differential expression of human granzymes A, B, and K in natural killer cells and during CD8+ T cell differentiation in peripheral blood. *European journal of immunology,* 35**,** 2608-2616.

BRENNAN, P. J., BRIGL, M. & BRENNER, M. B. 2013. Invariant natural killer T cells: an innate activation scheme linked to diverse effector functions. *Nature Reviews Immunology,* 13**,** 101-117.

BRINKMAN, C. C., ROUHANI, S. J., SRINIVASAN, N. & ENGELHARD, V. H. 2013. Peripheral tissue homing receptors enable T cell entry into lymph nodes and affect the anatomical distribution of memory cells. *The Journal of Immunology,* 191**,** 2412-2425.

BRODIN, P. & DAVIS, M. M. 2017. Human immune system variation. *Nature reviews immunology,* 17**,** 21-29.

BUBIEN, J. K., ZHOU, L.-J., BELL, P. D., FRIZZELL, R. A. & TEDDER, T. F. 1993. Transfection of the CD20 cell surface molecule into ectopic cell types generates a Ca2+ conductance found constitutively in B lymphocytes. *The Journal of cell biology,* 121**,** 1121-1132.

BUCHBINDER, E. I. & DESAI, A. 2016. CTLA-4 and PD-1 pathways: similarities, differences, and implications of their inhibition. *American journal of clinical oncology,* 39**,** 98.

CALDERÓN, L. & BOEHM, T. 2011. Three chemokine receptors cooperatively regulate homing of hematopoietic progenitors to the embryonic mouse thymus. *Proceedings of the National Academy of Sciences,* 108**,** 7517-7522.

CALL, M. E., PYRDOL, J., WIEDMANN, M. & WUCHERPFENNIG, K. W. 2002. The organizing principle in the formation of the T cell receptor-CD3 complex. *Cell,* 111**,** 967-979.

CALLENDER, L. A., CARROLL, E. C., BEAL, R. W., CHAMBERS, E. S., NOURSHARGH, S., AKBAR, A. N. & HENSON, S. M. 2018. Human CD 8+ EMRA T cells display a senescence-associated secretory phenotype regulated by p38 MAPK. *Aging Cell,* 17**,** e12675.

CARUSO, A., LICENZIATI, S., CORULLI, M., CANARIS, A. D., DE FRANCESCO, M. A., FIORENTINI, S., PERONI, L., FALLACARA, F., DIMA, F. & BALSARI, A. 1997. Flow cytometric analysis of activation markers on stimulated T cells and their correlation with cell proliferation. *Cytometry: The Journal of the International Society for Analytical Cytology,* 27**,** 71-76.

CHA, E., KLINGER, M., HOU, Y., CUMMINGS, C., RIBAS, A., FAHAM, M. & FONG, L. 2014. Improved survival with T cell clonotype stability after anti–CTLA-4 treatment in cancer patients. *Science translational medicine,* 6**,** 238ra70-238ra70.

CHAMBERS, C. A., KUHNS, M. S., EGEN, J. G. & ALLISON, J. P. 2001. CTLA-4-mediated inhibition in regulation of T cell responses: mechanisms and manipulation in tumor immunotherapy. *Annual review of immunology,* 19**,** 565-594.

CHAN, W. K., RUJKIJYANONT, P., NEALE, G., YANG, J., BARI, R., GUPTA, N. D., HOLLADAY, M., ROONEY, B. & LEUNG, W. 2013. Multiplex and genome-wide analyses reveal distinctive properties of KIR+ and CD56+ T cells in human blood. *The Journal of Immunology,* 191**,** 1625-1636.

CHANG, J. T., WHERRY, E. J. & GOLDRATH, A. W. 2014. Molecular regulation of effector and memory T cell differentiation. *Nature immunology,* 15**,** 1104.

CHEN, C., CHEN, D., ZHANG, Y., CHEN, Z., ZHU, W., ZHANG, B., WANG, Z. & LE, H. 2014. Changes of CD4+ CD25+ FOXP3+ and CD8+ CD28− regulatory T cells in non-small cell lung cancer patients undergoing surgery. *International immunopharmacology,* 18**,** 255-261.

CHEN, D. S., IRVING, B. A. & HODI, F. S. 2012. Molecular pathways: next-generation immunotherapy—inhibiting programmed death-ligand 1 and programmed death-1. *Clinical cancer research,* 18**,** 6580-6587.

CHEN, Y.-S., HUANG, T.-H., LIU, C.-L., CHEN, H.-S., LEE, M.-H., CHEN, H.-W. & SHEN, C.-R. 2019. Locally targeting the IL-17/IL-17RA axis reduced tumor growth in a murine B16F10 melanoma model. *Human gene therapy,* 30**,** 273-285.

CHEVRIER, S., LEVINE, J. H., ZANOTELLI, V. R. T., SILINA, K., SCHULZ, D., BACAC, M., RIES, C. H., AILLES, L., JEWETT, M. A. S. & MOCH, H. 2017. An immune atlas of clear cell renal cell carcinoma. *Cell,* 169**,** 736-749. e18.

CHIBA, T., OHTANI, H., MIZOI, T., NAITO, Y., SATO, E., NAGURA, H., OHUCHI, A., OHUCHI, K., SHIIBA, K. & KUROKAWA, Y. 2004. Intraepithelial CD8+ T-cell-count becomes a prognostic factor

after a longer follow-up period in human colorectal carcinoma: possible association with suppression of micrometastasis. *British journal of cancer,* 91**,** 1711-1717.
CLARK, E. A. & SHU, G. 1987. Activation of human B cell proliferation through surface Bp35 (CD20) polypeptides or immunoglobulin receptors. *The Journal of Immunology,* 138**,** 720-725.
COLLINS, A. V., BRODIE, D. W., GILBERT, R. J., IABONI, A., MANSO-SANCHO, R., WALSE, B., STUART, D. I., VAN DER MERWE, P. A. & DAVIS, S. J. 2002. The interaction properties of costimulatory molecules revisited. *Immunity,* 17**,** 201-210.
CORTHAY, A. 2009. How do regulatory T cells work? *Scandinavian journal of immunology,* 70**,** 326-336.
CRAGG, M. 2002. Asidipour A O'Brien L Opposing properties of anti-CD20 mAb. Leucocyte typing VII. Oxford Mason D Simmons D Schwartz-Albiez R Hadam M Saalmuller A Clark E ….
CRAGG, M. S. & GLENNIE, M. J. 2004. Antibody specificity controls in vivo effector mechanisms of anti-CD20 reagents. *Blood,* 103**,** 2738-2743.
CRAGG, M. S., MORGAN, S. M., CHAN, H. C., MORGAN, B. P., FILATOV, A., JOHNSON, P. W., FRENCH, R. R. & GLENNIE, M. J. 2003. Complement-mediated lysis by anti-CD20 mAb correlates with segregation into lipid rafts. *Blood, The Journal of the American Society of Hematology,* 101**,** 1045-1052.
CRAGG, M. S., WALSHE, C. A., IVANOV, A. O. & GLENNIE, M. J. 2005. The biology of CD20 and its potential as a target for mAb therapy. *B cell trophic factors and B cell antagonism in autoimmune disease,* 8**,** 140-174.
CROME, S., WANG, A. & LEVINGS, M. 2010. Translational mini-review series on Th17 cells: function and regulation of human T helper 17 cells in health and disease. *Clinical & Experimental Immunology,* 159**,** 109-119.
CROSS, A. H., STARK, J. L., LAUBER, J., RAMSBOTTOM, M. J. & LYONS, J.-A. 2006. Rituximab reduces B cells and T cells in cerebrospinal fluid of multiple sclerosis patients. *Journal of neuroimmunology,* 180**,** 63-70.
DANAHY, D. B., ANTHONY, S. M., JENSEN, I. J., HARTWIG, S. M., SHAN, Q., XUE, H.-H., HARTY, J. T., GRIFFITH, T. S. & BADOVINAC, V. P. 2017. Polymicrobial sepsis impairs bystander recruitment of effector cells to infected skin despite optimal sensing and alarming function of skin resident memory CD8 T cells. *PLoS pathogens,* 13**,** e1006569.
DAS, R., VERMA, R., SZNOL, M., BODDUPALLI, C. S., GETTINGER, S. N., KLUGER, H., CALLAHAN, M., WOLCHOK, J. D., HALABAN, R. & DHODAPKAR, M. V. 2015. Combination therapy with anti–CTLA-4 and anti–PD-1 leads to distinct immunologic changes in vivo. *The Journal of Immunology,* 194**,** 950-959.
DE BRUYN, M., WIERSMA, V. R., WOUTERS, M. C., SAMPLONIUS, D. F., KLIP, H. G., HELFRICH, W., NIJMAN, H. W., EGGLETON, P. & BREMER, E. 2015. CD20+ T cells have a predominantly Tc1 effector memory phenotype and are expanded in the ascites of patients with ovarian cancer. *Oncoimmunology,* 4**,** e999536.
DE VRIES, N. L., VAN UNEN, V., IJSSELSTEIJN, M. E., ABDELAAL, T., VAN DER BREGGEN, R., SARASQUETA, A. F., MAHFOUZ, A., PEETERS, K. C., HÖLLT, T. & LELIEVELDT, B. P. 2020. High-dimensional cytometric analysis of colorectal cancer reveals novel mediators of antitumour immunity. *Gut,* 69**,** 691-703.
DELECLUSE, S., TSAI, M.-H., SHUMILOV, A., BENCUN, M., ARROW, S., BESHIROVA, A., COTTIGNIES-CALAMARTE, A., LASITSCHKA, F., BULUT, O. C. & MÜNZ, C. 2019. Epstein-Barr virus induces expression of the LPAM-1 integrin in B cells in vitro and in vivo. *Journal of virology,* 93**,** e01618-18.
DERBINSKI, J., SCHULTE, A., KYEWSKI, B. & KLEIN, L. 2001. Promiscuous gene expression in medullary thymic epithelial cells mirrors the peripheral self. *Nature immunology,* 2**,** 1032.
DIAS, J., BOULOUIS, C., GORIN, J.-B., VAN DEN BIGGELAAR, R. H., LAL, K. G., GIBBS, A., LOH, L., GULAM, M. Y., SIA, W. R. & BARI, S. 2018. The CD4− CD8− MAIT cell subpopulation is a

functionally distinct subset developmentally related to the main CD8+ MAIT cell pool. *Proceedings of the National Academy of Sciences,* 115**,** E11513-E11522.
DONG, H., BUCKNER, A., PRINCE, J. & BULLOCK, T. 2019. Frontline Science: Late CD27 stimulation promotes IL-7Rα transcriptional re-expression and memory T cell qualities in effector CD8+ T cells. *Journal of leukocyte biology,* 106**,** 1007-1019.
DUDLEY, E. C., PETRIE, H. T., SHAH, L. M., OWEN, M. J. & HAYDAY, A. C. 1994. T cell receptor β chain gene rearrangement and selection during thymocyte development in adult mice. *Immunity,* 1**,** 83-93.
DUHEN, T., DUHEN, R., MONTLER, R., MOSES, J., MOUDGIL, T., DE MIRANDA, N. F., GOODALL, C. P., BLAIR, T. C., FOX, B. A. & MCDERMOTT, J. E. 2018. Co-expression of CD39 and CD103 identifies tumor-reactive CD8 T cells in human solid tumors. *Nature communications,* 9**,** 1-13.
DUSSEAUX, M., MARTIN, E., SERRIARI, N., PÉGUILLET, I., PREMEL, V., LOUIS, D., MILDER, M., LE BOURHIS, L., SOUDAIS, C. & TREINER, E. 2011. Human MAIT cells are xenobiotic-resistant, tissue-targeted, CD161hi IL-17–secreting T cells. *Blood, The Journal of the American Society of Hematology,* 117**,** 1250-1259.
DZHAGALOV, I. & PHEE, H. 2012. How to find your way through the thymus: a practical guide for aspiring T cells. *Cellular and Molecular Life Sciences,* 69**,** 663-682.
EARL, L. & BAUM, L. 2008. CD45 glycosylation controls T-cell life and death. *Immunology and Cell Biology,* 86**,** 608.
EDWARDS, J. C., SZCZEPAŃSKI, L., SZECHIŃSKI, J., FILIPOWICZ-SOSNOWSKA, A., EMERY, P., CLOSE, D. R., STEVENS, R. M. & SHAW, T. 2004. Efficacy of B-cell–targeted therapy with rituximab in patients with rheumatoid arthritis. *New England Journal of Medicine,* 350**,** 2572-2581.
EGER, K. A., SUNDRUD, M. S., MOTSINGER, A. A., TSENG, M., KAER, L. V. & UNUTMAZ, D. 2006. Human natural killer T cells are heterogeneous in their capacity to reprogram their effector functions. *PLoS One,* 1**,** e50.
ELIA, G., FERRARI, S. M., GALDIERO, M. R., RAGUSA, F., PAPARO, S. R., RUFFILLI, I., VARRICCHI, G., FALLAHI, P. & ANTONELLI, A. 2020. New insight in endocrine-related adverse events associated to immune checkpoint blockade. *Best Practice & Research Clinical Endocrinology & Metabolism,* 34**,** 101370.
EON KUEK, L., LEFFLER, M., MACKAY, G. A. & HULETT, M. D. 2016. The MS4A family: counting past 1, 2 and 3. *Immunology and cell biology,* 94**,** 11-23.
FALSCHLEHNER, C., SCHAEFER, U. & WALCZAK, H. 2009. Following TRAIL's path in the immune system. *Immunology,* 127**,** 145-154.
FARHOOD, B., NAJAFI, M. & MORTEZAEE, K. 2019. CD8+ cytotoxic T lymphocytes in cancer immunotherapy: a review. *Journal of cellular physiology,* 234**,** 8509-8521.
FAVORITI, P., CARBONE, G., GRECO, M., PIROZZI, F., PIROZZI, R. E. M. & CORCIONE, F. 2016. Worldwide burden of colorectal cancer: a review. *Updates in surgery,* 68**,** 7-11.
FEHLING, H., KROTKOVA, A., SAINT-RUF, C. & VON BOEHMER, H. 1995. Crucial role of the pre-T-cell receptor gene in development of but not T cells.[Published erratum appears in 1995 Nature 378: 419.]. *Nature,* 375**,** 795.
FEHLINGS, M., SIMONI, Y., PENNY, H., BECHT, E., LOH, C., GUBIN, M., WARD, J., WONG, S., SCHREIBER, R. & NEWELL, E. 2017. Checkpoint blockade immunotherapy reshapes the high-dimensional phenotypic heterogeneity of murine intratumoural neoantigen-specific CD8+ T cells. *Nature communications,* 8**,** 1-12.
FERGUSSON, J., HÜHN, M., SWADLING, L., WALKER, L., KURIOKA, A., LLIBRE, A., BERTOLETTI, A., HOLLÄNDER, G., NEWELL, E. & DAVIS, M. 2016. CD161 int CD8+ T cells: a novel population of highly functional, memory CD8+ T cells enriched within the gut. *Mucosal immunology,* 9**,** 401-413.
FERGUSSON, J. R., SMITH, K. E., FLEMING, V. M., RAJORIYA, N., NEWELL, E. W., SIMMONS, R., MARCHI, E., BJÖRKANDER, S., KANG, Y.-H. & SWADLING, L. 2014. CD161 defines a

transcriptional and functional phenotype across distinct human T cell lineages. *Cell reports,* 9**,** 1075-1088.
FIFE, B. T. & BLUESTONE, J. A. 2008. Control of peripheral T-cell tolerance and autoimmunity via the CTLA-4 and PD-1 pathways. *Immunological reviews,* 224**,** 166-182.
FLETCHER, A. L., ACTON, S. E. & KNOBLICH, K. 2015. Lymph node fibroblastic reticular cells in health and disease. *Nature Reviews Immunology,* 15**,** 350.
FRIDMAN, W. H., PAGES, F., SAUTES-FRIDMAN, C. & GALON, J. 2012. The immune contexture in human tumours: impact on clinical outcome. *Nature Reviews Cancer,* 12**,** 298-306.
FUERTES MARRACO, S. A., NEUBERT, N. J., VERDEIL, G. & SPEISER, D. E. 2015. Inhibitory Receptors Beyond T Cell Exhaustion. *Frontiers in Immunology,* 6**,** 310.
GASTEIGER, G. & RUDENSKY, A. Y. 2014. Interactions between innate and adaptive lymphocytes. *Nature Reviews Immunology,* 14**,** 631-639.
GATTINONI, L., JI, Y. & RESTIFO, N. P. 2010. Wnt/β-catenin signaling in T-cell immunity and cancer immunotherapy. *Clinical Cancer Research,* 16**,** 4695-4701.
GATTINONI, L., SPEISER, D. E., LICHTERFELD, M. & BONINI, C. 2017. T memory stem cells in health and disease. *Nature medicine,* 23**,** 18-27.
GERLACH, C., MOSEMAN, E. A., LOUGHHEAD, S. M., ALVAREZ, D., ZWIJNENBURG, A. J., WAANDERS, L., GARG, R., JUAN, C. & VON ANDRIAN, U. H. 2016. The chemokine receptor CX3CR1 defines three antigen-experienced CD8 T cell subsets with distinct roles in immune surveillance and homeostasis. *Immunity,* 45**,** 1270-1284.
GHERARDIN, N. A., SOUTER, M. N., KOAY, H. F., MANGAS, K. M., SEEMANN, T., STINEAR, T. P., ECKLE, S. B., BERZINS, S. P., D'UDEKEM, Y. & KONSTANTINOV, I. E. 2018. Human blood MAIT cell subsets defined using MR1 tetramers. *Immunology and cell biology,* 96**,** 507-525.
GLARÍA, E. & VALLEDOR, A. F. 2020. Roles of CD38 in the Immune Response to Infection. *Cells,* 9**,** 228.
GODFREY, D. I., KOAY, H.-F., MCCLUSKEY, J. & GHERARDIN, N. A. 2019. The biology and functional importance of MAIT cells. *Nature immunology,* 20**,** 1110-1128.
GONG, J., CHEHRAZI-RAFFLE, A., REDDI, S. & SALGIA, R. 2018. Development of PD-1 and PD-L1 inhibitors as a form of cancer immunotherapy: a comprehensive review of registration trials and future considerations. *Journal for immunotherapy of cancer,* 6**,** 1-18.
GOODNOW, C. C., SPRENT, J., DE ST GROTH, B. F. & VINUESA, C. G. 2005. Cellular and genetic mechanisms of self tolerance and autoimmunity. *Nature,* 435**,** 590-597.
GREENBERG, S. A., KONG, S. W., THOMPSON, E. & GULLA, S. V. 2019. Co-inhibitory T cell receptor KLRG1: human cancer expression and efficacy of neutralization in murine cancer models. *Oncotarget,* 10**,** 1399.
GROS, A., ROBBINS, P. F., YAO, X., LI, Y. F., TURCOTTE, S., TRAN, E., WUNDERLICH, J. R., MIXON, A., FARID, S. & DUDLEY, M. E. 2014. PD-1 identifies the patient-specific CD8+ tumor-reactive repertoire infiltrating human tumors. *The Journal of clinical investigation,* 124**,** 2246-2259.
GUO, X., ZHANG, Y., ZHENG, L., ZHENG, C., SONG, J., ZHANG, Q., KANG, B., LIU, Z., JIN, L. & XING, R. 2018. Global characterization of T cells in non-small-cell lung cancer by single-cell sequencing. *Nature medicine,* 24**,** 978-985.
HAINSWORTH, J. D., BURRIS, H. A., MORRISSEY, L. H., LITCHY, S., SCULLIN, D. C., BEARDEN, J. D., RICHARDS, P. & GRECO, F. A. 2000. Rituximab monoclonal antibody as initial systemic therapy for patients with low-grade non-Hodgkin lymphoma. *Blood,* 95**,** 3052-3056.
HAMANN, D., KOSTENSE, S., WOLTHERS, K. C., OTTO, S. A., BAARS, P. A., MIEDEMA, F. & VAN LIER, R. A. 1999. Evidence that human CD8+ CD45RA+ CD27–cells are induced by antigen and evolve through extensive rounds of division. *International Immunology,* 11**,** 1027-1033.
HAYWARD, A. R., LEE, J. & BEVERLEY, P. C. 1989. Ontogeny of expression of UCHL1 antigen on TcR-1+(CD4/8) and TcRδ+ T cells. *European journal of immunology,* 19**,** 771-773.
HENGEL, R. L., THAKER, V., PAVLICK, M. V., METCALF, J. A., DENNIS, G., YANG, J., LEMPICKI, R. A., SERETI, I. & LANE, H. C. 2003. Cutting edge: L-selectin (CD62L) expression distinguishes small

resting memory CD4+ T cells that preferentially respond to recall antigen. *The Journal of Immunology,* 170**,** 28-32.

HENSON, S. M., RIDDELL, N. E. & AKBAR, A. N. 2012. Properties of end-stage human T cells defined by CD45RA re-expression. *Current opinion in immunology,* 24**,** 476-481.

HOLDER, M., GRAFTON, G., MACDONALD, I., FINNEY, M. & GORDON, J. 1995. Engagement of CD20 suppresses apoptosis in germinal center B cells. *European journal of immunology,* 25**,** 3160-3164.

HOLLEY, J. E., BREMER, E., KENDALL, A. C., DE BRUYN, M., HELFRICH, W., TARR, J. M., NEWCOMBE, J., GUTOWSKI, N. J. & EGGLETON, P. 2014. CD20+ inflammatory T-cells are present in blood and brain of multiple sclerosis patients and can be selectively targeted for apoptotic elimination. *Multiple sclerosis and related disorders,* 3**,** 650-658.

HUANG, A. C., POSTOW, M. A., ORLOWSKI, R. J., MICK, R., BENGSCH, B., MANNE, S., XU, W., HARMON, S., GILES, J. R. & WENZ, B. 2017. T-cell invigoration to tumour burden ratio associated with anti-PD-1 response. *Nature,* 545**,** 60-65.

HULTIN, L. E., HAUSNER, M. A., HULTIN, P. M. & GIORGI, J. V. 1993. CD20 (pan-B cell) antigen is expressed at a low level on a subpopulation of human T lymphocytes. *Cytometry: The Journal of the International Society for Analytical Cytology,* 14**,** 196-204.

HUSTER, K. M., KOFFLER, M., STEMBERGER, C., SCHIEMANN, M., WAGNER, H. & BUSCH, D. H. 2006. Unidirectional development of CD8+ central memory T cells into protective Listeria-specific effector memory T cells. *European journal of immunology,* 36**,** 1453-1464.

INOZUME, T., HANADA, K.-I., WANG, Q. J., AHMADZADEH, M., WUNDERLICH, J. R., ROSENBERG, S. A. & YANG, J. C. 2010. Selection of CD8+ PD-1+ lymphocytes in fresh human melanomas enriches for tumor-reactive T-cells. *Journal of immunotherapy (Hagerstown, Md.: 1997),* 33**,** 956.

JAMESON, S. C. & MASOPUST, D. 2018. Understanding subset diversity in T cell memory. *Immunity,* 48**,** 214-226.

JOSHI, N. S., CUI, W., CHANDELE, A., LEE, H. K., URSO, D. R., HAGMAN, J., GAPIN, L. & KAECH, S. M. 2007. Inflammation directs memory precursor and short-lived effector CD8+ T cell fates via the graded expression of T-bet transcription factor. *Immunity,* 27**,** 281-295.

JUNG, D. & ALT, F. W. 2004. Unraveling V (D) J recombination: insights into gene regulation. *Cell,* 116**,** 299-311.

KAECH, S. M., HEMBY, S., KERSH, E. & AHMED, R. 2002. Molecular and functional profiling of memory CD8 T cell differentiation. *Cell,* 111**,** 837-851.

KAECH, S. M., TAN, J. T., WHERRY, E. J., KONIECZNY, B. T., SURH, C. D. & AHMED, R. 2003. Selective expression of the interleukin 7 receptor identifies effector CD8 T cells that give rise to long-lived memory cells. *Nature immunology,* 4**,** 1191-1198.

KAMPHORST, A. O., PILLAI, R. N., YANG, S., NASTI, T. H., AKONDY, R. S., WIELAND, A., SICA, G. L., YU, K., KOENIG, L. & PATEL, N. T. 2017a. Proliferation of PD-1+ CD8 T cells in peripheral blood after PD-1–targeted therapy in lung cancer patients. *Proceedings of the National Academy of Sciences,* 114**,** 4993-4998.

KAMPHORST, A. O., WIELAND, A., NASTI, T., YANG, S., ZHANG, R., BARBER, D. L., KONIECZNY, B. T., DAUGHERTY, C. Z., KOENIG, L. & YU, K. 2017b. Rescue of exhausted CD8 T cells by PD-1–targeted therapies is CD28-dependent. *Science,* 355**,** 1423-1427.

KANSAS, G. S. & TEDDER, T. F. 1991. Transmembrane signals generated through MHC class II, CD19, CD20, CD39, and CD40 antigens induce LFA-1-dependent and independent adhesion in human B cells through a tyrosine kinase-dependent pathway. *The Journal of Immunology,* 147**,** 4094-4102.

KANZAKI, M., LINDORFER, M. A., GARRISON, J. C. & KOJIMA, I. 1997. Activation of the calcium-permeable cation channel CD20 by α subunits of the Gi protein. *Journal of Biological Chemistry,* 272**,** 14733-14739.

KANZAKI, M., SHIBATA, H., MOGAMI, H. & KOJIMA, I. 1995. Expression of calcium-permeable cation channel CD20 accelerates progression through the G1 phase in Balb/c 3T3 cells. *Journal of Biological Chemistry,* 270**,** 13099-13104.

KEIR, M. E., BUTTE, M. J., FREEMAN, G. J. & SHARPE, A. H. 2008. PD-1 and its ligands in tolerance and immunity. *Annu. Rev. Immunol.,* 26**,** 677-704.

KHAIR, D. O., BAX, H. J., MELE, S., CRESCIOLI, S., PELLIZZARI, G., KHIABANY, A., NAKAMURA, M., HARRIS, R. J., FRENCH, E. & HOFFMANN, R. M. 2019. Combining immune checkpoint inhibitors: established and emerging targets and strategies to improve outcomes in melanoma. *Frontiers in immunology,* 10**,** 453.

KITAYAMA, S., ZHANG, R., LIU, T.-Y., UEDA, N., IRIGUCHI, S., YASUI, Y., KAWAI, Y., TATSUMI, M., HIRAI, N. & MIZORO, Y. 2016. Cellular adjuvant properties, direct cytotoxicity of re-differentiated Vα24 invariant NKT-like cells from human induced pluripotent stem cells. *Stem cell reports,* 6**,** 213-227.

KLÄSENER, K., JELLUSOVA, J., ANDRIEUX, G., SALZER, U., BÖHLER, C., STEINER, S. N., ALBINUS, J. B., CAVALLARI, M., SÜß, B. & VOLL, R. E. 2021. CD20 as a gatekeeper of the resting state of human B cells. *Proceedings of the National Academy of Sciences,* 118.

KLEIN, C., LAMMENS, A., SCHÄFER, W., GEORGES, G., SCHWAIGER, M., MÖSSNER, E., HOPFNER, K.-P., UMAÑA, P. & NIEDERFELLNER, G. Epitope interactions of monoclonal antibodies targeting CD20 and their relationship to functional properties. MAbs, 2013. Taylor & Francis, 22-33.

KLOCKE, K., SAKAGUCHI, S., HOLMDAHL, R. & WING, K. 2016. Induction of autoimmune disease by deletion of CTLA-4 in mice in adulthood. *Proceedings of the National Academy of Sciences,* 113**,** E2383-E2392.

KONDURI, V., OYEWOLE-SAID, D., VAZQUEZ-PEREZ, J., WELDON, S. A., HALPERT, M. M., LEVITT, J. M. & DECKER, W. K. 2021. CD8+ CD161+ T-Cells: Cytotoxic Memory Cells With High Therapeutic Potential. *Frontiers in Immunology,* 11**,** 3621.

KOTOV, D. I., MITCHELL, J. S., PENGO, T., RUEDL, C., WAY, S. S., LANGLOIS, R. A., FIFE, B. T. & JENKINS, M. K. 2019. TCR affinity biases Th cell differentiation by regulating CD25, Eef1e1, and Gbp2. *The Journal of Immunology,* 202**,** 2535-2545.

KRANICH, J. & KRAUTLER, N. J. 2016. How follicular dendritic cells shape the B-cell antigenome. *Frontiers in immunology,* 7**,** 225.

KRIJGSMAN, D., HOKLAND, M. & KUPPEN, P. J. 2018. The role of natural killer T cells in cancer—a phenotypical and functional approach. *Frontiers in immunology,* 9**,** 367.

KRUMMEL, M. F. & ALLISON, J. P. 1996. CTLA-4 engagement inhibits IL-2 accumulation and cell cycle progression upon activation of resting T cells. *The Journal of experimental medicine,* 183**,** 2533-2540.

KUIJPERS, T. W., BENDE, R. J., BAARS, P. A., GRUMMELS, A., DERKS, I. A., DOLMAN, K. M., BEAUMONT, T., TEDDER, T. F., VAN NOESEL, C. J. & ELDERING, E. 2010. CD20 deficiency in humans results in impaired T cell–independent antibody responses. *The Journal of clinical investigation,* 120**,** 214-222.

KUMAR, V. & DELOVITCH, T. L. 2014. Different subsets of natural killer T cells may vary in their roles in health and disease. *Immunology,* 142**,** 321-336.

KURIOKA, A., KLENERMAN, P. & WILLBERG, C. B. 2018. Innate-like CD 8+ T-cells and NK cells: converging functions and phenotypes. *Immunology,* 154**,** 547-556.

LANDAY, A., OHLSSON-WILHELM, B. & GIORGI, J. V. 1990. Application of flow cytometry to the study of HIV infection. *Aids,* 4**,** 479-498.

LARBI, A. & FULOP, T. 2014. From “truly naïve” to “exhausted senescent” T cells: when markers predict functionality. *Cytometry Part A,* 85**,** 25-35.

LARKIN, J., CHIARION-SILENI, V., GONZALEZ, R., GROB, J. J., COWEY, C. L., LAO, C. D., SCHADENDORF, D., DUMMER, R., SMYLIE, M. & RUTKOWSKI, P. 2015. Combined nivolumab and ipilimumab or monotherapy in untreated melanoma. *New England journal of medicine,* 373**,** 23-34.

LATCHMAN, Y. E., LIANG, S. C., WU, Y., CHERNOVA, T., SOBEL, R. A., KLEMM, M., KUCHROO, V. K., FREEMAN, G. J. & SHARPE, A. H. 2004. PD-L1-deficient mice show that PD-L1 on T cells, antigen-presenting cells, and host tissues negatively regulates T cells. *Proceedings of the National Academy of Sciences,* 101**,** 10691-10696.

LATHROP, S. K., BLOOM, S. M., RAO, S. M., NUTSCH, K., LIO, C.-W., SANTACRUZ, N., PETERSON, D. A., STAPPENBECK, T. S. & HSIEH, C.-S. 2011. Peripheral education of the immune system by colonic commensal microbiota. *Nature,* 478**,** 250-254.

LEE, C. H., ZHANG, H. H., SINGH, S. P., KOO, L., KABAT, J., TSANG, H., SINGH, T. P. & FARBER, J. M. 2018. C/EBPδ drives interactions between human MAIT cells and endothelial cells that are important for extravasation. *Elife,* 7**,** e32532.

LEI, Q., WANG, D., SUN, K., WANG, L. & ZHANG, Y. 2020. Resistance mechanisms of anti-PD1/PDL1 therapy in solid tumors. *Frontiers in Cell and Developmental Biology,* 8.

LÉVEILLÉ, C., AL-DACCAK, R. & MOURAD, W. 1999. CD20 is physically and functionally coupled to MHC class II and CD40 on human B cell lines. *European journal of immunology,* 29**,** 65-74.

LI, H., VAN DER LEUN, A. M., YOFE, I., LUBLING, Y., GELBARD-SOLODKIN, D., VAN AKKOOI, A. C., VAN DEN BRABER, M., ROZEMAN, E. A., HAANEN, J. B. & BLANK, C. U. 2020a. Dysfunctional CD8 T Cells Form a Proliferative, Dynamically Regulated Compartment within Human Melanoma. *Cell,* 181**,** 747.

LI, L., WAN, S., TAO, K., WANG, G. & ZHAO, E. 2016. KLRG1 restricts memory T cell antitumor immunity. *Oncotarget,* 7**,** 61670.

LI, Z., ZHENG, B., QIU, X., WU, R., WU, T., YANG, S., ZHU, Y., WU, X., WANG, S. & GU, Z. 2020b. The identification and functional analysis of CD8+ PD-1+ CD161+ T cells in hepatocellular carcinoma. *NPJ precision oncology,* 4**,** 1-10.

LIANG, Y., BUCKLEY, T. R., TU, L., LANGDON, S. D. & TEDDER, T. F. 2001. Structural organization of the human MS4A gene cluster on Chromosome 11q12. *Immunogenetics,* 53**,** 357-368.

LIM, S. Y., LEE, J. H., GIDE, T. N., MENZIES, A. M., GUMINSKI, A., CARLINO, M. S., BREEN, E. J., YANG, J. Y., GHAZANFAR, S. & KEFFORD, R. F. 2019. Circulating cytokines predict immune-related toxicity in melanoma patients receiving anti-PD-1–based immunotherapy. *Clinical Cancer Research,* 25**,** 1557-1563.

LINSLEY, P. S., BRADSHAW, J., GREENE, J., PEACH, R., BENNETT, K. L. & MITTLER, R. S. 1996. Intracellular trafficking of CTLA-4 and focal localization towards sites of TCR engagement. *Immunity,* 4**,** 535-543.

LIU, Y. J., ZHANG, J., LANE, P. J., CHAN, E. Y. T. & MACLENNAN, I. C. 1991. Sites of specific B cell activation in primary and secondary responses to T cell-dependent and T cell-independent antigens. *European journal of immunology,* 21**,** 2951-2962.

LUCAS, B., JAMES, K. D., COSWAY, E. J., PARNELL, S. M., TUMANOV, A. V., WARE, C. F., JENKINSON, W. E. & ANDERSON, G. 2016. Lymphotoxin β receptor controls T cell progenitor entry to the thymus. *The Journal of Immunology,* 197**,** 2665-2672.

LUGLI, E., GATTINONI, L., ROBERTO, A., MAVILIO, D., PRICE, D. A., RESTIFO, N. P. & ROEDERER, M. 2013. Identification, isolation and in vitro expansion of human and nonhuman primate T stem cell memory cells. *Nature protocols,* 8**,** 33-42.

MACKAY, L. K., RAHIMPOUR, A., MA, J. Z., COLLINS, N., STOCK, A. T., HAFON, M.-L., VEGA-RAMOS, J., LAUZURICA, P., MUELLER, S. N. & STEFANOVIC, T. 2013. The developmental pathway for CD103+ CD8+ tissue-resident memory T cells of skin. *Nature immunology,* 14**,** 1294-1301.

MACLEOD, M. K., KAPPLER, J. W. & MARRACK, P. 2010. Memory CD4 T cells: generation, reactivation and re-assignment. *Immunology,* 130**,** 10-15.

MAHNKE, Y. D., BRODIE, T. M., SALLUSTO, F., ROEDERER, M. & LUGLI, E. 2013. The who's who of T-cell differentiation: human memory T-cell subsets. *European journal of immunology,* 43**,** 2797-2809.

MARGONI, M., PREZIOSA, P., FILIPPI, M. & ROCCA, M. A. 2021. Anti-CD20 therapies for multiple sclerosis: current status and future perspectives. *Journal of Neurology***,** 1-19.

MARRERO, I., WARE, R. & KUMAR, V. 2015. Type II NKT cells in inflammation, autoimmunity, microbial immunity, and cancer. *Frontiers in immunology,* 6**,** 316.
MARTIN, E., TREINER, E., DUBAN, L., GUERRI, L., LAUDE, H., TOLY, C., PREMEL, V., DEVYS, A., MOURA, I. C. & TILLOY, F. 2009. Stepwise development of MAIT cells in mouse and human. *PLoS Biol,* 7**,** e1000054.
MASTELLER, E. L., CHUANG, E., MULLEN, A. C., REINER, S. L. & THOMPSON, C. B. 2000. Structural analysis of CTLA-4 function in vivo. *The Journal of Immunology,* 164**,** 5319-5327.
MELCHERS, F. 2005. The pre-B-cell receptor: selector of fitting immunoglobulin heavy chains for the B-cell repertoire. *Nature Reviews Immunology,* 5**,** 578-584.
MITTELBRUNN, M. & KROEMER, G. 2021. Hallmarks of T cell aging. *Nature Immunology,* 22**,** 687-698.
MOJUMDAR, K., VAJPAYEE, M., CHAUHAN, N. K., SINGH, A., SINGH, R. & KURAPATI, S. 2012. Altered T cell differentiation associated with loss of CD27 and CD28 in HIV infected Indian individuals. *Cytometry Part B: Clinical Cytometry,* 82**,** 43-53.
MOOSMANN, A., BIGALKE, I., TISCHER, J., SCHIRRMANN, L., KASTEN, J., TIPPMER, S., LEEPING, M., PREVALŠEK, D., JAEGER, G. & LEDDEROSE, G. 2010. Effective and long-term control of EBV PTLD after transfer of peptide-selected T cells. *Blood, The Journal of the American Society of Hematology,* 115**,** 2960-2970.
MORSY, D. E. D., SANYAL, R., ZAISS, A. K., DEO, R., MURUVE, D. A. & DEANS, J. P. 2013. Reduced T-dependent humoral immunity in CD20-deficient mice. *The Journal of Immunology,* 191**,** 3112-3118.
MUELLER, D. L. 2010. Mechanisms maintaining peripheral tolerance. *Nature immunology,* 11**,** 21.
MURAYAMA, Y., MUKAI, R., SATA, T., MATSUNAGA, S., NOGUCHI, A. & YOSHIKAWA, Y. 1996. Transient expression of CD20 antigen (pan B cell marker) in activated lymph node T cells. *Microbiology and immunology,* 40**,** 467-471.
MURPHY, K. & WEAVER, C. 2016. *Janeway's immunobiology*, Garland science.
MURPHY, K. M. & REINER, S. L. 2002. Decision making in the immune system: the lineage decisions of helper T cells. *Nature Reviews Immunology,* 2**,** 933.
NEMAZEE, D. & HOGQUIST, K. A. 2003. Antigen receptor selection by editing or downregulation of V (D) J recombination. *Current opinion in immunology,* 15**,** 182-189.
OHKAWA, T., SEKI, S., DOBASHI, H., KOIKE, Y., HABU, Y., AMI, K., HIRAIDE, H. & SEKINE, I. 2001. Systematic characterization of human CD8+ T cells with natural killer cell markers in comparison with natural killer cells and normal CD8+ T cells. *Immunology,* 103**,** 281-290.
ONITILO, A. A., STANKOWSKI, R. V., ENGEL, J. M. & DOI, S. A. 2013. Adequate lymph node recovery improves survival in colorectal cancer patients. *Journal of surgical oncology,* 107**,** 828-834.
OZGA, A. J., MOALLI, F., ABE, J., SWOGER, J., SHARPE, J., ZEHN, D., KREUTZFELDT, M., MERKLER, D., RIPOLL, J. & STEIN, J. V. 2016. pMHC affinity controls duration of CD8+ T cell–DC interactions and imprints timing of effector differentiation versus expansion. *Journal of Experimental Medicine,* 213**,** 2811-2829.
PALEY, M. A., KROY, D. C., ODORIZZI, P. M., JOHNNIDIS, J. B., DOLFI, D. V., BARNETT, B. E., BIKOFF, E. K., ROBERTSON, E. J., LAUER, G. M. & REINER, S. L. 2012. Progenitor and terminal subsets of CD8+ T cells cooperate to contain chronic viral infection. *Science,* 338**,** 1220-1225.
PARRY, R. V., CHEMNITZ, J. M., FRAUWIRTH, K. A., LANFRANCO, A. R., BRAUNSTEIN, I., KOBAYASHI, S. V., LINSLEY, P. S., THOMPSON, C. B. & RILEY, J. L. 2005. CTLA-4 and PD-1 receptors inhibit T-cell activation by distinct mechanisms. *Molecular and cellular biology,* 25**,** 9543-9553.
PELLICCI, D. G., KOAY, H.-F. & BERZINS, S. P. 2020. Thymic development of unconventional T cells: how NKT cells, MAIT cells and γδ T cells emerge. *Nature Reviews Immunology,* 20**,** 756-770.
PETRIE, R. J. & DEANS, J. P. 2002. Colocalization of the B cell receptor and CD20 followed by activation-dependent dissociation in distinct lipid rafts. *The Journal of Immunology,* 169**,** 2886-2891.
PIEPER, K., GRIMBACHER, B. & EIBEL, H. 2013. B-cell biology and development. *Journal of Allergy and Clinical Immunology,* 131**,** 959-971.

POLI, A., MICHEL, T., THÉRÉSINE, M., ANDRÈS, E., HENTGES, F. & ZIMMER, J. 2009. CD56bright natural killer (NK) cells: an important NK cell subset. *Immunology,* 126**,** 458-465.

POLYAK, M. J. & DEANS, J. P. 2002. Alanine-170 and proline-172 are critical determinants for extracellular CD20 epitopes; heterogeneity in the fine specificity of CD20 monoclonal antibodies is defined by additional requirements imposed by both amino acid sequence and quaternary structure. *Blood, The Journal of the American Society of Hematology,* 99**,** 3256-3262.

POLYAK, M. J., TAILOR, S. H. & DEANS, J. P. 1998. Identification of a cytoplasmic region of CD20 required for its redistribution to a detergent-insoluble membrane compartment. *The Journal of immunology,* 161**,** 3242-3248.

POONIA, B. & PAUZA, C. D. 2014. Levels of CD56+ TIM-3-effector CD8 T cells distinguish HIV natural virus suppressors from patients receiving antiretroviral therapy. *PLoS One,* 9**,** e88884.

PORRITT, H. E., RUMFELT, L. L., TABRIZIFARD, S., SCHMITT, T. M., ZÚÑIGA-PFLÜCKER, J. C. & PETRIE, H. T. 2004. Heterogeneity among DN1 prothymocytes reveals multiple progenitors with different capacities to generate T cell and non-T cell lineages. *Immunity,* 20**,** 735-745.

RADTKE, F. 1999. Wilson A, Stark B, Bauer M, vanMeerwijk J, MacDonald HR, Aguet M. *Deficient T cell fate specification in mice with an induced inactivation of Notch1. Immunity,* 10**,** 547-558.

RATHBONE, E. 2018. *Investigation of the adaptive immune response in multiple sclerosis.* University of Birmingham.

RAVI, R., MOOKERJEE, B., BHUJWALLA, Z. M., SUTTER, C. H., ARTEMOV, D., ZENG, Q., DILLEHAY, L. E., MADAN, A., SEMENZA, G. L. & BEDI, A. 2000. Regulation of tumor angiogenesis by p53-induced degradation of hypoxia-inducible factor 1α. *Genes & development,* 14**,** 34-44.

ROBERT, C., SCHACHTER, J., LONG, G. V., ARANCE, A., GROB, J. J., MORTIER, L., DAUD, A., CARLINO, M. S., MCNEIL, C. & LOTEM, M. 2015. Pembrolizumab versus ipilimumab in advanced melanoma. *New England Journal of Medicine,* 372**,** 2521-2532.

ROBERT, L., HARVIEW, C., EMERSON, R., WANG, X., MOK, S., HOMET, B., COMIN-ANDUIX, B., KOYA, R. C., ROBINS, H. & TUMEH, P. C. 2014. Distinct immunological mechanisms of CTLA-4 and PD-1 blockade revealed by analyzing TCR usage in blood lymphocytes. *Oncoimmunology,* 3**,** e29244.

ROCK, K. L., REITS, E. & NEEFJES, J. 2016. Present yourself! By MHC class I and MHC class II molecules. *Trends in immunology,* 37**,** 724-737.

ROCK, M. T., YODER, S. M., WRIGHT, P. F., TALBOT, T. R., EDWARDS, K. M. & CROWE, J. E. 2005. Differential regulation of granzyme and perforin in effector and memory T cells following smallpox immunization. *The Journal of Immunology,* 174**,** 3757-3764.

ROMERO, P., ZIPPELIUS, A., KURTH, I., PITTET, M. J., TOUVREY, C., IANCU, E. M., CORTHESY, P., DEVEVRE, E., SPEISER, D. E. & RUFER, N. 2007. Four functionally distinct populations of human effector-memory CD8+ T lymphocytes. *The Journal of Immunology,* 178**,** 4112-4119.

ROSSI, F. M., CORBEL, S. Y., MERZABAN, J. S., CARLOW, D. A., GOSSENS, K., DUENAS, J., SO, L., YI, L. & ZILTENER, H. J. 2005. Recruitment of adult thymic progenitors is regulated by P-selectin and its ligand PSGL-1. *Nature immunology,* 6**,** 626-634.

ROTTE, A. 2019. Combination of CTLA-4 and PD-1 blockers for treatment of cancer. *Journal of Experimental & Clinical Cancer Research,* 38**,** 1-12.

ROTTE, A., JIN, J. & LEMAIRE, V. 2018. Mechanistic overview of immune checkpoints to support the rational design of their combinations in cancer immunotherapy. *Annals of Oncology,* 29**,** 71-83.

SADE-FELDMAN, M., YIZHAK, K., BJORGAARD, S. L., RAY, J. P., DE BOER, C. G., JENKINS, R. W., LIEB, D. J., CHEN, J. H., FREDERICK, D. T. & BARZILY-ROKNI, M. 2019. Defining T cell states associated with response to checkpoint immunotherapy in melanoma. *Cell,* 176**,** 404.

SAWANT, D. V., YANO, H., CHIKINA, M., ZHANG, Q., LIAO, M., LIU, C., CALLAHAN, D. J., SUN, Z., SUN, T. & TABIB, T. 2019. Adaptive plasticity of IL-10+ and IL-35+ T reg cells cooperatively promotes tumor T cell exhaustion. *Nature immunology,* 20**,** 724-735.

SCHIETINGER, A., PHILIP, M., KRISNAWAN, V. E., CHIU, E. Y., DELROW, J. J., BASOM, R. S., LAUER, P., BROCKSTEDT, D. G., KNOBLAUGH, S. E. & HÄMMERLING, G. J. 2016. Tumor-specific T cell dysfunction is a dynamic antigen-driven differentiation program initiated early during tumorigenesis. *Immunity,* 45**,** 389-401.

SCHNEIDER, H., DOWNEY, J., SMITH, A., ZINSELMEYER, B. H., RUSH, C., BREWER, J. M., WEI, B., HOGG, N., GARSIDE, P. & RUDD, C. E. 2006. Reversal of the TCR stop signal by CTLA-4. *science,* 313**,** 1972-1975.

SCHUH, E., BERER, K., MULAZZANI, M., FEIL, K., MEINL, I., LAHM, H., KRANE, M., LANGE, R., PFANNES, K. & SUBKLEWE, M. 2016. Features of human CD3+ CD20+ T cells. *The Journal of Immunology,* 197**,** 1111-1117.

SHAH, D. K. & ZÚÑIGA-PFLÜCKER, J. C. 2014. An overview of the intrathymic intricacies of T cell development. *The Journal of Immunology,* 192**,** 4017-4023.

SHANNON-LOWE, C. & RICKINSON, A. 2019. The global landscape of EBV-associated tumors. *Frontiers in oncology,* 9**,** 713.

SHINKAI, Y., LAM, K.-P., OLTZ, E. M., STEWART, V., MENDELSOHN, M., CHARRON, J., DATTA, M., YOUNG, F., STALL, A. M. & ALT, F. W. 1992. RAG-2-deficient mice lack mature lymphocytes owing to inability to initiate V (D) J rearrangement. *Cell,* 68**,** 855-867.

SIMONI, Y., BECHT, E., FEHLINGS, M., LOH, C. Y., KOO, S.-L., TENG, K. W. W., YEONG, J. P. S., NAHAR, R., ZHANG, T. & KARED, H. 2018a. Bystander CD8+ T cells are abundant and phenotypically distinct in human tumour infiltrates. *Nature,* 557**,** 575.

SIMONI, Y., BECHT, E., FEHLINGS, M., LOH, C. Y., KOO, S.-L., TENG, K. W. W., YEONG, J. P. S., NAHAR, R., ZHANG, T. & KARED, H. 2018b. Bystander CD8+ T cells are abundant and phenotypically distinct in human tumour infiltrates. *Nature,* 557**,** 575-579.

SINGER, A. 2002. New perspectives on a developmental dilemma: the kinetic signaling model and the importance of signal duration for the CD4/CD8 lineage decision. *Current opinion in immunology,* 14**,** 207-215.

SMELAND, E. B., BEISKE, K., EK, B., WATT, R., PFEIFER-OHLSSON, S., BLOMHOFF, H. K., GODAL, T. & OHLSSON, R. 1987. Regulation of c-myc transcription and protein expression during activation of normal human B cells. *Experimental cell research,* 172**,** 101-109.

SMITH-GARVIN, J. E., KORETZKY, G. A. & JORDAN, M. S. 2009. T cell activation. *Annu Rev Immunol,* 27**,** 591-619.

SONG, H., LIM, Y., IM, H., BAE, J. M., KANG, G. H., AHN, J., BAEK, D., KIM, T.-Y., YOON, S.-S. & KOH, Y. 2019. Interpretation of EBV infection in pan-cancer genome considering viral life cycle: LiEB (Life cycle of Epstein-Barr virus). *Scientific reports,* 9**,** 3465.

SPIDLEN, J., BREUER, K., ROSENBERG, C., KOTECHA, N. & BRINKMAN, R. R. 2012. FlowRepository: A resource of annotated flow cytometry datasets associated with peer-reviewed publications. *Cytometry Part A,* 81**,** 727-731.

STORIE, I., WILSON, G., GRANGER, V., BARNETT, D. & REILLY, J. 1995. Circulating CD20dim T-lymphocytes increase with age: evidence for a memory cytotoxic phenotype. *Clinical & Laboratory Haematology,* 17**,** 323-328.

SUBRAHMANYAM, P. B., DONG, Z., GUSENLEITNER, D., GIOBBIE-HURDER, A., SEVERGNINI, M., ZHOU, J., MANOS, M., EASTMAN, L. M., MAECKER, H. T. & HODI, F. S. 2018. Distinct predictive biomarker candidates for response to anti-CTLA-4 and anti-PD-1 immunotherapy in melanoma patients. *Journal for immunotherapy of cancer,* 6**,** 1-14.

TAKAMI, A., SAITO, M., NAKAO, S., ASAKURA, H., NOZUE, T., ONOE, Y., YACHIE, A., SHIOBARA, S. & MATSUDA, T. 1998. CD20-positive T-cell chronic lymphocytic leukaemia. *British journal of haematology,* 102**,** 1327-1329.

TEDDER, T., BOYD, A., FREEDMAN, A., NADLER, L. & SCHLOSSMAN, S. 1985. The B cell surface molecule B1 is functionally linked with B cell activation and differentiation. *The Journal of Immunology,* 135**,** 973-979.

TEDDER, T. F. & ENGEL, P. 1994. CD20: a regulator of cell-cycle progression of B lymphocytes. *Immunology today,* 15**,** 450-454.

TEDDER, T. F., FORSGREN, A., BOYD, A. W., NADLER, L. M. & SCHLOSSMAN, S. F. 1986. Antibodies reactive with the B1 molecule inhibit cell cycle progression but not activation of human B lymphocytes. *European journal of immunology,* 16**,** 881-887.

THOME, J. J., YUDANIN, N., OHMURA, Y., KUBOTA, M., GRINSHPUN, B., SATHALIYAWALA, T., KATO, T., LERNER, H., SHEN, Y. & FARBER, D. L. 2014. Spatial map of human T cell compartmentalization and maintenance over decades of life. *Cell,* 159**,** 814-828.

THOMMEN, D. S., KOELZER, V. H., HERZIG, P., ROLLER, A., TREFNY, M., DIMELOE, S., KIIALAINEN, A., HANHART, J., SCHILL, C. & HESS, C. 2018. A transcriptionally and functionally distinct PD-1+ CD8+ T cell pool with predictive potential in non-small-cell lung cancer treated with PD-1 blockade. *Nature medicine,* 24**,** 994-1004.

THOMMEN, D. S., SCHREINER, J., MÜLLER, P., HERZIG, P., ROLLER, A., BELOUSOV, A., UMANA, P., PISA, P., KLEIN, C. & BACAC, M. 2015. Progression of lung cancer is associated with increased dysfunction of T cells defined by coexpression of multiple inhibitory receptors. *Cancer immunology research,* 3**,** 1344-1355.

TIROSH, I., IZAR, B., PRAKADAN, S. M., WADSWORTH, M. H., TREACY, D., TROMBETTA, J. J., ROTEM, A., RODMAN, C., LIAN, C. & MURPHY, G. 2016. Dissecting the multicellular ecosystem of metastatic melanoma by single-cell RNA-seq. *Science,* 352**,** 189-196.

TIVOL, E. A., BORRIELLO, F., SCHWEITZER, A. N., LYNCH, W. P., BLUESTONE, J. A. & SHARPE, A. H. 1995. Loss of CTLA-4 leads to massive lymphoproliferation and fatal multiorgan tissue destruction, revealing a critical negative regulatory role of CTLA-4. *Immunity,* 3**,** 541-547.

TOGHI ESHGHI, S., AU-YEUNG, A., TAKAHASHI, C., BOLEN, C. R., NYACHIENGA, M. N., LEAR, S. P., GREEN, C., MATHEWS, W. R. & O'GORMAN, W. E. 2019. Quantitative comparison of conventional and t-SNE-guided gating analyses. *Frontiers in immunology,* 10**,** 1194.

TONEGAWA, S. 1983. Somatic generation of antibody diversity. *Nature,* 302**,** 575-581.

TUGIZOV, S. M., HERRERA, R. & PALEFSKY, J. M. 2013. Epstein-Barr virus transcytosis through polarized oral epithelial cells. *Journal of virology,* 87**,** 8179-8194.

TURVEY, S. E. & BROIDE, D. H. 2010. Innate immunity. *Journal of Allergy and Clinical Immunology,* 125**,** S24-S32.

UCHIDA, J., LEE, Y., HASEGAWA, M., LIANG, Y., BRADNEY, A., OLIVER, J. A., BOWEN, K., STEEBER, D. A., HAAS, K. M. & POE, J. C. 2004. Mouse CD20 expression and function. *International immunology,* 16**,** 119-129.

VAN ACKER, H. H., ANGUILLE, S., WILLEMEN, Y., VAN DEN BERGH, J. M., BERNEMAN, Z. N., LION, E., SMITS, E. L. & VAN TENDELOO, V. F. 2016. Interleukin-15 enhances the proliferation, stimulatory phenotype, and antitumor effector functions of human gamma delta T cells. *Journal of hematology & oncology,* 9**,** 1-13.

VAN DER LEUN, A. M., THOMMEN, D. S. & SCHUMACHER, T. N. 2020. CD8+ T cell states in human cancer: insights from single-cell analysis. *Nature Reviews Cancer,* 20**,** 218-232.

VAN MEIR, H., NOUT, R., WELTERS, M., LOOF, N., DE KAM, M., VAN HAM, J., SAMUELS, S., KENTER, G., COHEN, A. & MELIEF, C. 2017. Impact of (chemo) radiotherapy on immune cell composition and function in cervical cancer patients. *Oncoimmunology,* 6**,** e1267095.

VICKERS, N. J. 2017. Animal communication: when i'm calling you, will you answer too? *Current biology,* 27**,** R713-R715.

VO, A. A., LUKOVSKY, M., TOYODA, M., WANG, J., REINSMOEN, N. L., LAI, C.-H., PENG, A., VILLICANA, R. & JORDAN, S. C. 2008. Rituximab and intravenous immune globulin for desensitization during renal transplantation. *New England Journal of Medicine,* 359**,** 242-251.

VOLPE, E., SAMBUCCI, M., BATTISTINI, L. & BORSELLINO, G. 2016. Fas–fas ligand: Checkpoint of t cell functions in multiple sclerosis. *Frontiers in immunology,* 7**,** 382.

VON ESSEN, M. R., AMMITZBØLL, C., HANSEN, R. H., PETERSEN, E. R., MCWILLIAM, O., MARQUART, H. V., DAMM, P. & SELLEBJERG, F. 2019. Proinflammatory CD20+ T cells in the pathogenesis of multiple sclerosis. *Brain,* 142**,** 120-132.

VOSKOBOINIK, I., WHISSTOCK, J. C. & TRAPANI, J. A. 2015. Perforin and granzymes: function, dysfunction and human pathology. *Nature Reviews Immunology,* 15**,** 388-400.

WAGNER, J., RAPSOMANIKI, M. A., CHEVRIER, S., ANZENEDER, T., LANGWIEDER, C., DYKGERS, A., REES, M., RAMASWAMY, A., MUENST, S. & SOYSAL, S. D. 2019. A single-cell atlas of the tumor and immune ecosystem of human breast cancer. *Cell,* 177**,** 1330-1345. e18.

WAHID, M., AKHTER, N., JAWED, A., DAR, S. A., MANDAL, R. K., LOHANI, M., AREESHI, M. Y., KHAN, S. & HAQUE, S. 2017. Pembrolizumab's non-cross resistance mechanism of action successfully overthrown ipilimumab. *Critical reviews in oncology/hematology,* 111**,** 1-6.

WALKER, L. J., KANG, Y.-H., SMITH, M. O., THARMALINGHAM, H., RAMAMURTHY, N., FLEMING, V. M., SAHGAL, N., LESLIE, A., OO, Y. & GEREMIA, A. 2012. Human MAIT and CD8αα cells develop from a pool of type-17 precommitted CD8+ T cells. *Blood, The Journal of the American Society of Hematology,* 119**,** 422-433.

WELTERS, M. J., MA, W., SANTEGOETS, S. J., GOEDEMANS, R., EHSAN, I., JORDANOVA, E. S., VAN HAM, V. J., VAN UNEN, V., KONING, F. & VAN EGMOND, S. I. 2018. Intratumoral HPV16-specific T cells constitute a type I–oriented tumor microenvironment to improve survival in HPV16-driven oropharyngeal cancer. *Clinical Cancer Research,* 24**,** 634-647.

WHERRY, E. J. 2011. T cell exhaustion. *Nature immunology,* 12**,** 492-499.

WHERRY, E. J., BLATTMAN, J. N., MURALI-KRISHNA, K., VAN DER MOST, R. & AHMED, R. 2003a. Viral persistence alters CD8 T-cell immunodominance and tissue distribution and results in distinct stages of functional impairment. *Journal of virology,* 77**,** 4911-4927.

WHERRY, E. J., TEICHGRÄBER, V., BECKER, T. C., MASOPUST, D., KAECH, S. M., ANTIA, R., VON ANDRIAN, U. H. & AHMED, R. 2003b. Lineage relationship and protective immunity of memory CD8 T cell subsets. *Nature immunology,* 4**,** 225-234.

WILK, E., WITTE, T., MARQUARDT, N., HORVATH, T., KALIPPKE, K., SCHOLZ, K., WILKE, N., SCHMIDT, R. E. & JACOBS, R. 2009. Depletion of functionally active CD20+ T cells by rituximab treatment. *Arthritis & Rheumatism: Official Journal of the American College of Rheumatology,* 60**,** 3563-3571.

WILLINGER, T., FREEMAN, T., HASEGAWA, H., MCMICHAEL, A. J. & CALLAN, M. F. 2005. Molecular signatures distinguish human central memory from effector memory CD8 T cell subsets. *The Journal of Immunology,* 175**,** 5895-5903.

WONG, E. B., AKILIMALI, N. A., GOVENDER, P., SULLIVAN, Z. A., COSGROVE, C., PILLAY, M., LEWINSOHN, D. M., BISHAI, W. R., WALKER, B. D. & NDUNG'U, T. 2013. Low levels of peripheral CD161++ CD8+ mucosal associated invariant T (MAIT) cells are found in HIV and HIV/TB co-infection. *PloS one,* 8**,** e83474.

XU, H., WILLIAMS, M. S. & SPAIN, L. M. 2006. Patterns of expression, membrane localization, and effects of ectopic expression suggest a function for MS4a4B, a CD20 homolog in Th1 T cells. *Blood,* 107**,** 2400-2408.

YAN, Y., LI, Z., ZHANG, G.-X., WILLIAMS, M. S., CAREY, G. B., ZHANG, J., ROSTAMI, A. & XU, H. 2013. Anti-MS4a4B treatment abrogates MS4a4B-mediated protection in T cells and ameliorates experimental autoimmune encephalomyelitis. *Apoptosis,* 18**,** 1106-1119.

YOKOSE, N., OGATA, K., SUGISAKI, Y., MORI, S., YAMADA, T., AN, E. & DAN, K. 2001. CD20-positive T cell leukemia/lymphoma: case report and review of the literature. *Annals of hematology,* 80**,** 372-375.

ZHANG, L., YU, X., ZHENG, L., ZHANG, Y., LI, Y., FANG, Q., GAO, R., KANG, B., ZHANG, Q. & HUANG, J. Y. 2018. Lineage tracking reveals dynamic relationships of T cells in colorectal cancer. *Nature,* 564**,** 268-272.

ZHANG, Y., GARCIA-IBANEZ, L. & TOELLNER, K. M. 2016. Regulation of germinal center B-cell differentiation. *Immunological reviews,* 270**,** 8-19.

ZHANG, Y., JOE, G., HEXNER, E., ZHU, J. & EMERSON, S. G. 2005. Host-reactive CD8+ memory stem cells in graft-versus-host disease. *Nature medicine,* 11**,** 1299-1305.
ZÚÑIGA-PFLÜCKER, J. C. 2004. T-cell development made simple. *Nature Reviews Immunology,* 4**,** 67.